Post-Punching Shear Behaviour of Full-Scale Slab Structure with Edge and Corner Columns

Li Zhang

Department of Civil Engineering and Applied Mechanics

McGill University

Montreal, Quebec, Canada

September 2014

A thesis submitted to McGill University in partial fulfilment of the requirements of the degree of Master of Engineering

ABSTRACT

The provision of structural integrity reinforcement provides a secondary defence mechanism after punching shear failure in two-way slab systems and prevents progressive collapse. The effectiveness of structural integrity reinforcement in a slab system, designed in accordance with the 2014 CSA A23.3 standard, was investigated in this experimental program. A full-scale slab structure, consisting of two continuous 3.0 × 3.0 m bays and supported by six exterior columns, was subjected to extreme overloading, causing punching shear failure in all of the slab-column connections. The sequence of punching shear failures was monitored and the post- punching shear behaviour due to the presence of structural integrity reinforcement was examined.

In order to estimate the response of individual columns, the load distribution ratio at the columns was calculated using the SAP2000 structural analysis software, with the stiffness of slab-column connections failing in punching shear being adjusted using the analytical model developed by Habibi et al. (2014). The responses of the individual slab-column connections suggested that the code provides conservative predictions of the punching shear resistance due to shear and moment transfer. The torsional cracking due to the moments being transferred at the edge and corner columns reduced the concrete breakout strength after punching shear and limited the performance of the structural integrity reinforcing bars.

The assessment of the overall performance indicated that the slab structure was able to provide overall post-punching shear resistance which was significantly higher than the design service load.

RÉSUMÉ

Le renforcement d'intégrité structurelle par armature est une mesure qui apporte un support secondaire lors d'une rupture par poinçonnement en cisaillement dans un système à dalles à deux voies et qui prévient l'effondrement progressif dans les structures à étages. L'efficacité du renforcement de l'intégrité structurelle dans un système à dalles, conçu selon le standard 2014 CSA A23.3, a été testée dans ce programme expérimental. Une structure de dalles pleine grandeur, constituée de deux baies continues de 3.0 × 3.0 m et supportée par six colonnes externes, a été soumise à une surcharge extrême, causant un échec par poinçonnement dans tous les raccordements dalle-colonne. La séquence des ruptures par poinçonnement été observée et le comportement post-poinçonnement dû à la présence de renforcement d'intégrité structurelle été examiné.

Afin d'estimer le résultat pour chaque colonne individuelle, le ratio de distribution de la charge par colonne a été calculé par le programme d'analyse structurelle SAP2000, avec la rigidité des raccordements dalle-colonne, caractérisé par une rupture par poinçonnement, et ajusté en accord avec le modèle analytique développé par Habibi et al. (2014). Le comportement des raccordements dalle-colonne individuels suggère que le code donne des prédictions conservatrices de la résistance au poinçonnement dû au cisaillement et au transfert de moments. Les fissures par torsion causées par les moments transférés à la périphérie et aux coins réduisent la force tronconique du béton et limitent la performance des barres qui renforcent l'intégrité structurelle de la structure.

L'évaluation générale de la performance a indiqué que la structure en dalles a fait preuve d'une meilleure résistance globale au poinçonnement en cisaillement sous une charge plus élevée que ce que la conception de service permettait.

ACKNOWLEDGEMENTS

I would like to take this opportunity to express my deepest gratitude to Professor Denis Mitchell and Dr. William Cook for their sharing of knowledge, tremendous support and continual guidance throughout my graduate program.

I would like to extend my appreciation to laboratory technicians John Bartczak and Gerard Bechard for their contribution of expertise in construction of the slab structure. The structure would not have been successfully built without their help.

I also wish to thank fellow students Aram Torikian, Abram Selim and Heidy Botero Villegas for their assistance and sharing of good times in the early stage of test structure construction; and Pascal Vézina and Sophie Goulet for their involvement in developing and revising the RÉSUMÉ in French.

Finally, I would like to extend special thanks my parents, grandparents and friends for their continuous inspiration and unconditional support.

Li Zhang

September 2014

TABLE OF CONTENTS

LIST OF FIGURES

LIST OF TABLES

1. INTRODUCTION AND LITERATURE REVIEW

1.1 Introduction

Punching shear failure is one of the common concerns in the design of two-way slab systems. It occurs when the effects from the applied shear and moment transfer exceeds the shear strength of the slab in the slab-column connection. This type of failure is extremely brittle and can lead to progressive collapse unless a secondary defence mechanism is provided.

Punching shear failure can occur due to design or construction errors, corrosion of reinforcement, overloading from construction or seismic effects. If a secondary post-punching shear failure support is absent, then the loss of support at the first failed connection will lead to load redistribution, resulting in additional punching shear failures at adjacent slab-column connections. In this case an initial punching shear failure can lead to partial or total progressive collapse of the building.

Numerous research programs have been carried out to develop means of preventing progressive collapse. In 1984, the provision of structural integrity reinforcement in flat plate systems was required in CSA Standard A23.3-84, to provide a secondary support mechanism after punching shear failure and prevent progressive collapse (CSA, 1984).

1.2 Previous Research

Hawkins and Mitchell (1979) investigated factors which influence the initiation of punching shear failures and the propagation of progressive collapse of flat plate structures. They also examined four proposed methods to prevent progressive collapse. These methods include the design with higher live loads, the provision of integral beam stirrup reinforcement, the provision of continuous bottom reinforcement, and the provision of a tensile membrane action developed in the slab by providing proper anchorage of rebar into supports. The design with higher live loads is uneconomic and impractical as it will increase the slab thickness and be unable to prevent progressive collapse. The adoption of integral beam stirrup reinforcement can develop effective shear strength at the connection but the stirrup placement problem renders this method undesirable in construction practice.

In their slab-column tests with slabs having continuous reinforcement through the columns, Hawkins and Mitchell (1979) discovered that bottom reinforcement was much more effective in transferring residual shear to the support after punching shear failure than top reinforcement did, as the top reinforcement tended to tear out from the slab and lose load carrying capacity (Figure 1-1 and Figure 1-2). They concluded that continuous bottom reinforcement through a column or properly anchored into support is an effective and economic method to prevent progressive collapse, and the post-punching shear strength V was estimated to be:

$$V = 0.5A_s' f_y \tag{1.1}$$

where:

A_s' = total area of bottom reinforcement passing through the column or column capital.

f_y = specified yield strength of reinforcement.

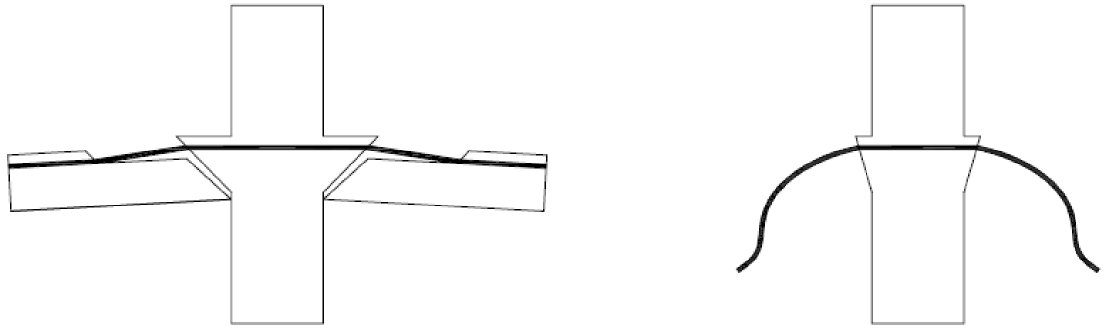

(a) (b)

Figure 1-1: Slab-column connection with only continuous top reinforcement: (a) top steel rips out from concrete cover after punching shear failure; (b) collapse of slab following ineffective support from top steel (Hawkins and Mitchell, 1979; Mitchell and Cook, 1984)

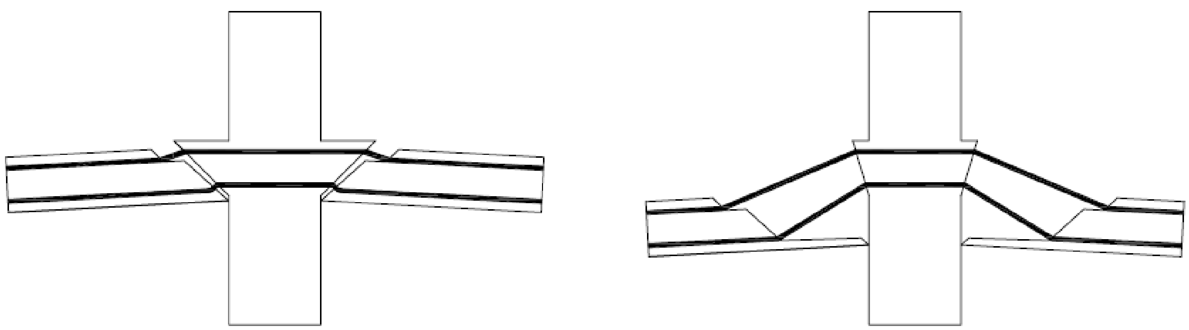

(a) (b)

Figure 1-2: Slab-column connection with continuous top and bottom reinforcement: (a) top and bottom steel supporting the slab after initial punching shear failure; (b) bottom structural integrity reinforcement supporting the slab after top steel become ineffective (Hawkins and Mitchell, 1979; Mitchell and Cook, 1984)

Mitchell and Cook (1984) discussed the post-failure behaviour of a two-way slab structure in the regions of edge and corner panels. They speculated that an overloaded edge panel will form a one-way membrane supported by one-way catenaries which are perpendicular to the free edge and hung from adjacent columns; an overloaded corner panel will result in slab folding and a one-way catenary forming diagonally across the slab supported by adjacent edge panels (Figure 1-3).

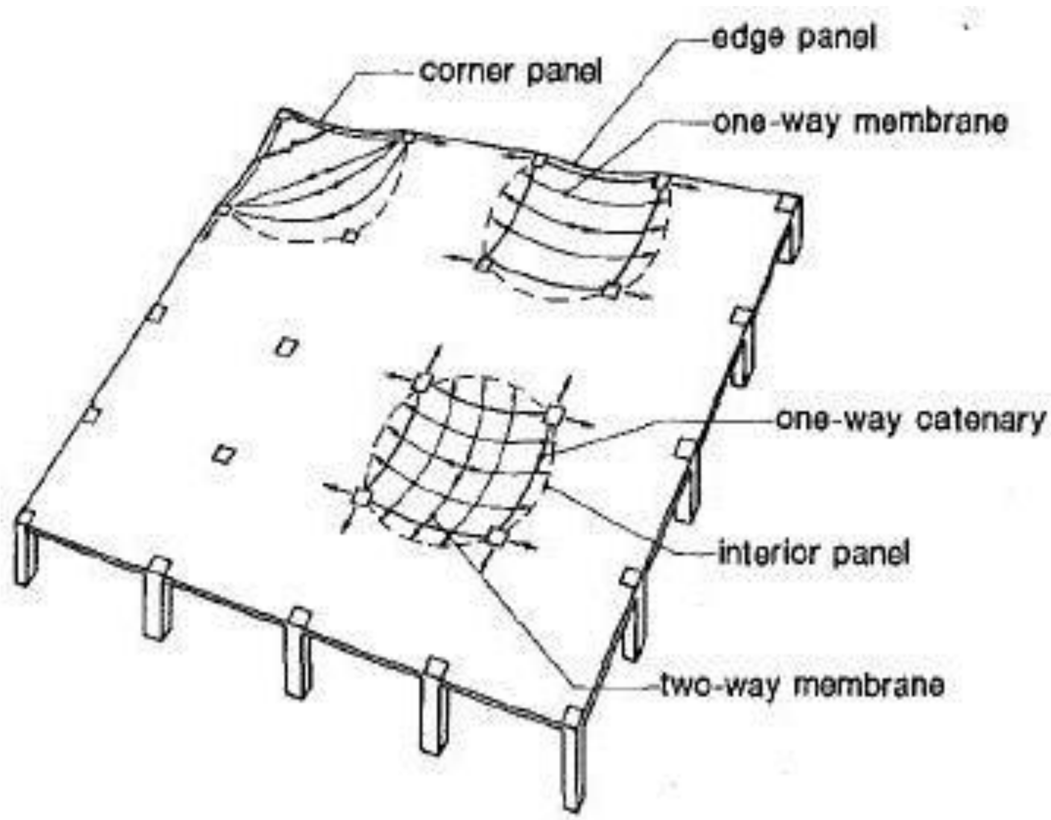

Figure 1-3: Development of "hanging nets" in panels of two-way slab structures (Mitchell and Cook, 1984)

To determine the minimum amount of horizontal restraint, namely the structural integrity reinforcement, required to provide sufficient post-failure resistance, Mitchell and Cook (1984) carried out tests on a one-quarter scale two-way slab structure with improved detailing of bottom reinforcement well-anchored into the columns in addition to the reinforcement required by the ACI Code 318-77 (ACI 318 Committee, 1977). The test result indicated that, by hanging the slab from the column after punching shear failure, the continuous bottom reinforcement was able to provide effective secondary load resisting mechanism to the structure. They proposed the equation to calculate the required area of continuous bottom steel as:

$$A_{sb} = \frac{0.5 w_s l_n l_2}{\phi f_y} \tag{1.2}$$

where:

A_{sb} = minimum area of effective continuous bottom steel in the direction of l_n.

l_n = clear span in the direction considered and measured face-to-face of supports.

w_s = uniform load after initial failure, which is the larger of the existing service load or twice the slab dead load.

l_2 = centre-to-centre distance between two adjacent panels on the two sides of one catenary.

ϕ = capacity reduction factor, 0.9.

f_y = specified yield strength of reinforcement.

The detailing of continuous bottom reinforcement must conform to one of the three specifications: 1) the bottom bars passing through the column are lap spliced over a length of l_d in the support reaction region; 2) the bottom bars passing through the column are lap spliced with other bottom slab bars over a length of $2l_d$ outside of the support reaction region; 3) and the bottom bars are bent, hooked or anchored at discontinuous edges to fully achieve yield stress at the support face.

Mitchell and Cook (1984) concluded that the provision of structural integrity reinforcement capable of developing an effective secondary load resisting mechanism is essential to prevent progressive collapse.

Mitchell (1993) developed a simplified equation for the required amount of structural integrity reinforcement. This equation is based on the theory that after initial punching shear, the structural integrity reinforcement will be inclined at 30 degrees from the horizontal and be capable of developing the yield strength. Instead of calculating the area of steel in each span direction, this equation calculates ΣA_{sb}, the minimum cumulative area of structural integrity reinforcing bars around the column faces connecting to the slab to the column. The required amount of structural integrity reinforcement is given by:

$$\Sigma A_{sb} = \frac{2V_{se}}{\phi f_y} \tag{1.3}$$

where:

V_{se} = total shear around the slab-column connection induced by the larger of specific loads or twice the dead load of the slab.

ϕ = capacity reduction factor, 0.9.

f_y = specified yield strength of reinforcement.

This equation was adopted in the 1994 CSA A23.3 Standard (CSA, 1994). In the 2004 edition of the CSA A23.3 Standard, the capacity reduction factor has been modified to 1 (CSA, 2004). Thus, the equation was further simplified as:

$$\Sigma A_{sb} = \frac{2V_{se}}{f_y} \tag{1.4}$$

Melo and Regan (1998) conducted series of tests to study three assumed failure modes after punching shear failure of interior slab-column connections with the presence of structural integrity reinforcement: 1) ripping out of the bottom reinforcement; 2) rupture of the bottom reinforcing bars; 3) and crushing of the concrete under the structural integrity reinforcing bars in the column. From the results of tests they concluded that the post-punching resistance can be governed either by the first or the second assumption; the crushing of the concrete in the column was unlikely to occur with the structural integrity reinforcement properly embedded through the column reinforcement cage.

In the case that the post-punching resistance was governed by the failure of the concrete surrounding the punching shear zone, their observation suggested that this type of post-punching resistance could be estimated by adopting the breakout resistance of reinforcement in concrete from the ACI code for nuclear safety related structures (ACI Committee 349, 1978):

$$P_u = 0.33\sqrt{f_c'}A_{ch} \tag{1.5}$$

where:

P_u = ultimate post-punching resistance.

$0.33\sqrt{f_c'}$ = average concrete tensile strength.

A_{ch} = horizontal projection of the 45 degree failure section of the steel bar.

In the second series of tests where the post-punching resistance was governed by the ultimate strength of the structural integrity reinforcement, Melo and Regan (1998) observed the ratio of $P_u /(\Sigma A_s f_u)$ was approximately 0.44. This implies that the bottom reinforcement was inclined by an angle of 26.1 degrees from the horizontal. Therefore, the equation of this type of post-punching resistance was derived as:

$$P_u = 0.44\Sigma A_s f_u \tag{1.6}$$

where:

ΣA_s = total area of structural integrity reinforcement around slab-column connection.

f_u = ultimate strength of reinforcement.

If only the yield stress was known, Melo and Regan suggested that $1.15f_y$ could be used as replacement of f_u. Hence, the equation can be rewritten as:

$$P_u = 0.5\Sigma A_s f_y \tag{1.7}$$

which is the same as the equation used in CSA A23.3-04 standard (CSA 2004).

In 2012, Habibi et al. (2012) verified the post-punching strength of slab-column connections detailed in accordance with CSA A23.3-04. Seven isolated interior connection specimens were tested to study four factors which might influence the effectiveness of structural integrity reinforcement, including: 1) the thickness of slab; 2) the length of structural integrity reinforcement; 3) the rectangularity of the slab-column connection; 4) and the effect of placing structural integrity reinforcement into the bottom of drop panels.

From the test results Habibi et al. (2012) concluded that the predicted capacities using the CSA A23.3-04 Standard expressions were conservative for both punching shear resistance and post-punching shear resistance. It was also concluded that: 1) the increase of slab thickness improves the breakout resistance of concrete above structural integrity reinforcement to the extent that the steel can yield, exhibiting strains well into the strain-hardening range; 2) the increase of structural integrity reinforcement length results in a slight improvement of the post-punching resistance but resulting in an additional 28% of ultimate post-punching deflection than specimens without the modification; 3) the column rectangularity and the structural integrity reinforcement arrangement play no significant effect on the post-punching resistance; 4) and the structural integrity reinforcing bars placed in the bottom of drop panel are effective in providing the post-punching resistance.

1.3 Design Provisions

1.3.1 2004 CSA A23.3 Standard and 2014 CSA A23.3 Standard

1.3.1.1 Punching Shear Stress Resistance

In Clause 13.3.4 of CSA A23.3-04, the standard states that for flat plate slabs without shear reinforcement, the slab maximum shear stress, v_r, is the smallest of the three equations Eq. 1.8, 1.9 and 1.10, where Eq. 1.9 accounts for the rectangularity of the column with β_c and Eq. 1.10 accounts for the location of the column, i.e. interior, edge and corner (CSA, 2004).

$$v_r = \left(1 + \frac{2}{\beta_c}\right) 0.19 \lambda \phi_c \sqrt{f_c'} \tag{1.8}$$

$$v_r = \left(\frac{\alpha_s d}{b_0} + 0.19\right) \lambda \phi_c \sqrt{f_c'} \tag{1.9}$$

$$v_r = 0.38\lambda\phi_c\sqrt{f_c'} \tag{1.10}$$

$$v_n = 0.33\lambda\sqrt{f_c'} \tag{1.11}$$

where:

β_c = ratio of long side to short side of the concentrate load or reaction area.

α_s = factor used to adjust for connection locations: 4 for interior connection, 3 for edge connection, and 2 for corner connection.

d = distance from extreme compression fibre to centroid of longitudinal tension reinforcement.

b_0 = perimeter of critical section.

λ = factor to account for low-density concrete.

ϕ_c = resistance factor for concrete.

The coefficient in Eq. 1.11 is reduced from 0.38 to 0.33 to give the nominal punching shear resistance and the material resistance factor for concrete, ϕ_c, is taken as 1.0. Similarly, the factors 0.19 in Eq. 1.8 and 1.9 are adjusted to 0.17 and ϕ_c is taken as 1.0 in order to obtain the nominal resistance.

1.3.1.2 Factored Shear Stress at Critical Section

Clause 13.3.5 of CSA A23.3-04 states that the estimation of the factored shear stress at a slab-column connection should account for both the shear stress due to the factored shear V_f, and the shear stress due to the unbalanced moment M_f transferred by the eccentricity of shear (CSA, 2004).

$$v_f = \frac{V_f}{b_0 d} + \left(\frac{\gamma_v M_f e}{J}\right)_x + \left(\frac{\gamma_v M_f e}{J}\right)_y \tag{1.12}$$

$$\gamma_v = 1 - \frac{1}{1 + \frac{2}{3}\sqrt{\frac{b_1}{b_2}}} \tag{1.13}$$

where:

γ_v = fraction of the unbalanced moment transferred by the eccentricity of shear at the connection.

e = distance from centroid of section for critical shear to point where shear stress is being calculated.

b_1 = width of the critical section for shear measured in the direction of the span for which moments are determined.

b_2 = width of the critical section for shear measured in the direction perpendicular to b_1.

J = property of the critical section for shear analogous to the polar moment of inertia.

1.3.1.3 One-Way Shear Stress for Corner Slab-Column Connections

Clause 13.3.6.2 of CSA A23.3-04 also specifies an equation (Eq. 1.14) to calculate, for corner slab-column connections, the one-way shear stress v_c along the critical shear section located not farther than *d/2* from the edge of the column or column capital (CSA, 2004).

.

$$v_c = \beta\lambda\phi_c\sqrt{f_c'} \tag{1.14}$$

where:

β = factor accounting for shear resistance of cracked concrete, specified in Clause 11.3.6.2 and 11.3.6.3.

1.3.1.4 Structural Integrity Reinforcement

The 2004 CSA A23.3 Standard (CSA, 2004) was updated with the simplified equation developed by Mitchell (1993) to calculate the required amount of the structural integrity reinforcement in a slab-column connection. In Clause 13.10.6, the Standard states that the minimum total area of bottom reinforcement, ΣA_s, connecting the slab, drop panel or slab band to column or column capital on all faces of the periphery of the column or column capital should be calculated as:

$$\Sigma A_{sb} = \frac{2V_{se}}{f_y} \tag{1.15}$$

where:

V_{se} = total shear around the slab-column connection induced by the larger of the shear corresponding to the specified loading or twice the self-weight of the slab.

f_y = specified yield strength of reinforcement.

The structural integrity reinforcement must consist of at least two bars or two tendons in each direction through the column or column capital, and must satisfy one or more of the listed requirement for reinforcement continuity (Figure 1-4): a) using Class A tension lap splice over a column or column capital; b) using additional bottom reinforcement passing over a column or column capital which has $2l_d$ overlaps with bottom reinforcement of adjacent spans; c) at discontinuous edges, using extended bottom reinforcement that is bent, hooked, or otherwise anchored over the column or column capital to develop yield stress.

The 2014 CSA A23.3 Standard (CSA, 2014) has the same requirements as the 2004 CSA A23.3 Standard except that for the design of the amount of structural integrity reinforcement required the term, V_{se}, is taken as the shear transmitted to the column due to specified loads without consideration of construction loading (i.e., twice the self-weight of the slab).

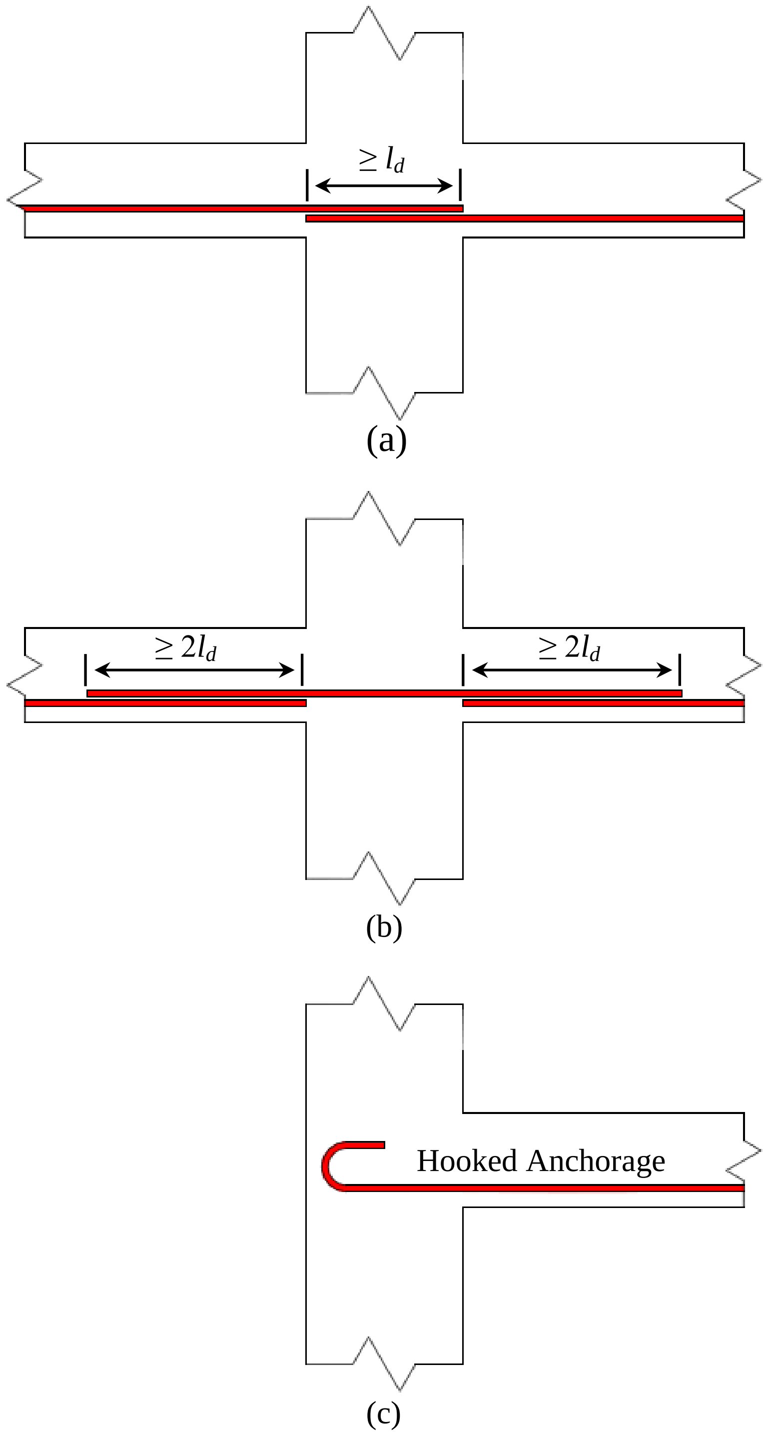

Figure 1-4: Requirement of continuity for structural integrity reinforcement: (a) Class A tension lap splice over the support; (b) $2l_d$ splice outside the support; (c) bent reinforcement anchored over the support

1.3.2 ACI 318M-11

The requirement of the structural integrity reinforcement for nonprestressed two-way slab construction is explained in Clause 13.3.8.5 of the ACI standard. This code requires that bottom reinforcement within the column strip in each direction must maintain continuity by using Class B tension splices, or using mechanical or welded splices which can develop strength at least $1.25f_y$ of the reinforcement, in either tension or compression. At exterior supports, the bottom reinforcement must be anchored such that the yield stress can be developed at the face of the support. The ACI Code also requires that there should be a minimum amount of two bottom bars passing through the region bounded by the longitudinal reinforcement of the column or column capital in each direction (ACI 318 Committee, 2011).

1.4 Experiment Objectives

Previous study has found that the structural integrity reinforcement required by the CSA A23.3-04 standard could provide considerable post-punching shear strength for interior slab-column connections in a flat plate structure (Habibi et al., 2012). However, experimental data are still lacking on whether the code requirement can provide satisfactory post-punching strength for exterior edge and corner slab-column connections.

Although the edge and corner slab-column connections share less tributary loads in a structure, they are eccentrically loaded and have less structural integrity reinforcement placed across the connection. It is also of interest to study the sequence of punching shear failures and post-punching failure load redistribution through the interaction of a group of exterior connections. This thesis investigates the sequence of punching shear failures and examines the post-punching shear behaviour of structural integrity reinforcing bars in a system of corner and edge slab-column connections that have been designed in accordance with the 2014 CSA A23.3 Standard.

1.5 Overview of Thesis

Chapter 1 provides the introduction to the research program, summary of previous research on the phenomenon of punching shear failure of flat plate structure, progress on the development of preventing the failure, and review of code provisions for punching shear resistance and the details of structural integrity reinforcement in the 2014 CSA Standard and in the 2011 ACI Code.

Chapter 2 explains the experimental program, including the dimensions of the slab structure, the details of reinforcement, material properties, the test setup, instrumentation and the test procedure.

Chapter 3 reports the overall response of the slab structure, as well as the post-punching response of individual slab-column connections.

Chapter 4 contains an analysis of the experimental results, including the punching shear and post-punching shear performance of individual slab-column connections, as well as the overall performance of the slab structure. The results are compared to the predictions by the 2014 CSA A23.3 Standard.

Chapter 5 provides conclusions based on the result of the test program and analysis that were carried out.

2. EXPERIMENTAL PROGRAM

2.1 Introduction

The goal of this experiment was to study the post-punching shear resistance of corner and edge slab-column connections detailed in accordance with the 2014 CSA A23.3 design standard, as well as to investigate the failure sequence and load redistribution after initial punching failure while these exterior columns and slab interact as a whole system. A full-scale slab structure with four corner columns and two edge columns was constructed and tested in the Jamieson Structures Laboratory at McGill University. The design and detailing of the concrete reinforcement and structural integrity reinforcing bars strictly followed the provision contained in CSA A23.3-14 (CSA, 2014).

2.2 Prototype Structure

The full-scale slab structure was designed to represent a typical building floor in accordance with the CSA A23.3 Standard and the ACI Code (ACI 318 Committee, 2011). The components of the structure included two continuous bays of 3.0 × 3.0 m, supported by six square exterior columns of 250 × 250 mm with column stubs extended 350 mm above the slab surface. The slab thickness was 150 mm. A superimposed dead load of 1.5 kPa and a live load of 10.0 kPa were considered in the design along with load factors of 1.25 and 1.5, for dead load and live load, respectively. The minimum required concrete compressive strength of 35 MPa and reinforcing bar yield strength of 400 MPa were assumed in the design of the slab structure. The slab structure was designed in accordance with the equivalent frame method of the 2014 CSA Standard A23.3. The relatively small columns, thin slab and an excess of flexural reinforcement resulted in shear being critical at the edge and corner columns. The slab-column connections were designed for combined direct shear as well as transfer of moments from the slab to the columns. The factored shear stress resistance was taken as $0.65\phi_c\sqrt{f_c'} = 0.65 \times 0.38\sqrt{35} = 1.46\ MPa$. The nominal shear stress resistance was taken as $0.33\sqrt{f_c'} = 0.33\sqrt{43} = 2.16\ MPa$. A summary of the resulting overall factored and service load, carried out in accordance with the CSA A23.3-14 Standard, is given below:

Minimum slab thickness (Clause 13.2):

$$h_s \geq 120\ mm$$

$$l_n = 3000 - 250 = 2750\ mm = 2.75\ m$$

$$h_s \geq \frac{l_n(0.6 + f_y/1000)}{30} = \frac{2750 \times (0.6 + 400/1000)}{30} = 91.6\ mm$$

Self-weight of the concrete slab:

$$w_{DL-self} = 24 \times 0.15 = 3.6\ kPa$$

Design factored load:

$$w_f = 1.25 \times (3.6 + 1.5) + 1.5 \times 10 = 21.4\ kPa$$

Total factored load:

$$V_{f-total} = 21.4 \times (3 + 3 + 0.25) \times (3 + 0.25) = 434.7\ kN$$

Total service load:

$$V_{se} = (3.6 + 1.5 + 10) \times (3 + 3 + 0.25) \times (3 + 0.25) = 306.7\ kN$$

Corresponding nominal resistance:

$$V_n = \frac{2.16}{1.46} \times V_{f-total} = 643.1\ kN$$

2.3 Description of the Slab Structure

2.3.1 Slab Structure Overview

The slab was designed with 25 mm cover and 150 mm thickness. It was support by four corner columns: NW, NE, SW and SE, and two edge columns: N and S. The columns were 250 × 250 mm in cross section. The reinforcing bars placed in the N-S direction were the outermost reinforcement as stronger moments were predicted in this direction. The column and the slab were cast monolithically with the same concrete and the concrete was moist cured for 7 days. The plan view and elevation view in two directions of the slab structure are as shown in Figure 2-1, 2-2 and 2-3.

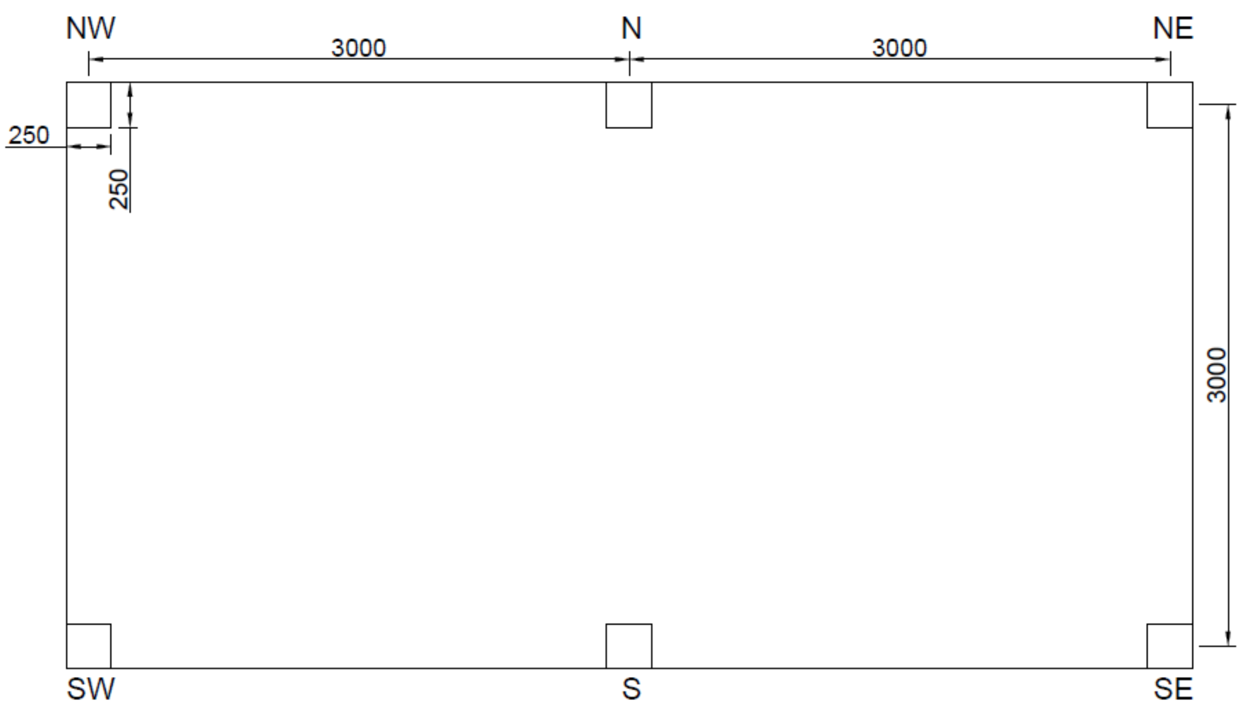

Figure 2-1: Plan view of slab structure (units: mm)

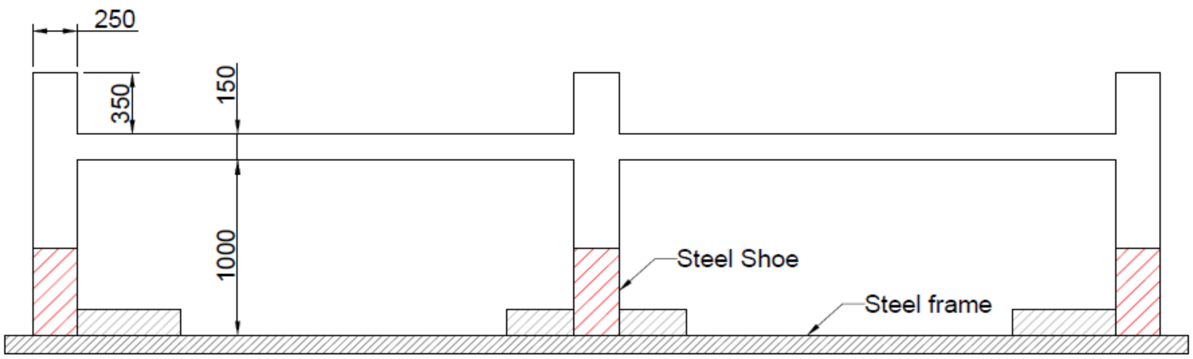

Figure 2-2: E-W elevation view of slab structure (units: mm)

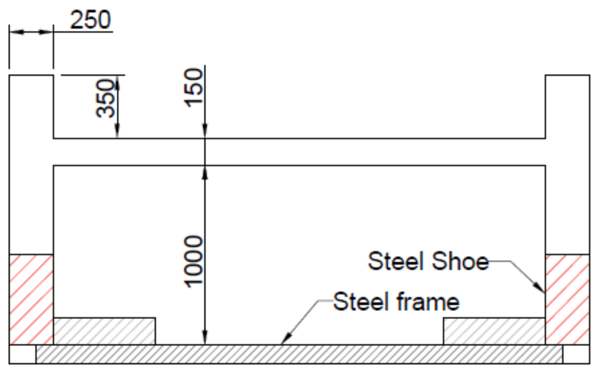

Figure 2-3: N-S elevation view of slab structure (units: mm)

2.3.2 Details of Slab Top Flexural Reinforcement

The top reinforcement was designed to provide sufficient moment resistance in the negative moment region. The outermost reinforcing bars were placed in the N-S direction. In the N-S direction, 4-15M top bars were anchored with hooks in each column and extended into the slab, while 8-10M bars were placed at 320 mm spacing in the slab between the columns, as shown in Figure 2-4. The anchorage details for the top reinforcement at the column locations are shown in Figure 2-4(b). Due to larger moments occurring at the edge columns, two additional 15M bars were placed in the slab perpendicular to the free edge and located close to the edge column faces.

In the E-W, innermost layer, direction, 3-15M hooked bars were anchored in the four corner columns and extended into the slab, while 9-10M bars were placed at 300 mm spacing in between the corner columns; 15M bars at a spacing of 100 mm were placed in the column strip of the two edge columns, as shown in Figure 2-5.

The 825 mm extension satisfied the $0.3l_n$ curtailment required by the CSA A23.3-14 (CSA, 2014), where the clear span l_n is 2750 mm. The 90 degree hook dimension satisfied the $12d_b$ specification required by the ACI standard (ACI 318 Committee 2011).

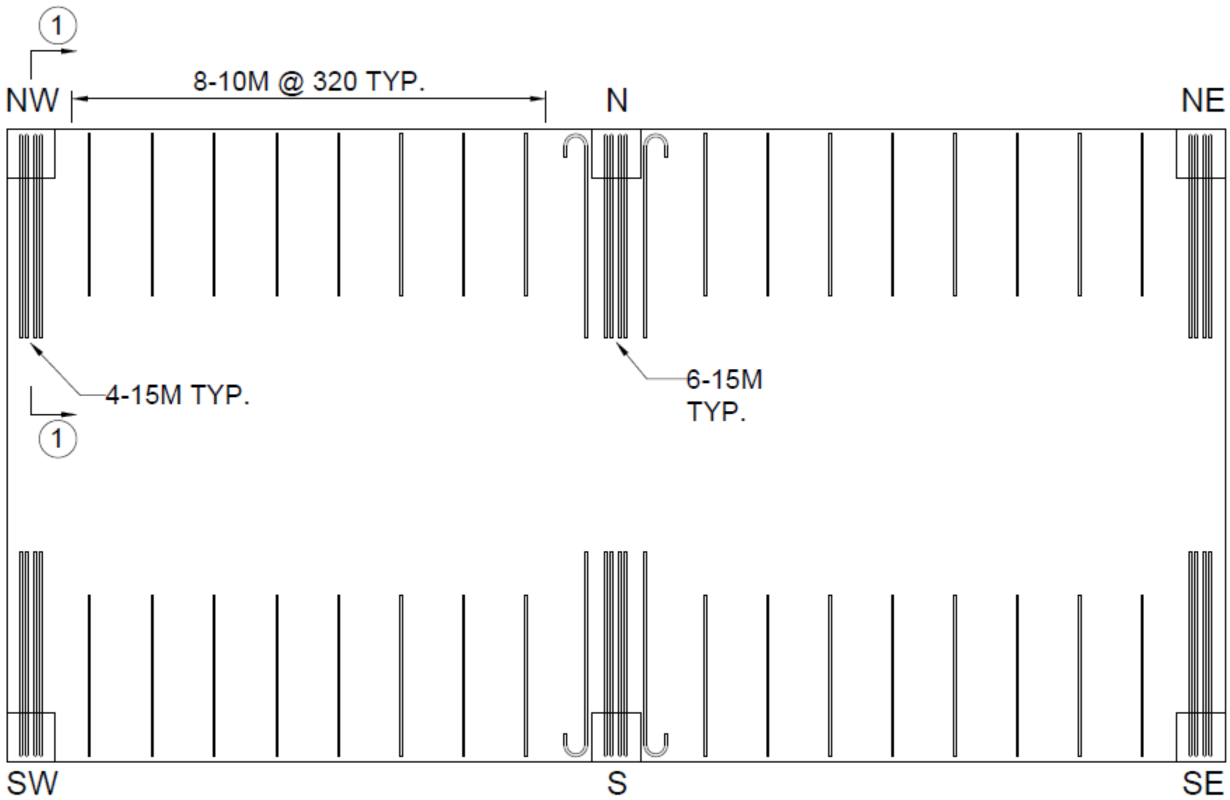

(a)

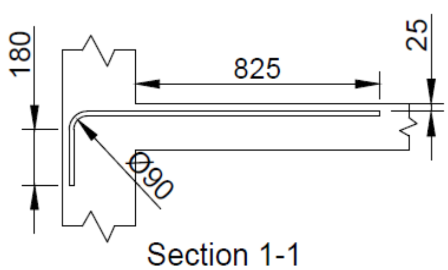

(b)

Figure 2-4: (a) Top reinforcement layout – N-S direction (outermost reinforcement direction); (b) Section 1-1: Embedment of top reinforcement in column (units: mm)

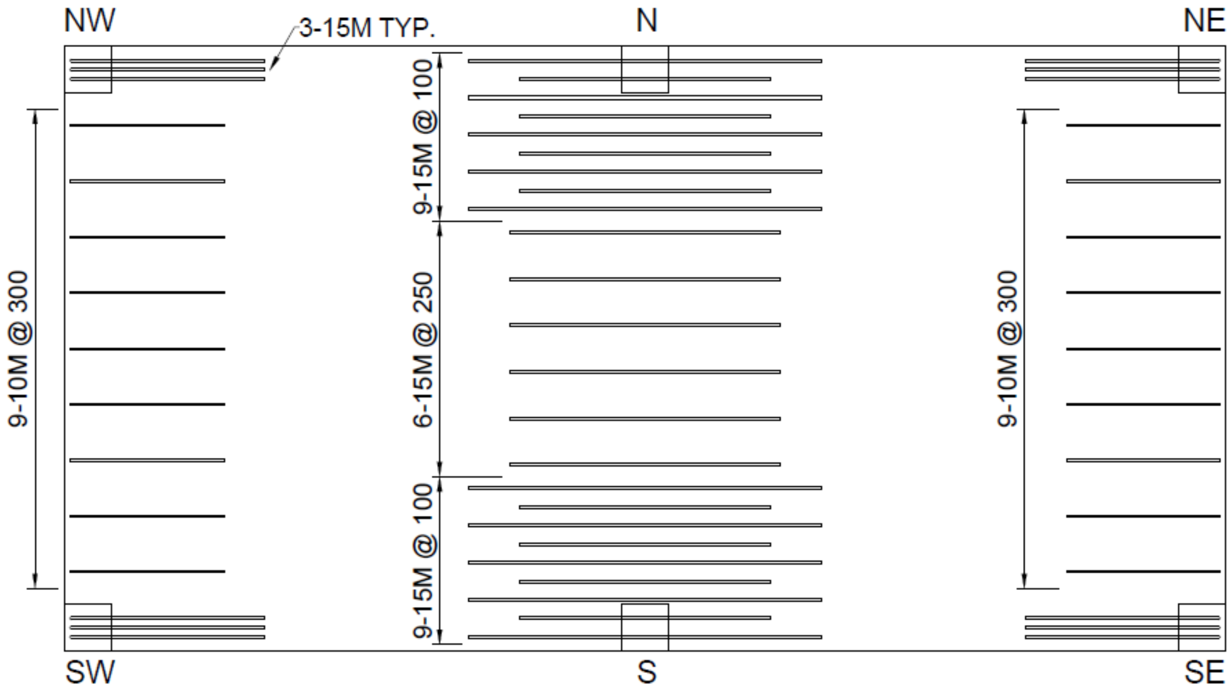

Figure 2-5: Top reinforcement layout – E-W direction (innermost reinforcement direction, units: mm)

2.3.3 Details of Slab Bottom Flexural Reinforcement

In the N-S, outermost layer direction, 7-10M bars with spacing of 120 mm were placed in the two half edge column strips; 10M bars spaced at 100 mm are placed in the central column strip and 10M bars with spacing of 150 mm were placed in the middle strips, as shown in Figure 2-6. In the E-W, innermost layer direction, 10M bars spaced at 100 mm were placed in the two edge half column strips and 10M bars spaced at 160 mm were placed in the middle strips, as shown in Figure 2-7.

It was noted that care was taken to curtail the bottom reinforcing bars that were directly in line with the columns right at the column faces so that they would not contribute to the post-punching shear resistance.

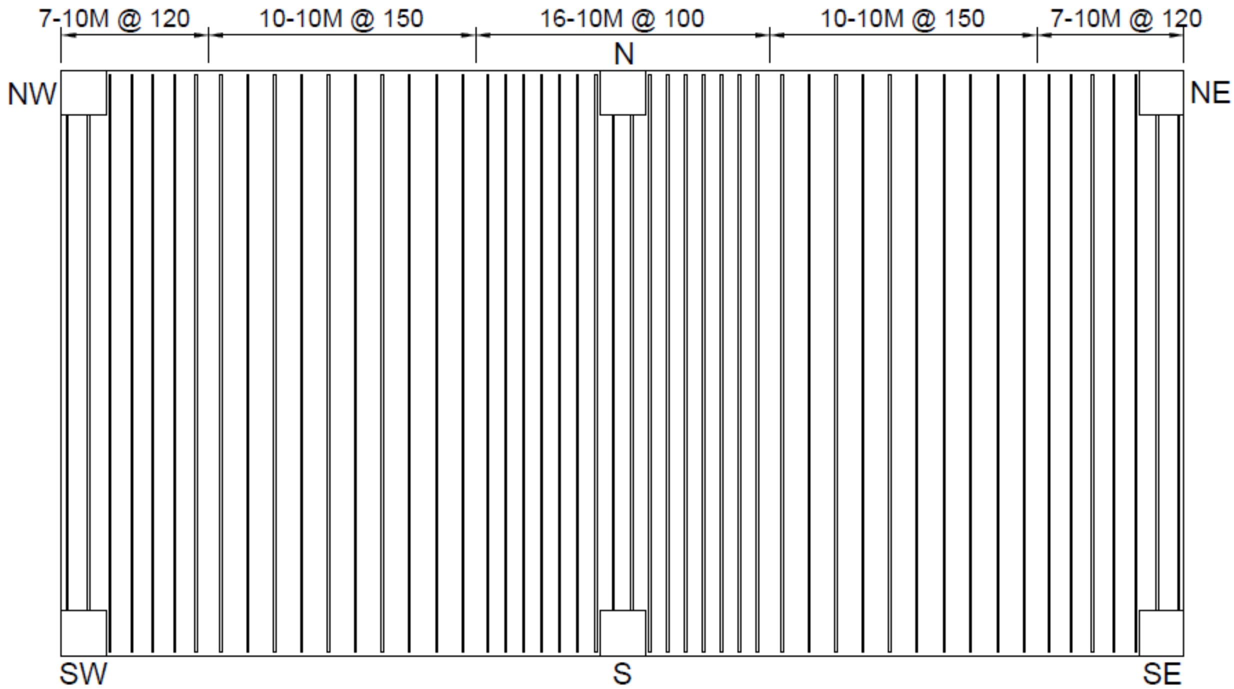

Figure 2-6: Bottom reinforcement layout – N-S direction (outermost reinforcement direction, units: mm)

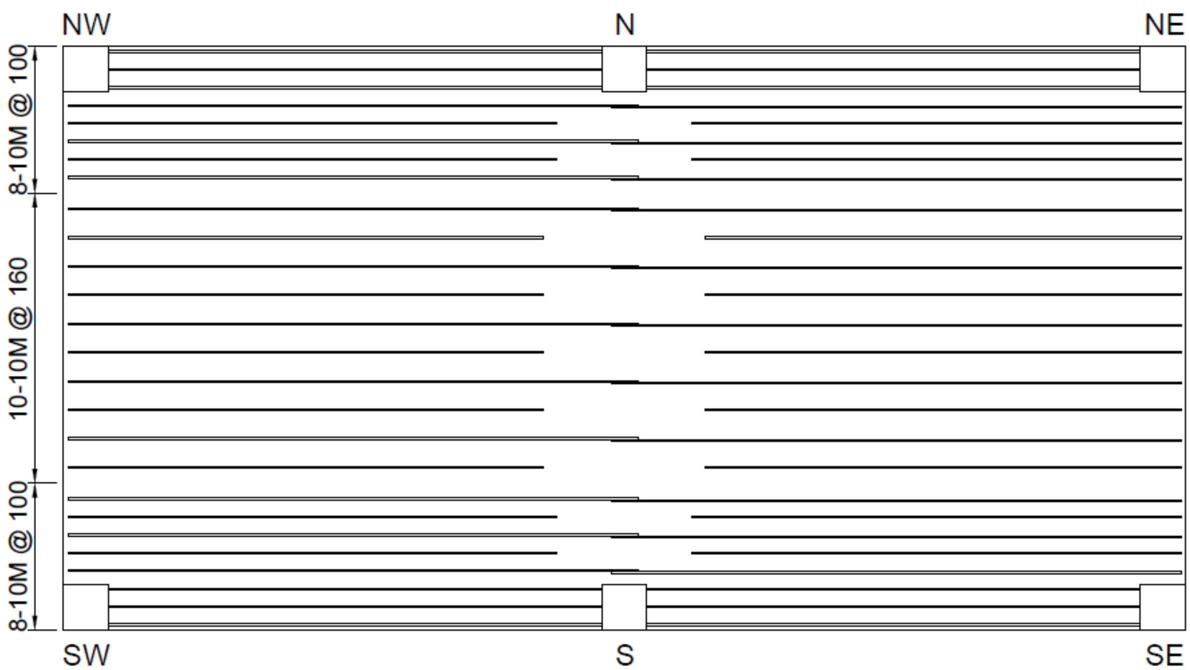

Figure 2-7: Bottom reinforcement layout – E-W direction (innermost reinforcement direction, units: mm)

2.3.4 Details of Structural Integrity Reinforcement

The 2014 CSA A23.3 Standard specified that, for the structural integrity reinforcement design, a minimum amount of two bars or two tendons must be provided through a column core or column capital region in each span direction. In a corner slab-column connection, the minimum of 2-10M structural integrity reinforcement extended out of the two interior column faces could offer a predicted post-punching shear strength of $V_{se} = 0.5\Sigma A_{sb} f_y = 0.5 \times 4 \times 100 \times 400/1000 = 80\ kN$. The edge slab-column connection had double the tributary area as the corner slab-column connection did. Therefore, it was designed to provide a post-punching shear strength of 160 kN which was twice the amount as the corner slab-column connection provides.

Structural integrity reinforcement was placed at the same level as the bottom reinforcement. On each side of the corner columns, as well as on the N-S direction of the edge columns, 2-10M bars, anchored with hooks, were embedded into the columns and extended 600 mm out of the column faces. In the E-W direction, continuous 3-10M bars were placed parallel to the free edge and through the edge columns and extended 600 mm out of two sides of the column faces, as shown in Figure 2-8.

The 600 mm extension satisfied the $2l_d$ overlap of the structural integrity reinforcement with the bottom reinforcement required by the CSA A23.3-14 Standard (CSA, 2014), where the tension development length, l_d, for a 10M bar was 300 mm. The 90 degree hook dimension satisfied the $12d_b$ specification required by the ACI standard (ACI 318 Committee, 2011).

It was noted that the amount of the structural integrity reinforcing bars provided was somewhat larger than that required to resist the service loading on the slab. The total service load acting on the slab from the design was 306.7 kN. The total post-punching resistance from the two edge columns (160 kN each) and the four corner columns (80 kN each) was 640 kN.

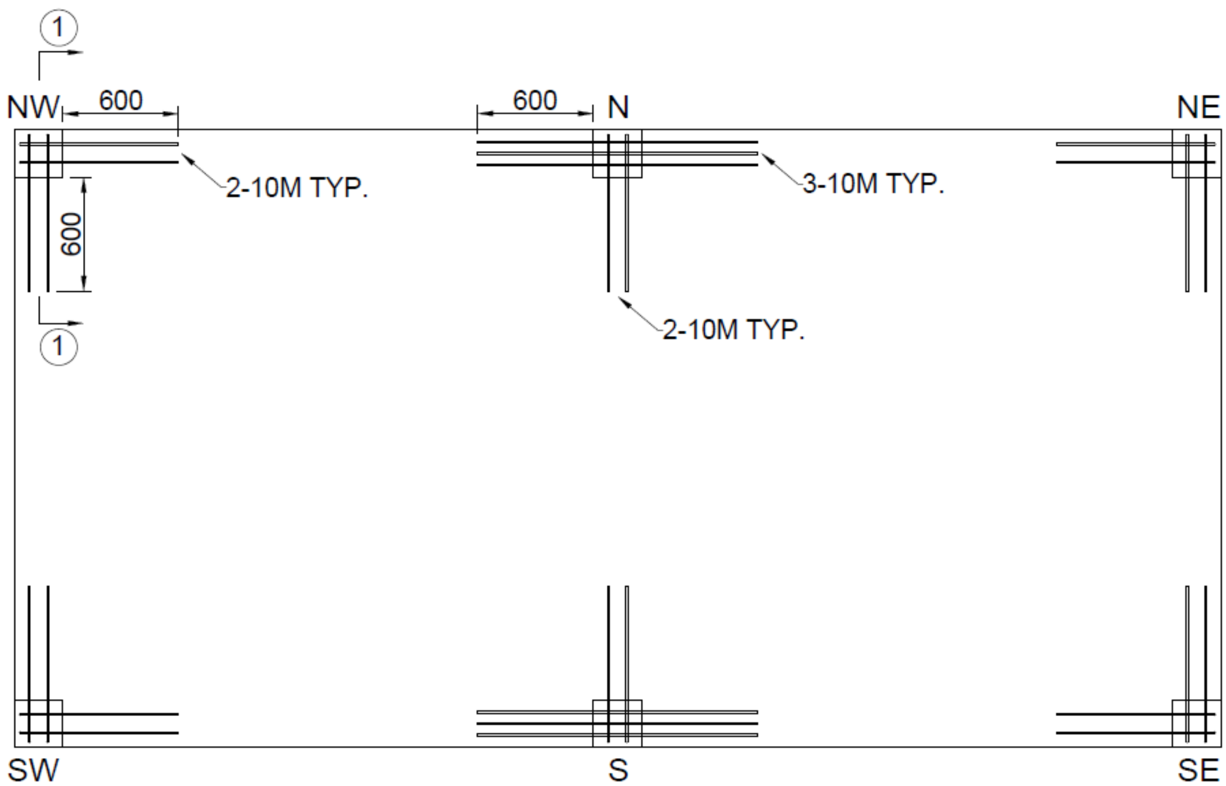

(a)

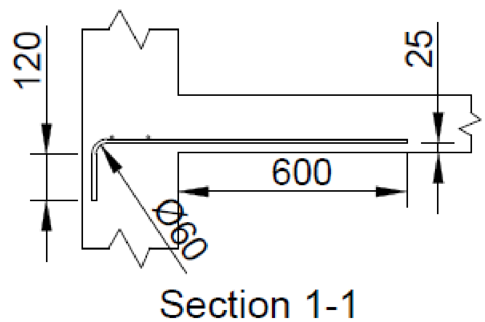

(b)

Figure 2-8: (a) Structural integrity reinforcement layout; (b) Section 1-1: Embedment of structural integrity reinforcement in column (units: mm)

2.3.5 Details of Columns

The slab structure simulated a typical building floor support by the columns. Because the slab was designed to be shear critical, relatively small columns were used to reduce the punching shear periphery. The 250 × 250 mm concrete square columns extended 1000 mm below the slab and 350 mm above the slab to provide sufficient development length for the vertical column reinforcement.

The following design details were applied to the columns to enhance their resistance against the maximum moment expected to occur before and after punching shear failure: 1) 15M reinforcing bars were used; 2) the column cover was reduced to 15 mm; 3) 500 mm high HSS 254×254×12.7 shoes at the bottom of corner columns and HSS 254×254×6.4 shoes at the bottom of edge columns; 4) and the steel shoes were welded to a steel frame at the bases of the columns. The welded steel shoes provided fixity at the column bases.

The column reinforcement details are shown in Figure 2-9 and the construction of the steel frame and welded HSS shoe details are shown in Figure 2-10.

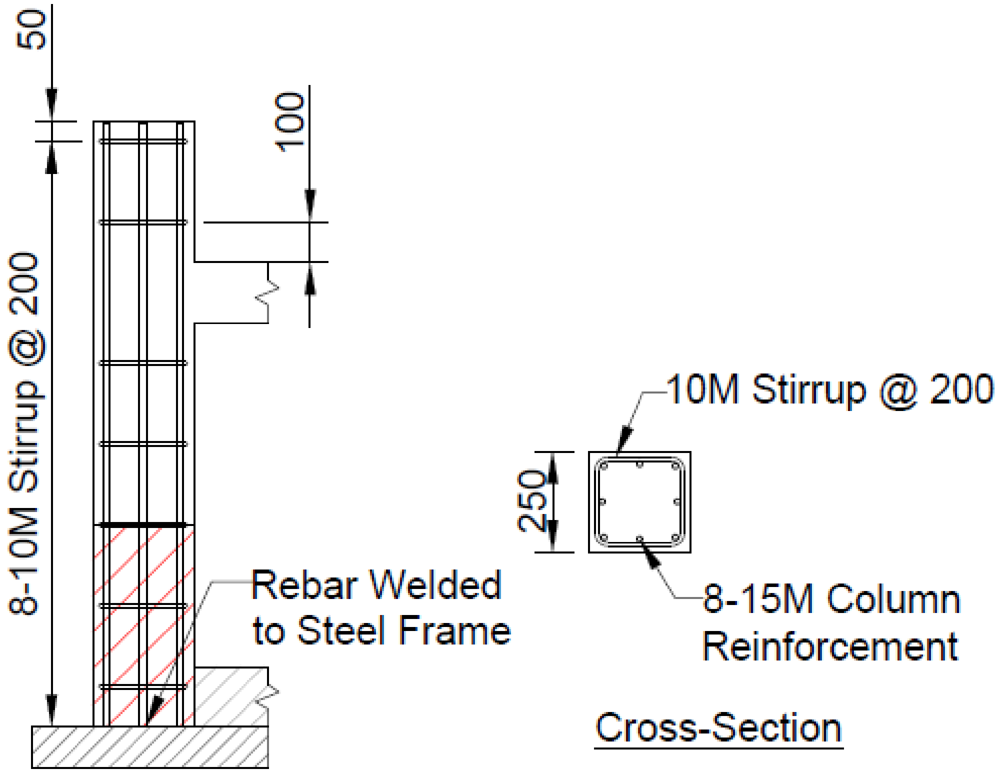

Figure 2-9: Elevation and cross-section view of column reinforcement

(a)

(b)

(c)

Figure 2-10: (a) Steel frame base; (b) Welding column reinforcement to the steel frame; (c) Welding HSS steel shoes to the steel frame

2.4 Material Properties

2.4.1 Reinforcing Steel

The 10M and 15M hot-rolled, weldable and deformed reinforcing steel bars used in the construction of the slab structure had a minimum yield stress of 400 MPa (CSA G30.18, 1992). Three randomly chosen test coupons of each group of 10M and 15M bars were tested in accordance with ASTM A370 standard (ASTM, 2014).

The mean values obtained from the test, including yield strength, ultimate strength, yield strain, strain at strain hardening and ultimate strain are given in Table 2-1. The typical stress-strain response of the reinforcing steel bars of each size are plotted in Figure 2-11.

Table 2-1: Reinforcing steel properties

Bar Size	Area (mm^2)	f_y (MPa)	f_u (MPa)	ε_y	ε_{sh}	ε_u
10M	100	451.9	645.1	0.00226	0.01307	0.118
15M	200	452.0	642.0	0.00226	0.00959	0.129

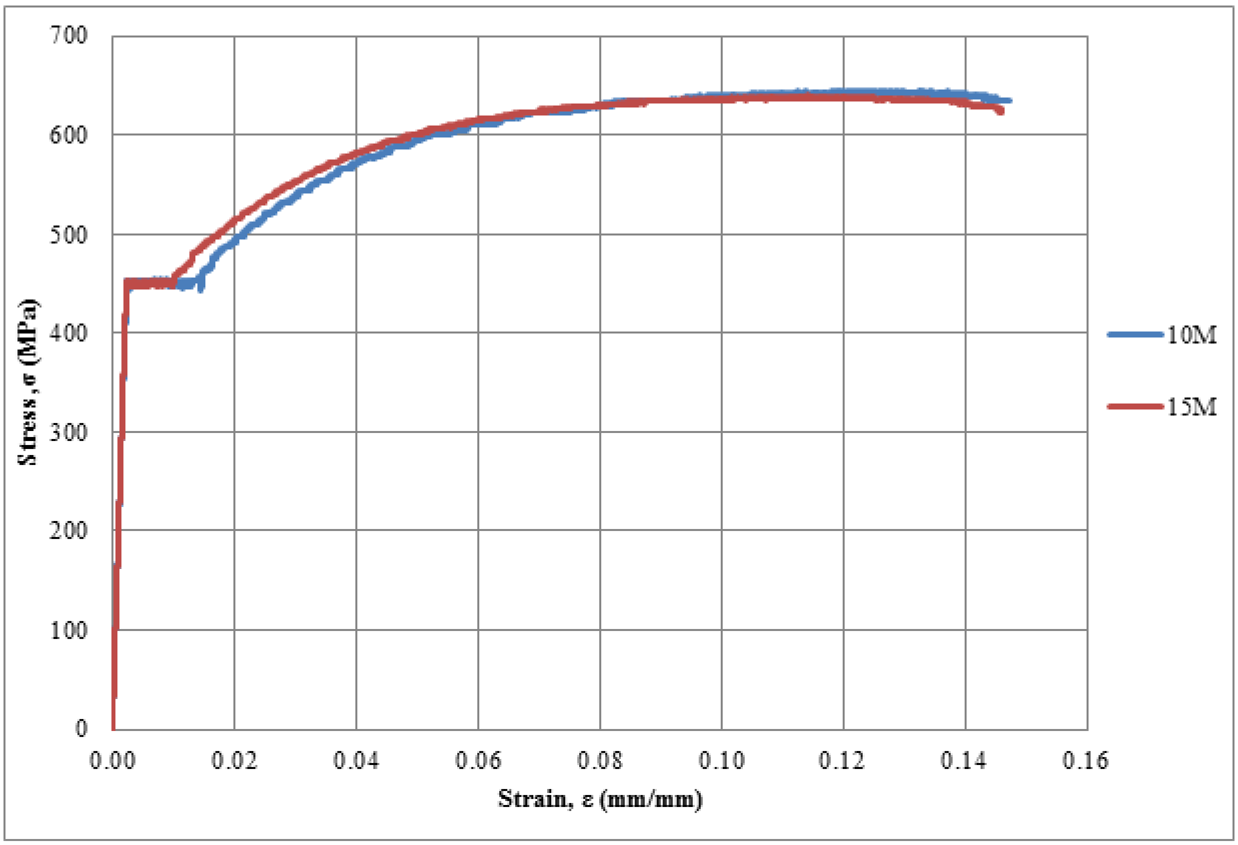

Figure 2-11: Typical stress-strain curve of reinforcing steel

2.4.2 Concrete

Normal density ready-mix concrete with a specified 28-day compressive strength of 35 MPa was ordered in one batch from a local supplier and used for the construction of the slab structure. Standard concrete cylinders of 100 mm in diameter and 200 mm in height and standard concrete flexural beams with dimensions of 100 × 100 × 400 mm were prepared on the day of construction for the tests of material properties. All the samples were kept in 100% humidity environment for moist-curing until material tests were conducted.

Three standard concrete cylinders were tested in compression test to determine the concrete compressive strength, f'_c; another group of three standard concrete cylinders were used to determine the splitting-tensile strength, f_{sp}; and three standard concrete beams were tested in four point flexure test to determine the modulus of rupture, f_r. The test results, as well as the mean values calculated for the results, are listed in Table 2-2. A typical concrete compressive stress-strain curve is presented in Figure 2-12.

Table 2-2: Concrete properties

Samples	f'_c (MPa)	f_{sp} (MPa)	f_r (MPa)
1	42.4	4.32	6.33
2	44.9	4.12	6.07
3	41.6	4.02	6.85
Average	43.0	4.15	6.42
Std. Dev.	1.41	0.12	0.33

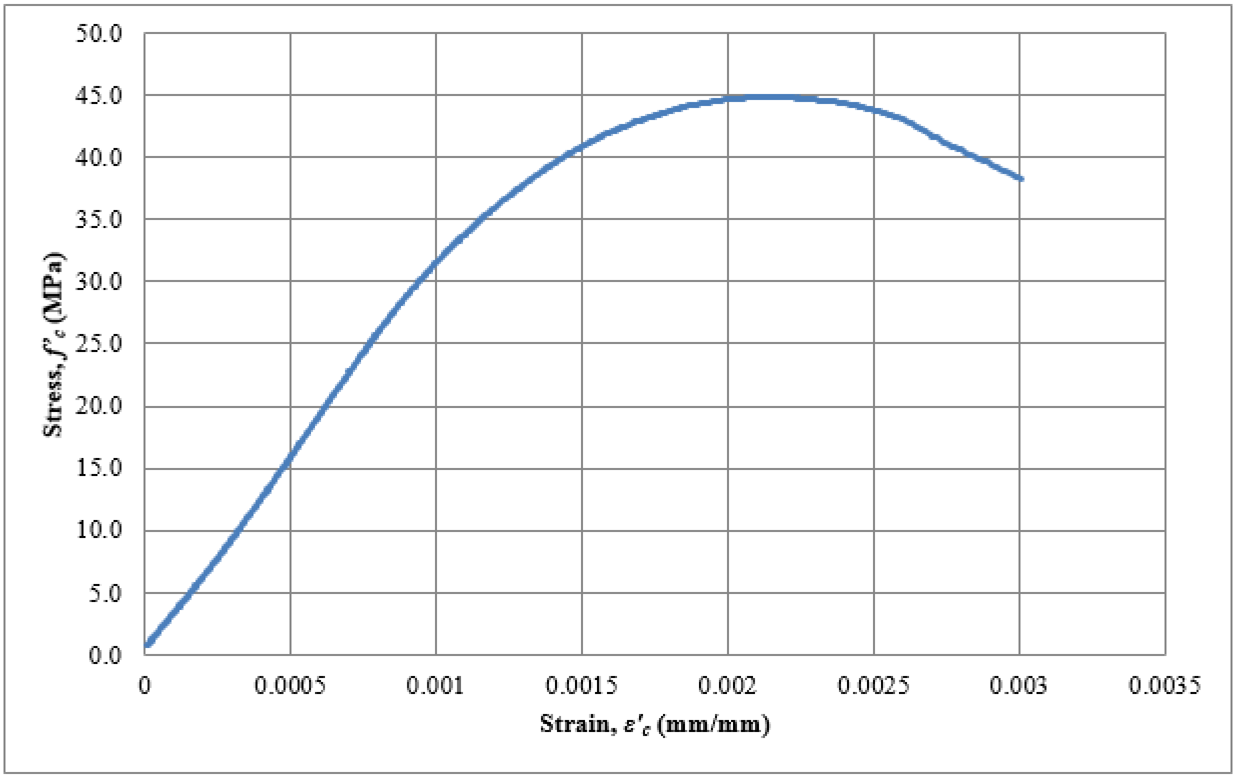

Figure 2-12: Typical compressive stress-strain curve of concrete

2.5 Test Setup

The columns of the slab structure were mounted in steel shoes made from HSS sections which were welded upon the steel frame base, as shown in Figure 2-8. On each bay, loads were applied at four locations at the quarter-points of each slab panel to simulate uniformly distributed load. The layout of the total eight loading points is as shown in Figure 2-13.

A 50 mm diameter hole located at each loading point allowed threaded steel rod to pass through the slab, connecting a circular steel plate installed on top of the slab and a hydraulic jack mounted underneath the strong floor. A manual hydraulic pump was connected to all of the jacks by interconnected hydraulic hoses such that the applied loads would be equal. Load cells were placed at the bottom of each hydraulic jack to monitor the applied loads. The setup of the loading apparatus is shown in Figure 2-14.

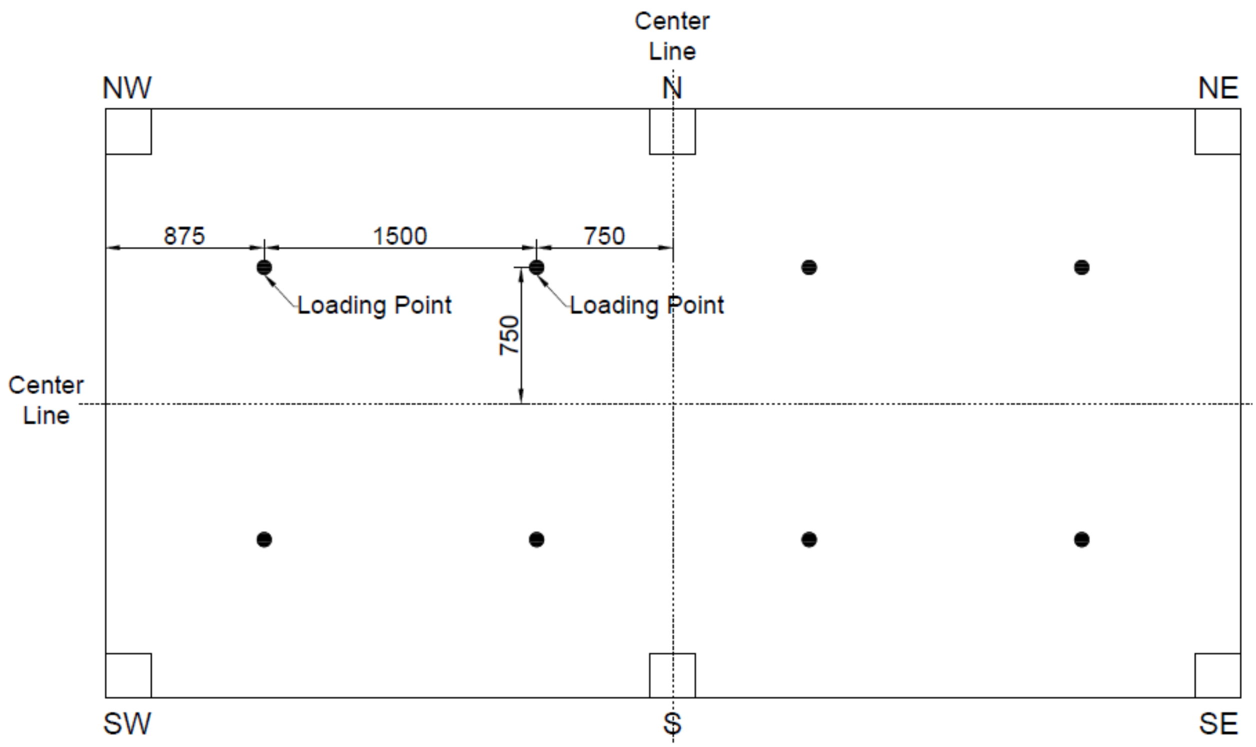

Figure 2-13: Layout of loading points

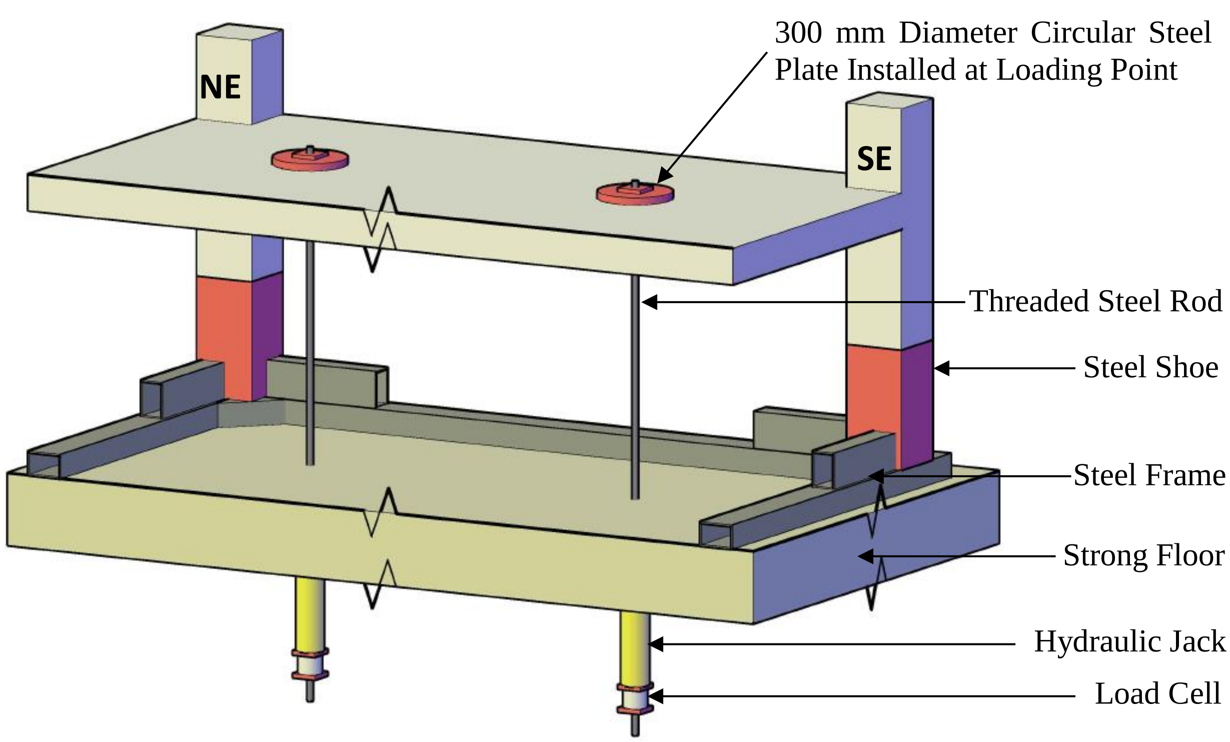

Figure 2-14: Sectional view of loading apparatus setup

2.6 Instrumentation

2.6.1 Displacement Transducers

The system of displacement transducers consisted of two types of devices: LVDTs and String Potentiometers. These devices were set up under the slab at locations near the column, loading point and slab center to measure slab displacement. The locations and arrangement of the system are shown in Figure 2-15.

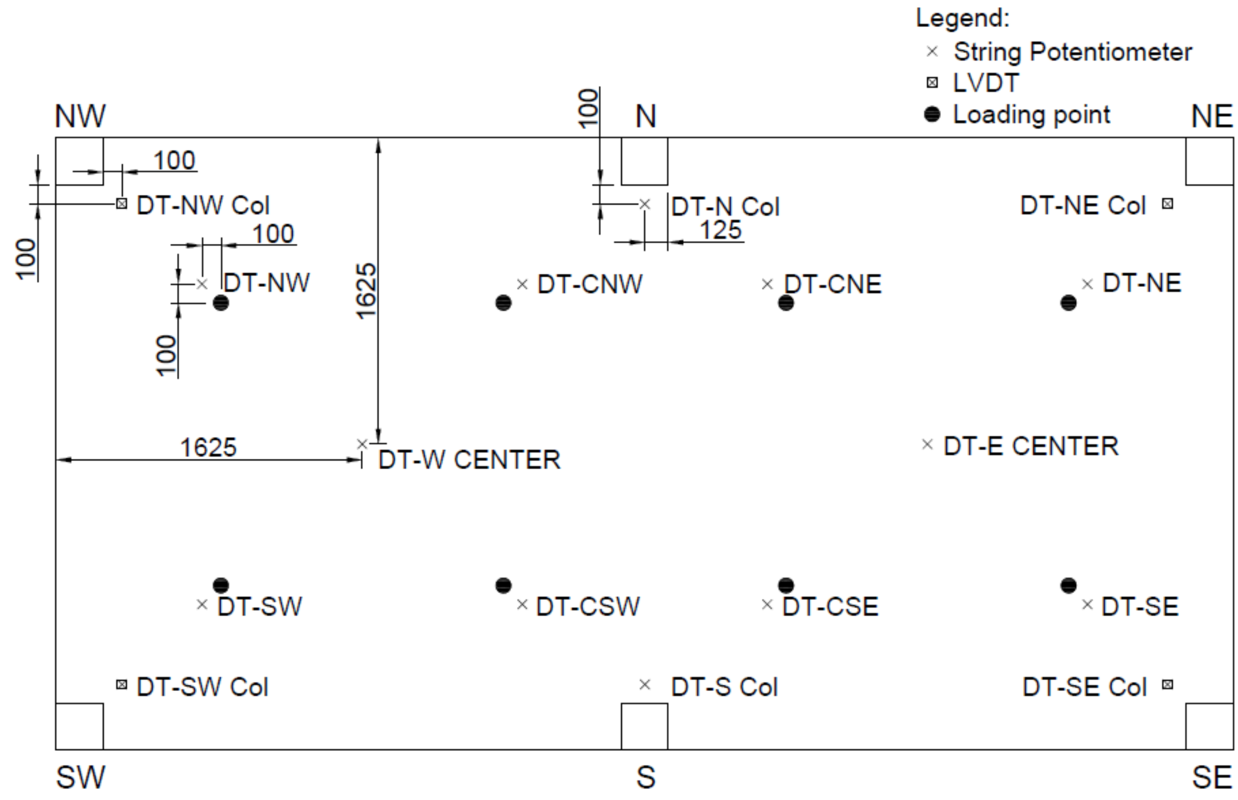

Figure 2-15: Configuration of displacement transducers

2.6.2 Load Cells

The applied loads were measured using load cells installed under the hydraulic jacks. The measured load, the self-weight of slab and loading apparatus, weighing 0.72 kN each, were accounted for in determining the total loading applied to the slab structure.

2.6.3 Strain Gauges

A total of 42 – 2 mm strain gauges were glued to the structural integrity reinforcement and 14 – 5 mm strain gauges were glued to the top reinforcing bars passing through the slab-column connections to measure the steel strain throughout the testing process. The strain gauges attached on selected structural integrity bars were located 5 mm, 200 mm and 400 mm from the column face. The strain gauges on selected top reinforcing bars were placed at 5 mm away from column face. The numbering and layout of structural integrity reinforcement strain gauges are shown in Figure 2-16; the numbering and layout of top reinforcement strain gauges are shown in Figure 2-17.

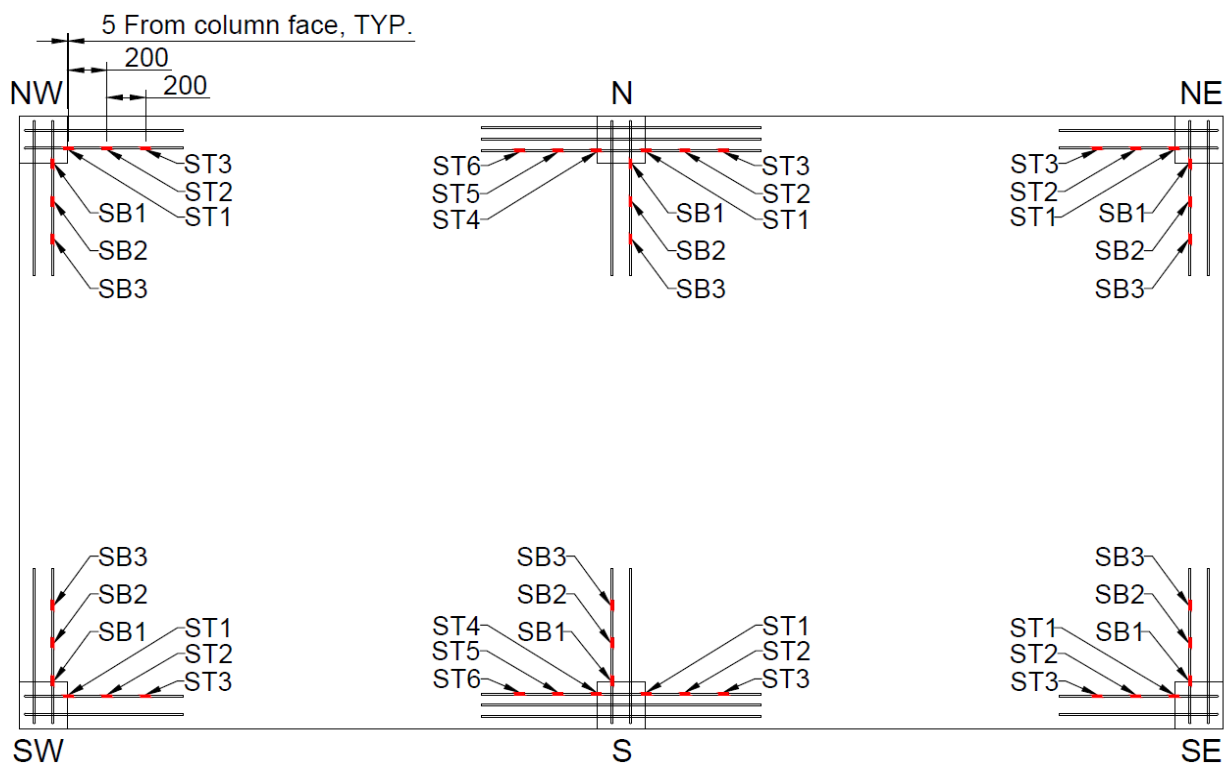

Figure 2-16: Layout of structural integrity reinforcement strain gauges (units: mm)

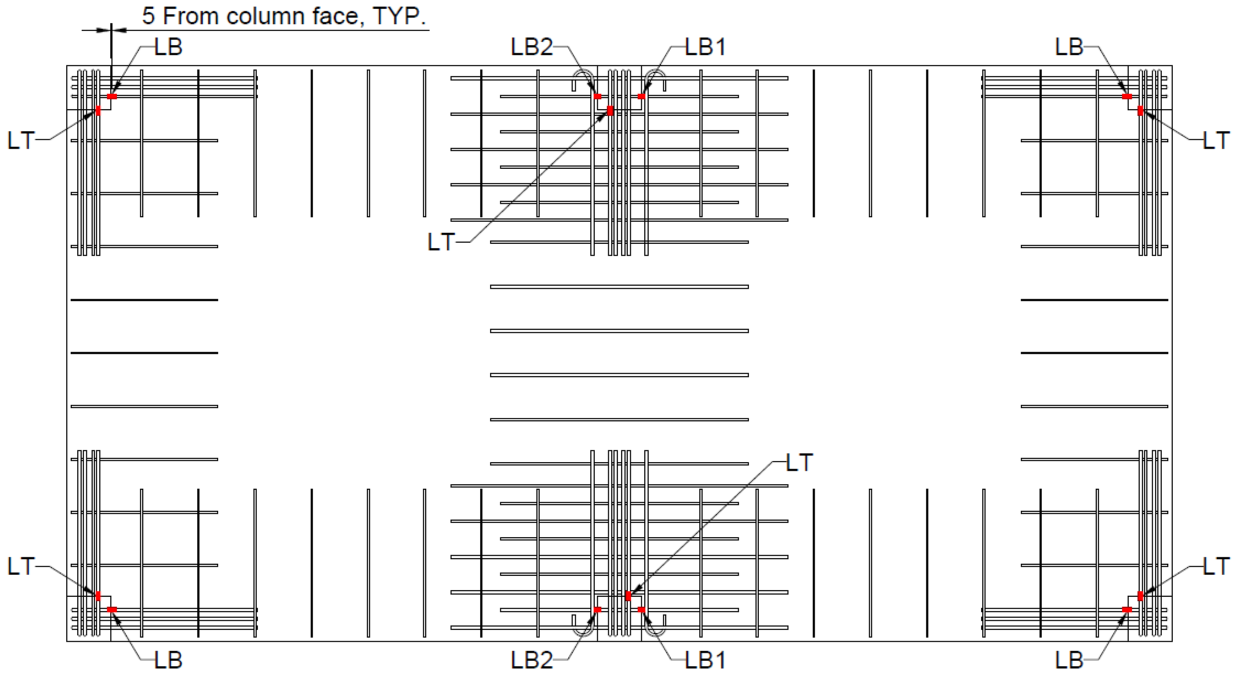

Figure 2-17: Layout of top reinforcement strain gauges (units: mm)

2.7 Test Procedure

Load was applied gradually from a manual hydraulic pump to the slab. Loading stage 1 was reached when hairline cracks started to appear. After stage 1, the loading stages were taken at 10 kN increments per load cell. At each stage, the cracks were marked, crack widths were measured, and photographs were taken of each slab-column connection. After punching shear failure, the loading was applied to the slab continuously to monitor the post-punching shear behaviour of the structural integrity reinforcement until the reading from load cells stopped increasing.

3. RESPONSE OF SLAB STRUCTURE

3.1 Introduction

The test results of this full-scale slab structure are reported in this chapter. The recorded data in this test include the concrete crack development, the applied load from each hydraulic jack, the vertical displacements of the slab, and the strains of top reinforcement and structural integrity reinforcing bars at each slab-column connection.

The deflection data used for plotting the responses of the individual slab-column connections were obtained from LVDTs at locations close to the columns. The shear at each connection was calculated based on load distribution ratios at key load stages which were obtained using structural analysis software SAP2000 (CSI, 2010) with inputs consisting of self-weight of slab and loading apparatus, and applied load from hydraulic jacks. The calculations of the shears at each column were explained in detail in Section 4.2 of this thesis. For the overall response of the slab structure the total loading was reported along with the average deflection measurement from all the displacement transducers.

3.3 Description of Overall Response

3.3.1 Introduction

The initial objective of the test was to apply constant loading in each hydraulic jack until all six slab-column connections failed in punching shear. This loading is referred to as Part 1 loading. After punching shear failures of the slab-column connections at the N, S, NW and SW columns, it was speculated that the continuation of uniform loading might cause collapse of the west bay before punching shear occurs to the slab-column connections at the NE and SE columns. Hence, the testing was continued in Part 2 loading, by increasing the loading in only the two hydraulic jacks adjacent to columns NE and SE, while the other six jacks were disconnected from the hydraulic system with the loads in these jacks being monitored using the load cells.

3.3.2 Part 1 of Overall Response

Figure 3-1 shows the total load, including dead load and applied load, versus average displacement of the slab. The average displacement was taken as the average of all the slab displacement measurements. At each loading stage, the applied load increased by approximately 10 kN per loading point, resulting in an estimated 80 kN increment in the total load until punching shear takes place. The loading stages were marked with numbers on the curve. As observed in the plot, each pause of applied load was subsequently followed by a drop in load as measured by the load cells. This phenomenon was caused by the reduction of slab stiffness resulted from development of concrete flexural cracks.

At load stage 1, at a total load of approximately 198.1 kN, a few hairline cracks started to appear at both edge slab-column connections N and S, and at corner connection SE (see Figure 3-2). The decline of load reading after stage 1 was unnoticeable in Figure 3-1. When the total load reached 275 kN at load stage 2, hairline cracks could be observed at all six slab-column connections. As loading proceeded, under the influence of increasing negative moment, the crack widths widened, and more flexural cracks were developed on the slab surface around the column stub at each slab-column connection, and on the slab surface spanning between the two edge columns (see Figure 3-4). Horizontal cracks also appeared on the outward faces of the columns, indicating that the typical eccentric loading at exterior connections caused bending moment in the columns (see Figure 3-3).

The crack width reached a maximum of 0.30 mm at load stage 8 with a maximum total load of 754 kN, where thin layers of concrete cover started breaking out around the two edge slab-column connections, and the measured load dropped rapidly, suggesting the initiation of shear failure (see Figure 3-5). The applied load was gradually increased after load stage 8. The expected complete punching shear failure occurred first at edge connection N at a total load of 696.9 kN, resulting in a large displacement and load drop. The shear failure of edge connection S followed subsequently with the continuation of loading at a total load of 567.6 kN (see Figure 3-6 and 3-7).

Due to ongoing concrete breakout after punching shear failure of the two edge slab-column connections, the loading process led to large slab deflections, with reduced stiffness. The failure of corner connections NW and SW took place at load stage 11 with a total load of 555.1 kN, where the top slab cover broke out in a diagonal pattern across the slab surface near the column stubs (see Figure 3-8 and 3-9).

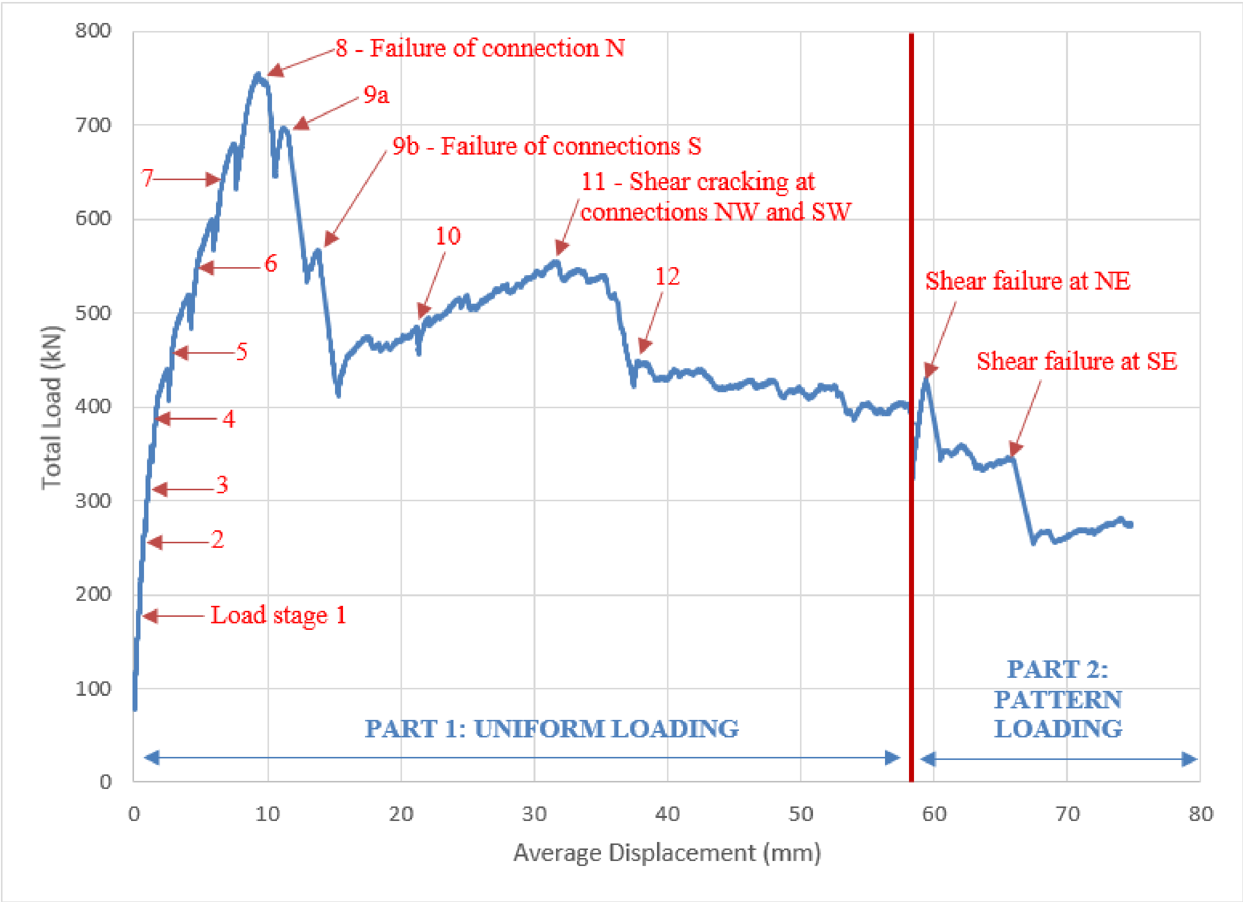

Figure 3-1: The total load vs. average displacement curve of slab structure

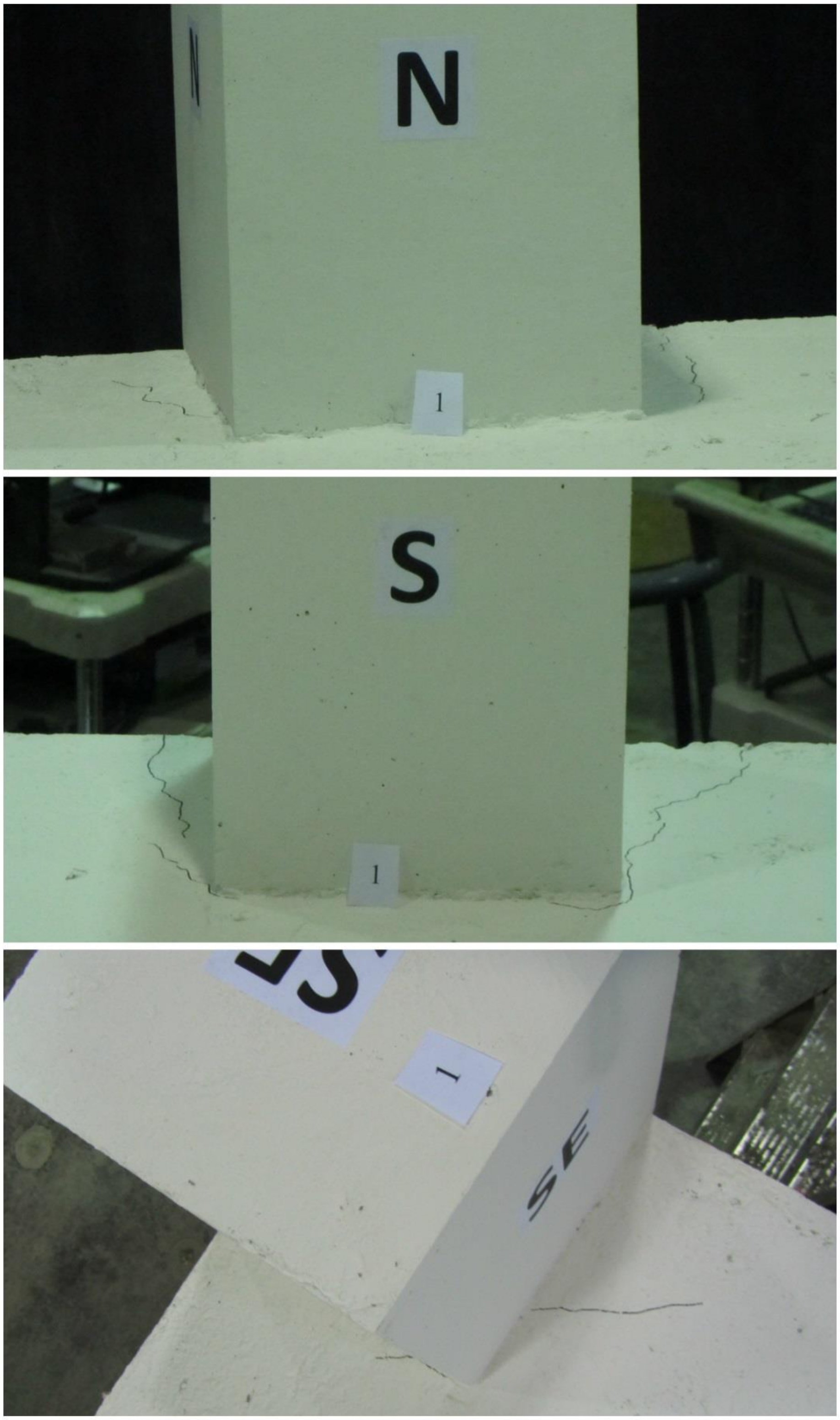

Figure 3-2: Appearance of hairline cracks at load stage 1 at N, S and SE slab-column connections

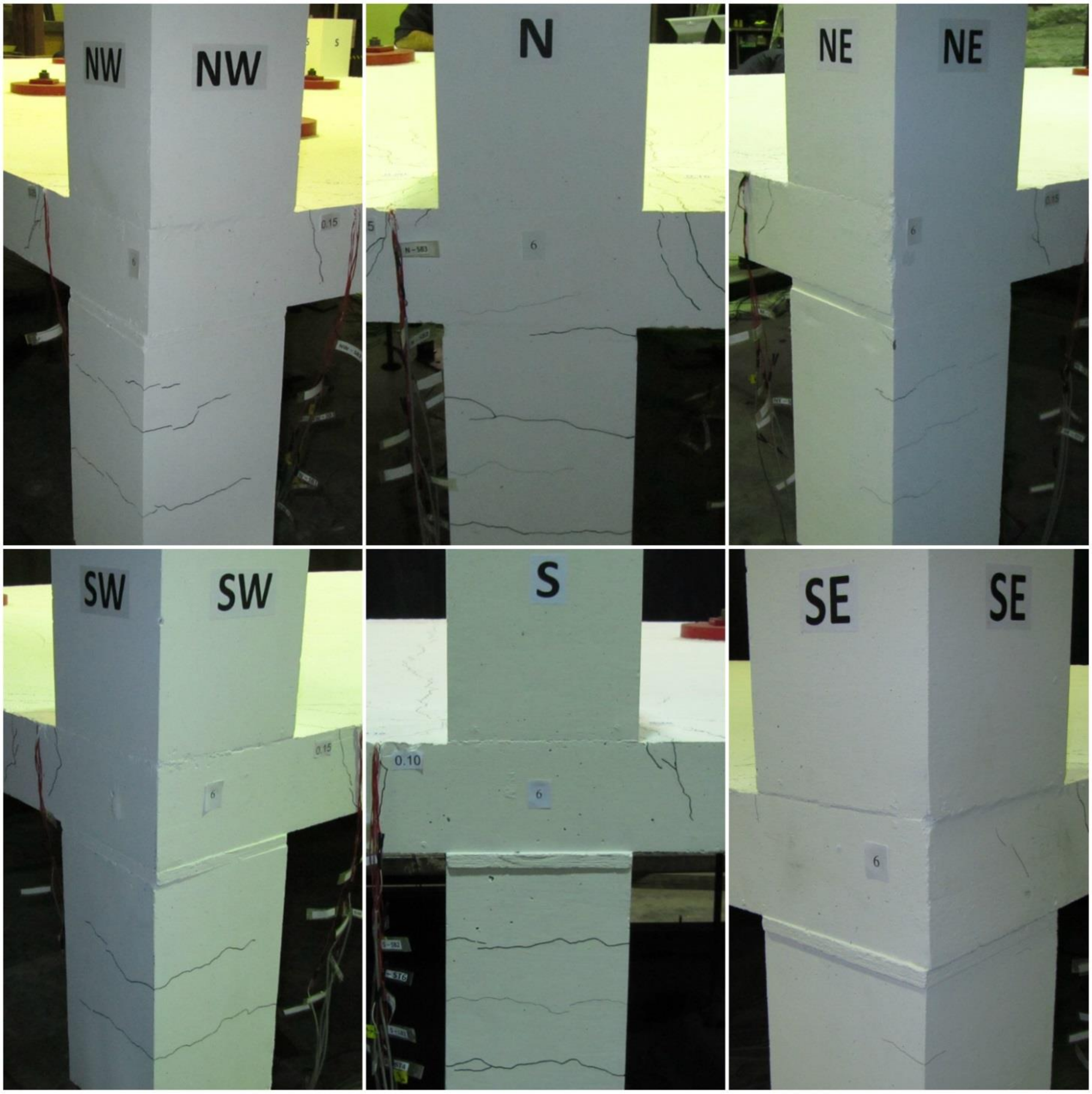

Figure 3-3: Horizontal cracks on the exterior faces of the columns at load stage 6

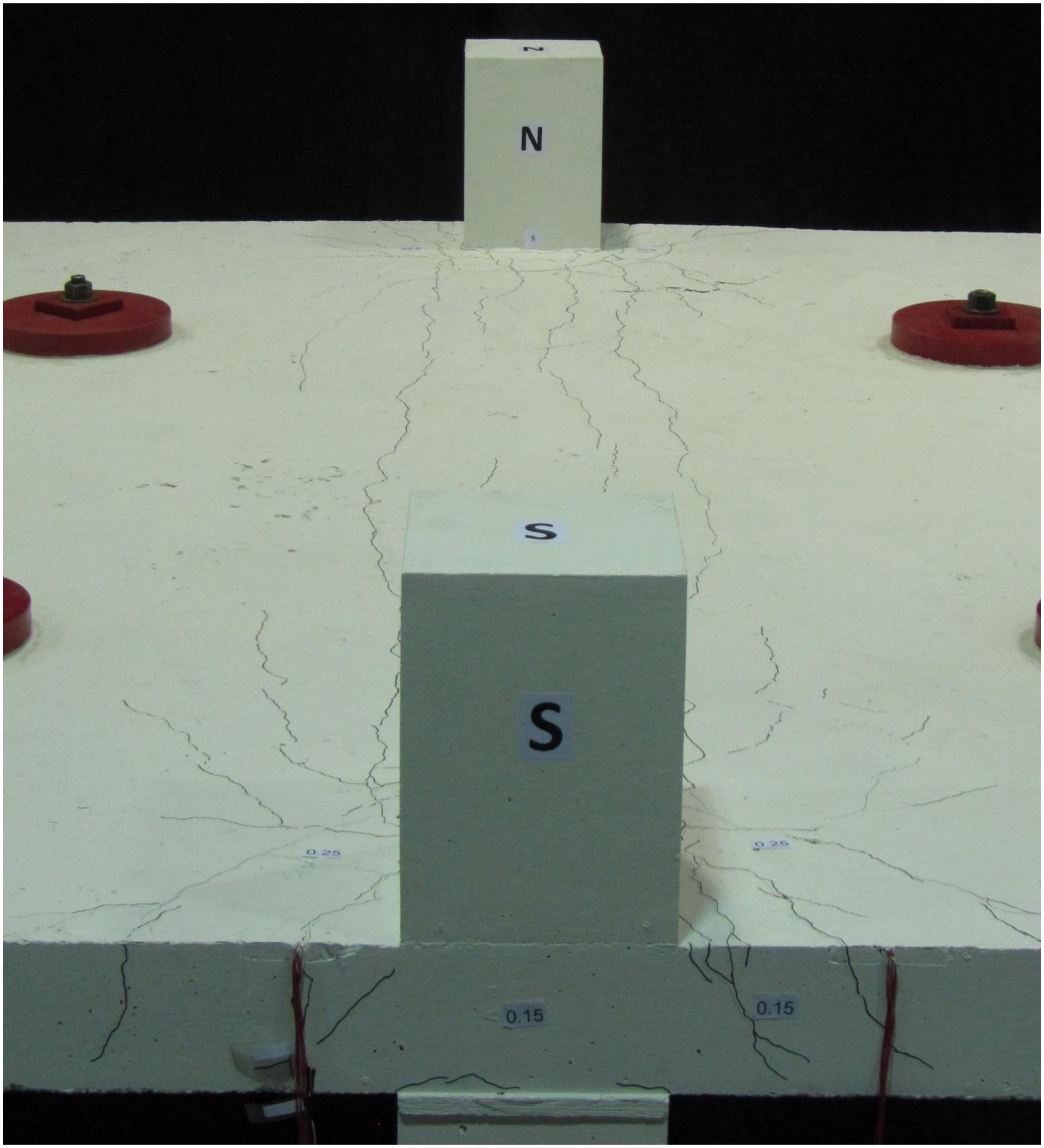

Figure 3-4: Cracks developed across the span between two edge slab-column connections at load stage 8

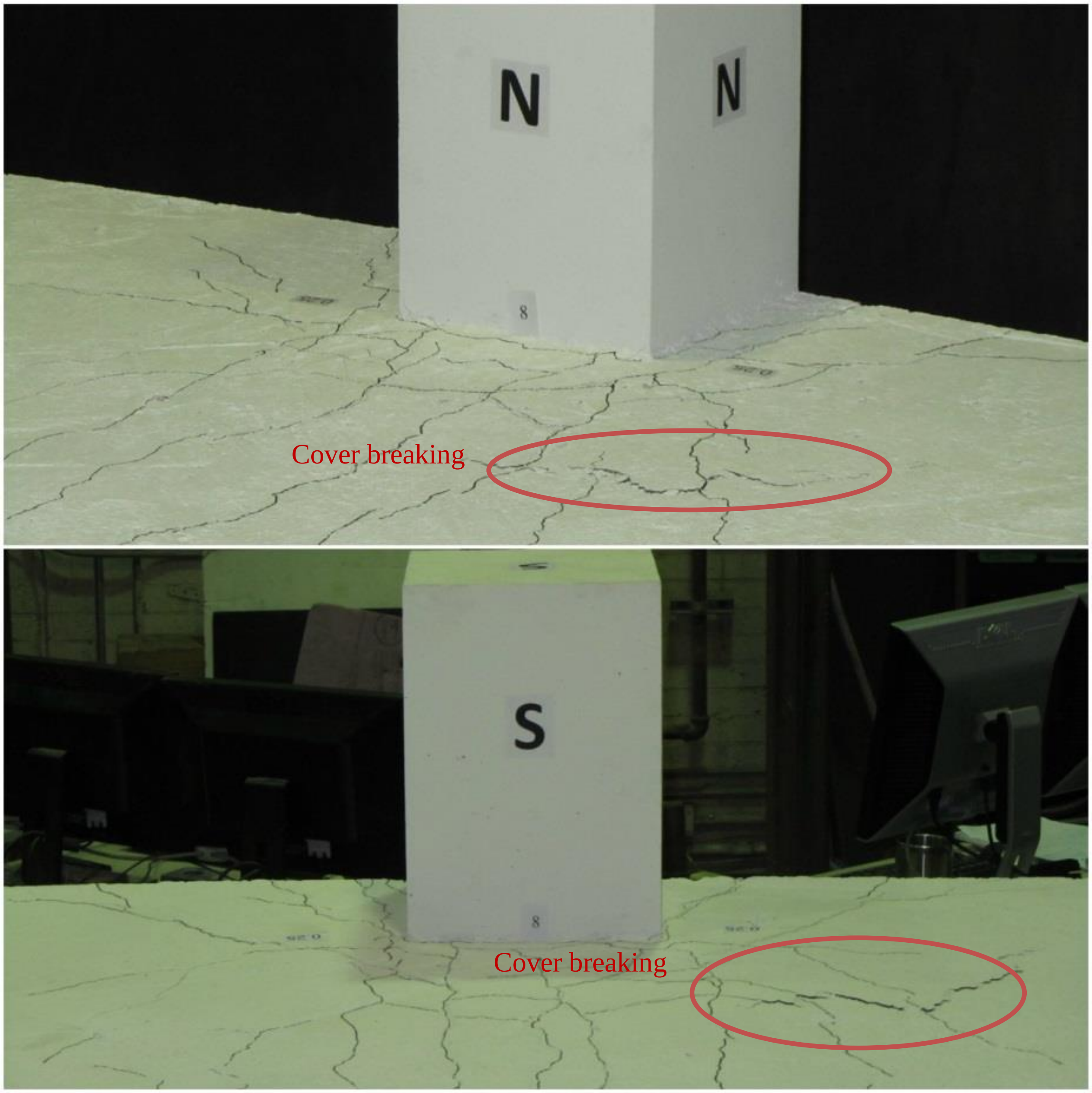

Figure 3-5: Slab cover breaking out at edge slab-column connections at load stage 8

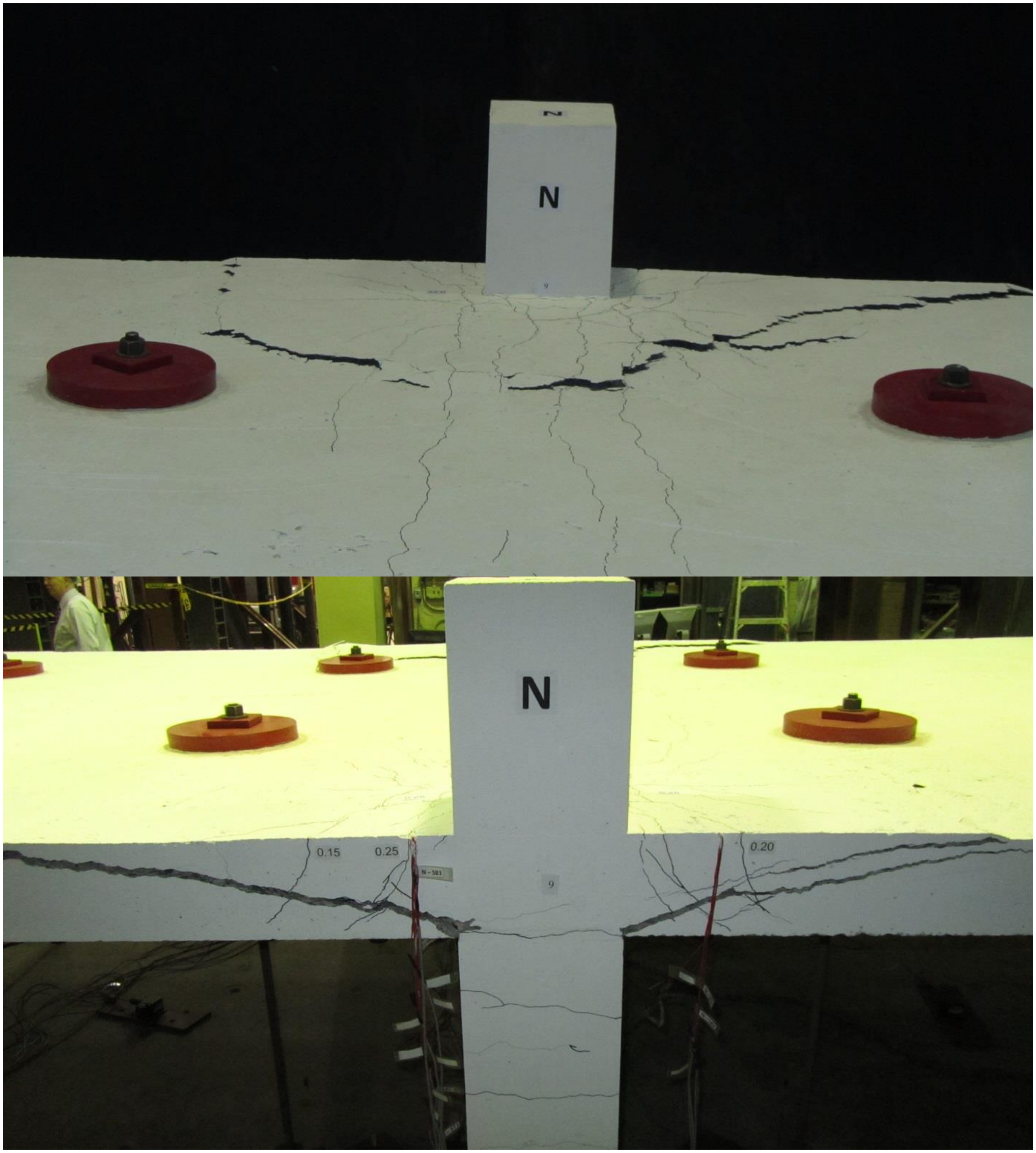

Figure 3-6: Punching shear failure of edge slab-column connection N at load stage 9a

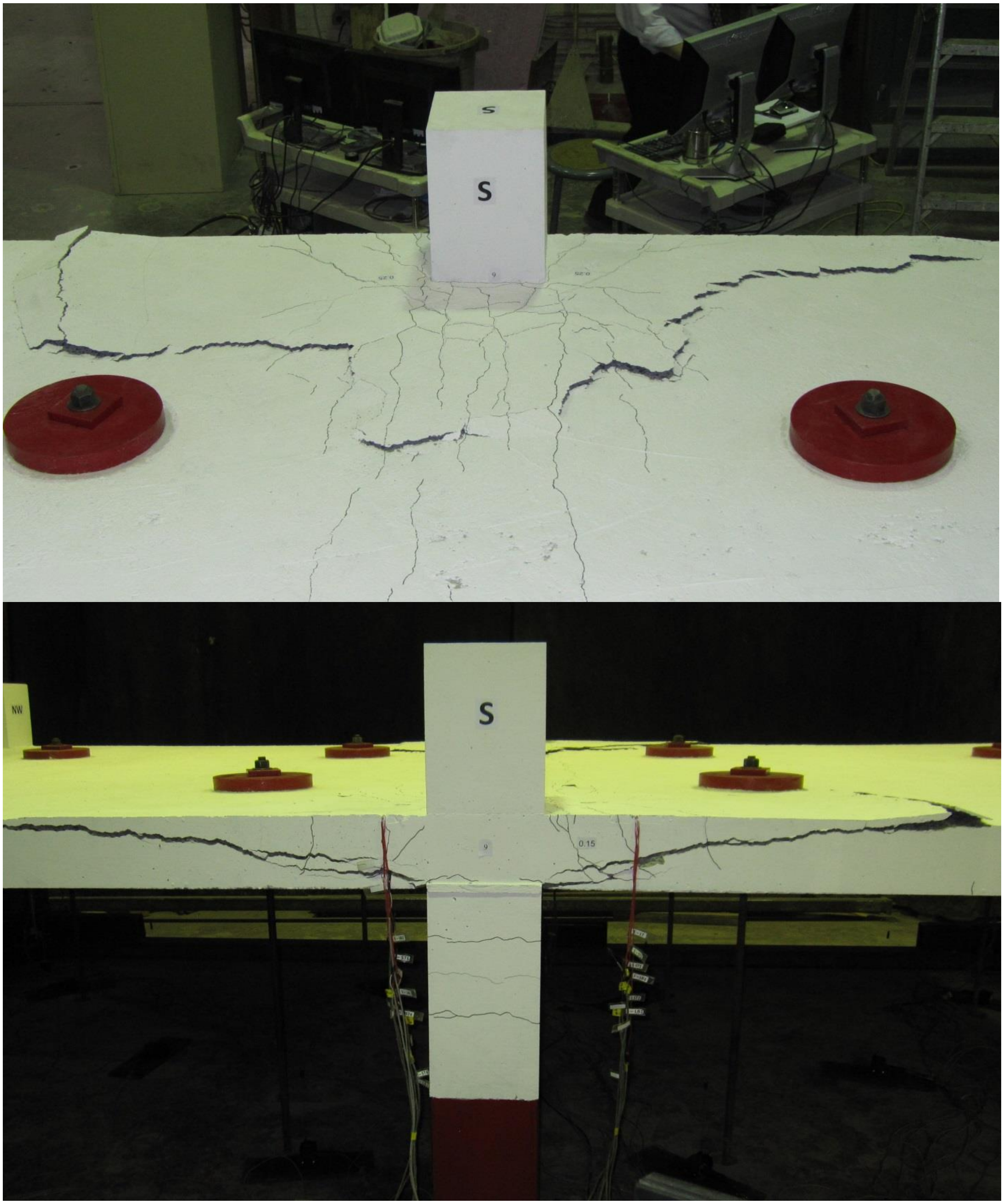

Figure 3-7: Punching shear failure of edge slab-column connection S at load stage 9b

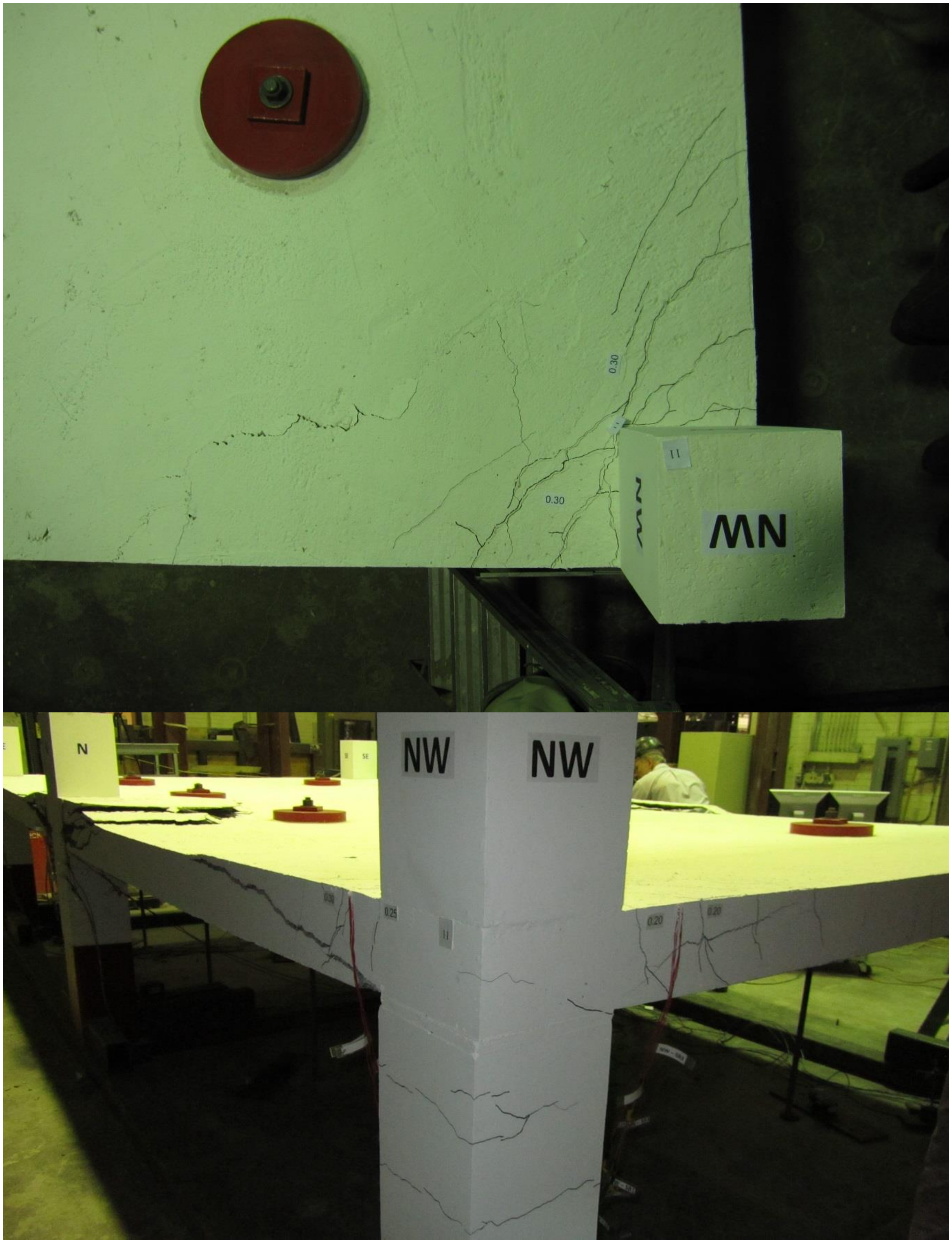

Figure 3-8: Punching shear failure of corner slab-column connection NW at load stage 11

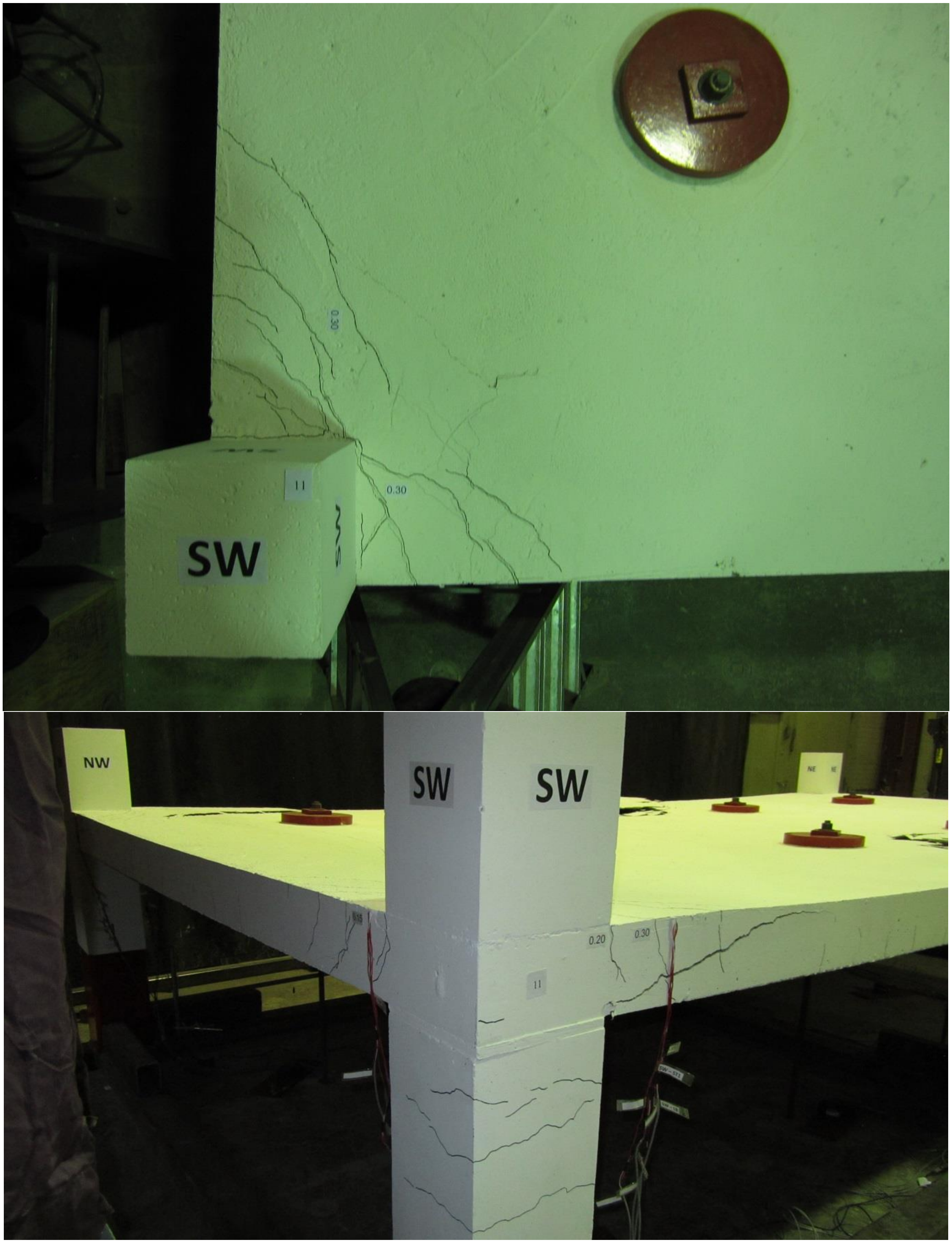

Figure 3-9: Punching shear failure of corner slab-column connection SW at load stage 11

3.3.3 Part 2 of Overall Response

In order to ensure punching shear failure at corner slab-column connections NE and SE, only the hydraulic jacks adjacent to columns NE and SE were used to apply additional force to the slab in Part 2 of the loading process. The total load vs. average displacement curve for part 2 is plotted following Part 1 in Figure 3-1. The corner slab-column connections NE and SE failed in punching at a total load of 429.0 kN and 345.8 kN, respectively (see Figure 3-1 and 3-10).

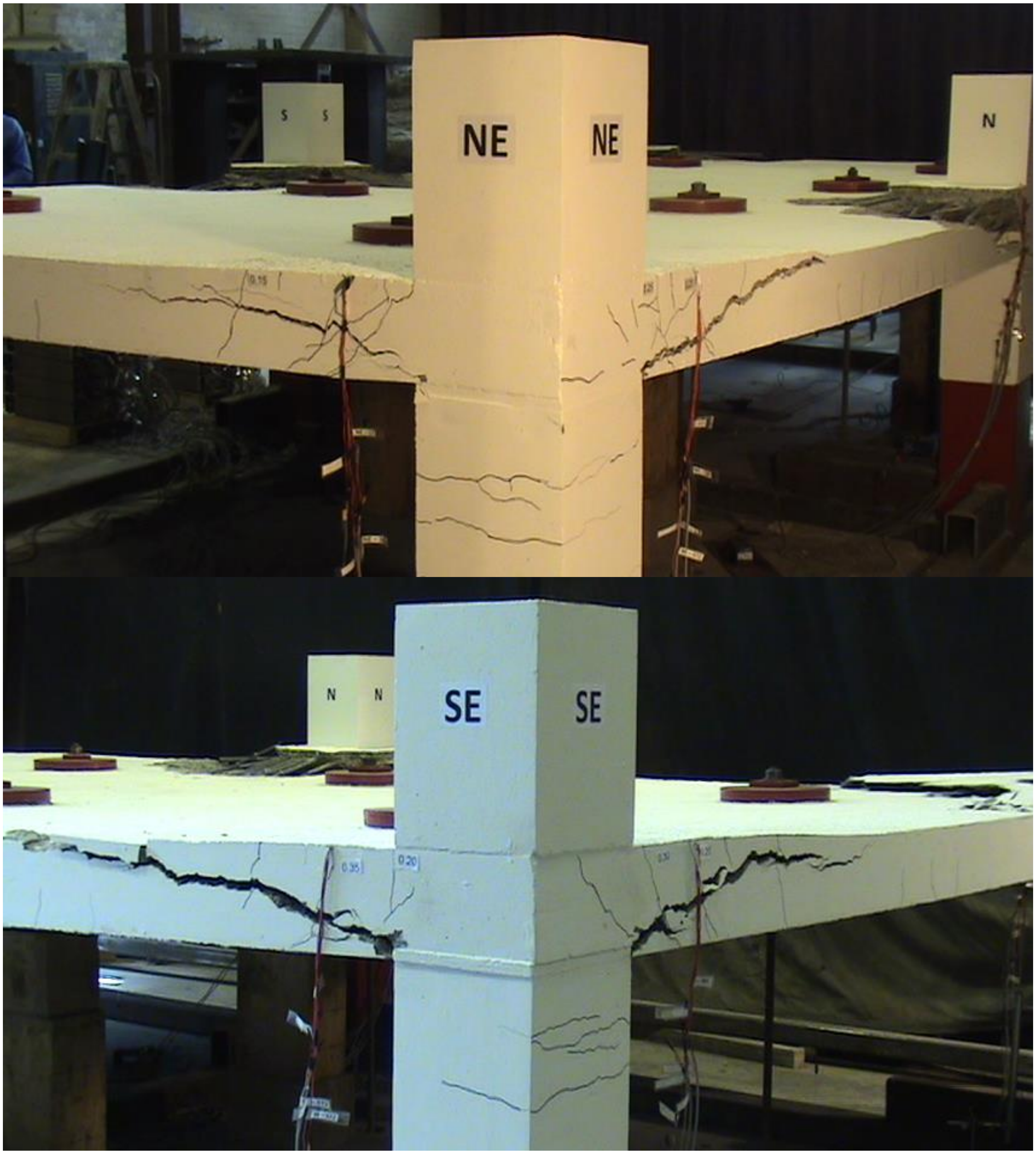

Figure 3-10: Punching shear failures of corner slab-column connections NE and SE in Part 2 of loading sequence

3.4 Edge Slab-Column Connections

It is noted that the shears occurring at each column during testing were determined by structural analyses, knowing the total applied loading and calculating the stiffness of the slab-column connections at different stages of loading. This calculation procedure is described in Chapter 4.

3.4.1 Edge Slab-Column Connection N

3.4.1.1 Test Results

Figure 3-11 shows the shear vs. slab displacement response of the edge slab-column connection N. Table 3-1 provides the corresponding shear and connection displacement values at key load stages which include first flexural cracking, first yielding of top reinforcement and structural integrity reinforcement, punching shear failure and maximum post-punching load.

The first flexural cracking occurred at load stage 1 where the shear at the connection was 57.4 kN. These hairline cracks on the surface of the slab in the region around column N are shown in Figure 3-2. The process of shear failure initiated at stage 8 with a maximum shear of 217.6 kN (see Figure 3-5), with the development of a complete punching shear surface at load stage 9a at 200.7 kN (see Figure 3-6).

The maximum post-punching failure load was reached at load stage 12 at a shear of 105.3 kN. After the completion of the test, the loose concrete at the connection was removed to examine the post-punching condition of the reinforcement. As shown in Figure 3-12, sections of the structural integrity reinforcement with significant length ripped out of the top surface of the concrete, suggesting that concrete breakout failure governed the post-punching shear strength of the connection.

The angles from horizontal of the reinforcement, including top reinforcement and structural integrity reinforcement, were measured and presented in Table 3-2 and Table 3-3, respectively. The average inclination angles are 10.6 degrees for the top reinforcement, and 11.3 degrees for the structural integrity reinforcement.

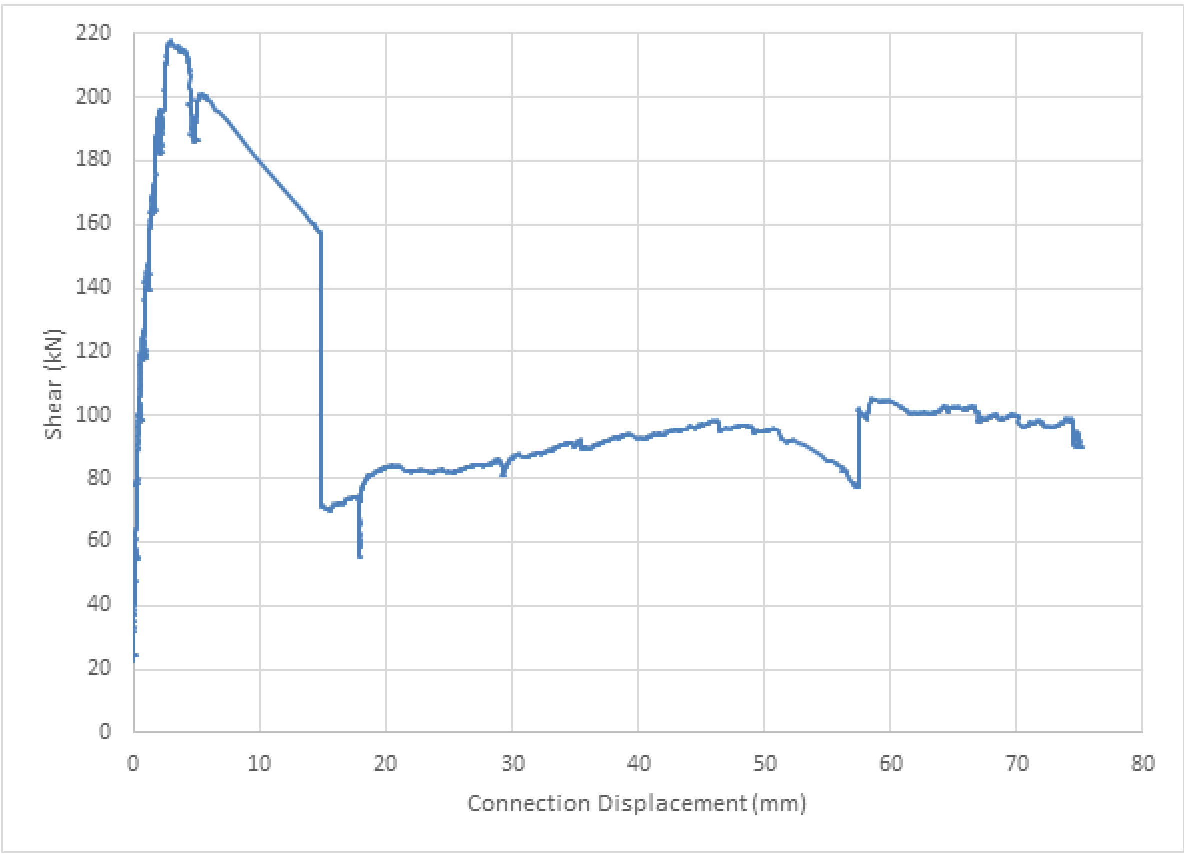

Figure 3-11: Shear vs. connection displacement curve for edge slab-column connection N

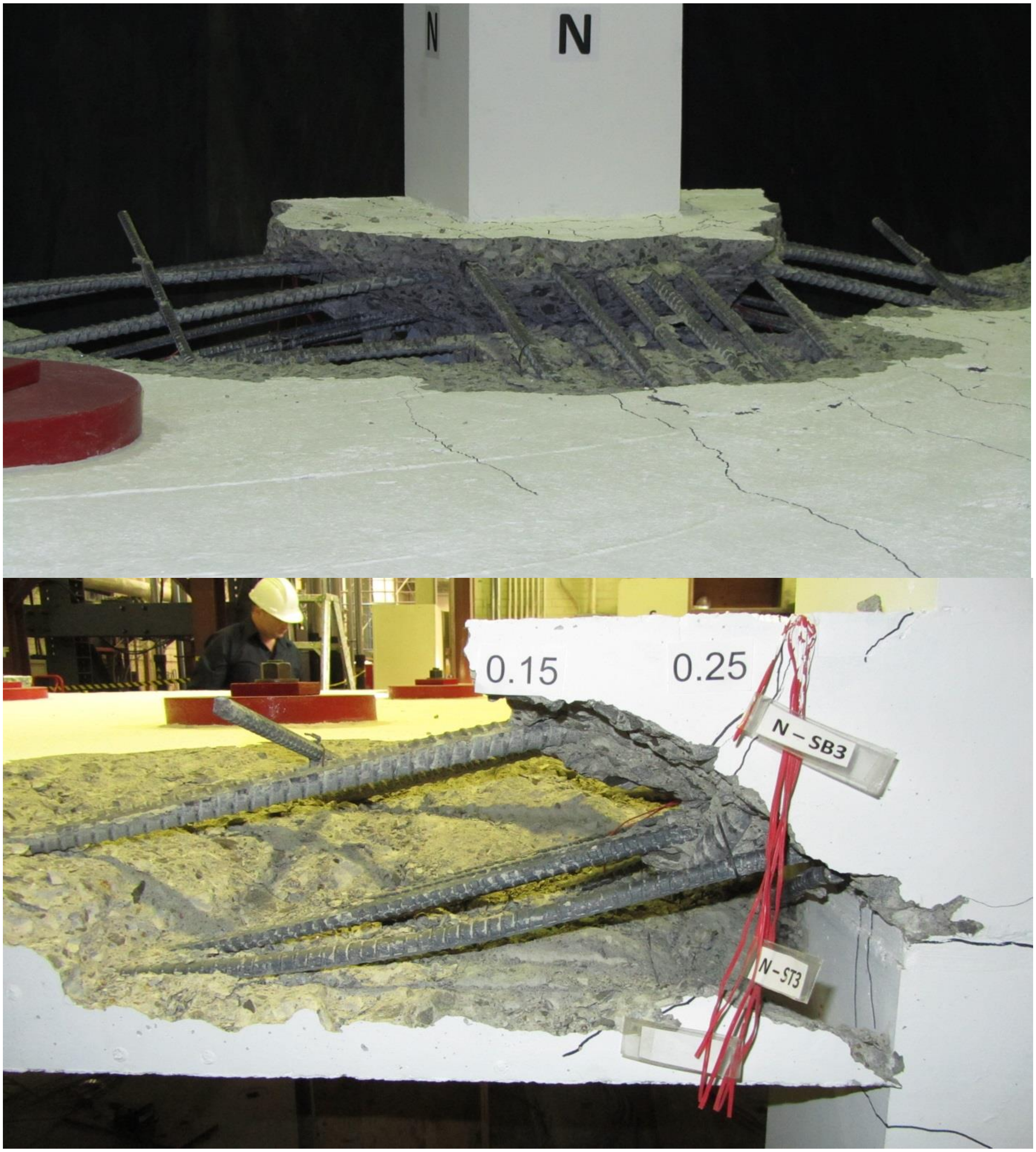

Figure 3-12: Post-punching shear condition of the edge slab-column connection N at the end of testing

Table 3-1: Summary of key load stages for edge slab-column connection N

Stage	Load (kN)	Displacement (mm)
First Cracking	57.4	0.17
First Yield (Top Bars)	NA	NA
First Yield (Structural Integrity Bars)	200.4	5.5
Punching Shear Failure	217.6	2.9
Max. Post-Punching Load	105.3	58.5

Table 3-2: Angle of top reinforcement for edge slab-column connection N

Steel Layout	Labels	Angle from Horizontal (Degree)
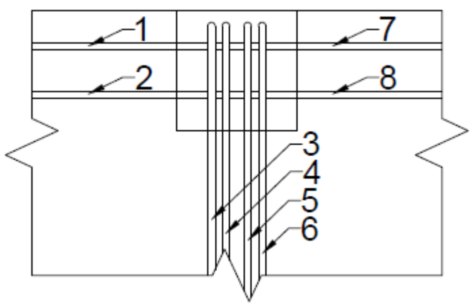	1	9
	2	Free
	3	11
	4	12
	5	11
	6	12
	7	10
	8	9

Table 3-3: Angle of structural integrity reinforcement for edge slab-column connection N

Steel Layout	Labels	Angle from Horizontal (Degree)
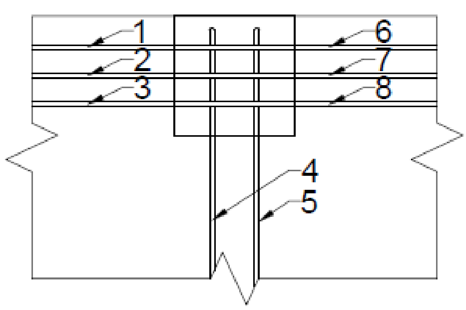	1	12
	2	12
	3	12
	4	NA
	5	NA
	6	11
	7	10
	8	11

3.4.1.2 Concrete Cracking

Flexural cracks occurring on the top surface of the slab around the column appeared and widened as the applied load increased. The shear vs. maximum crack width curve for edge slab-column connection N is presented in Figure 3-13. The crack width was monitored at each load stage until shear cracking appeared at the observed slab-column connection. The maximum flexural crack width of connection N was 0.25 mm.

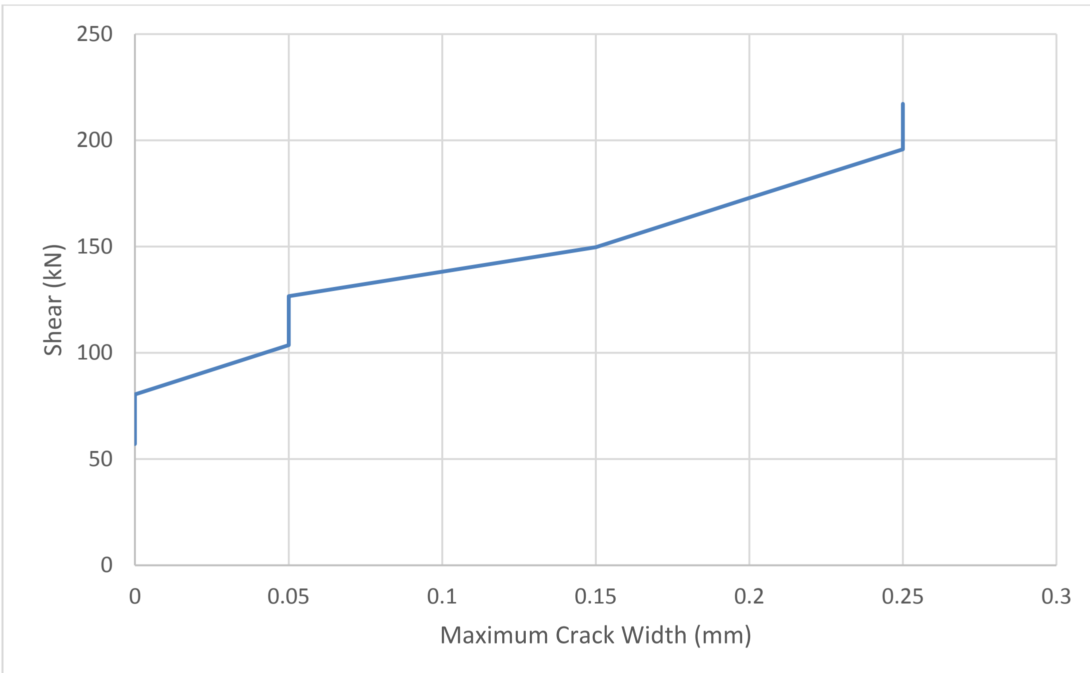

Figure 3-13: Shear vs. maximum crack width response for edge slab-column connection N

3.4.1.3 Top Reinforcement Strains

The relationship between strains measured in the top reinforcement and slab displacement close to the connection are presented in Figure 3-14. It can be seen that after achieving maximum strain, punching shear failure caused rapid decline of strain in the top reinforcement. In the N-S direction, gauge LT regained strain during post-punching loading until the strain gauge malfunctioned; in the E-W direction, the strain in LB1 and LB2 continuously declined. The comparison of the curves indicated that higher negative moment was induced at the south face of the connection before the shear failure. After punching failure, the top reinforcement in the N-S direction provided limited contribution in supporting the slab, while reinforcement in the E-W direction lost anchorage in the slab.

The yield strain of 15M steel bars used in this test is 2260 $\mu\varepsilon$. None of the top reinforcement reached yield strength at this connection.

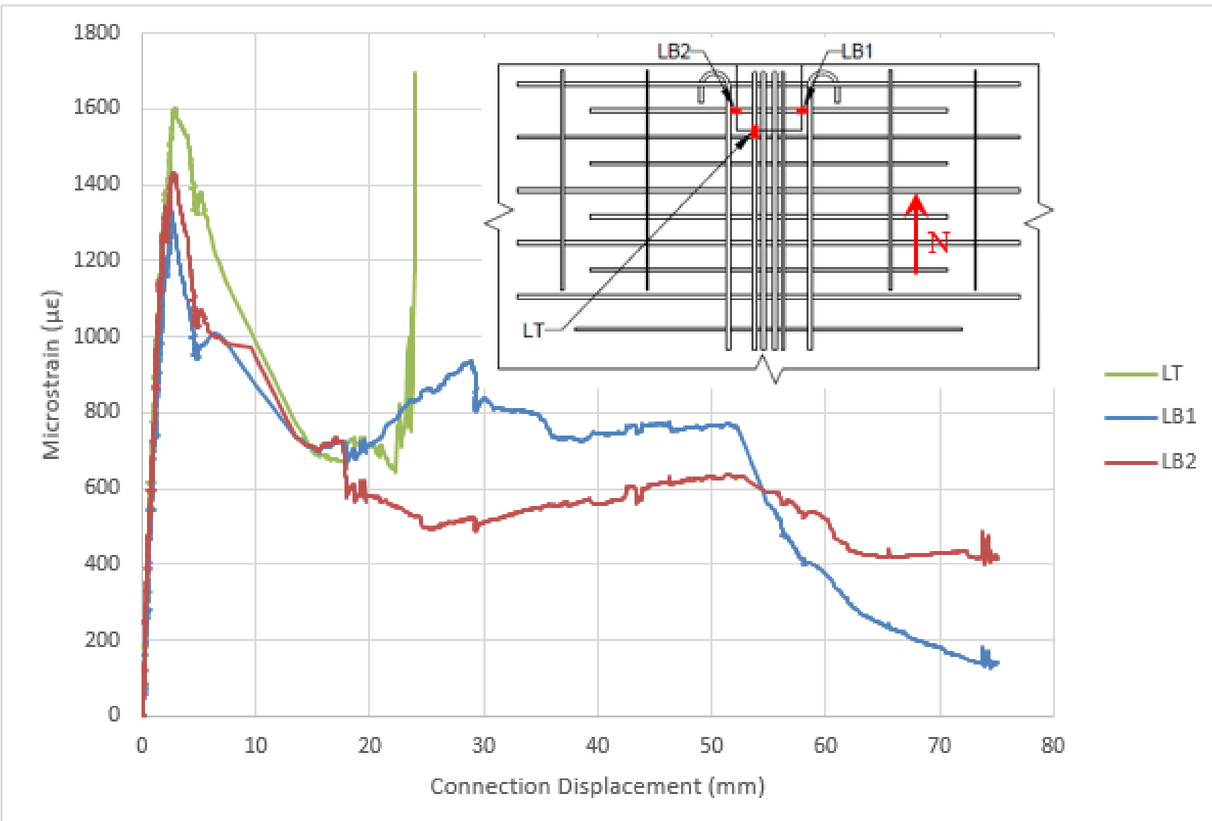

Figure 3-14: Measured strains in the top reinforcement vs. connection displacement for edge slab-column connection N

3.4.1.4 Structural Integrity Reinforcement Strains

At each face of the connection, three strain gauges were placed on the bars at regular intervals away from the column face on a selected bar, so that strain development at different locations along the bar can be determined. Figure 3-15 presents the strain versus deflection responses of the selected reinforcement.

Gauges ST1, ST4 and SB1 displayed noticeable increases of strain before the punching shear failure occurred, and reached the yield strain of 2260 $\mu\varepsilon$ for 10M bars after punching shear failure. The data acquisition system can record strain values up to 16000 $\mu\varepsilon$. Therefore, a discontinuity occurred in the curve of SB1 when its strain surpassed this limit. Gauges SB2 and SB3 were immediately damaged after punching occurred. Gauges ST5 and ST6 reached higher post-punching strains than gauges ST2 and ST3 due to the subsequent failure occurring at the west side corner slab-column connections.

Figure 3-16 and 3-17 provide the strain distribution in the structural integrity reinforcement around the edge connection at each load stage. The strain development was mostly concentrated at the location closest to the connection, and it decreased progressively as the rebar extends further from the connection. The strains throughout the structural integrity reinforcing bars increased as the load increased. In the N-S direction, strain gauges malfunctioned immediately after the connection failure. In the E-W direction, yield strain was achieved and exceeded after punching shear failure of connection N in the region around the column. There were stages of strain regain in the gauges during post-punching loading, especially in gauge SB1, suggesting that the structural integrity reinforcement was ripping out of the concrete intermittently during increased deflections.

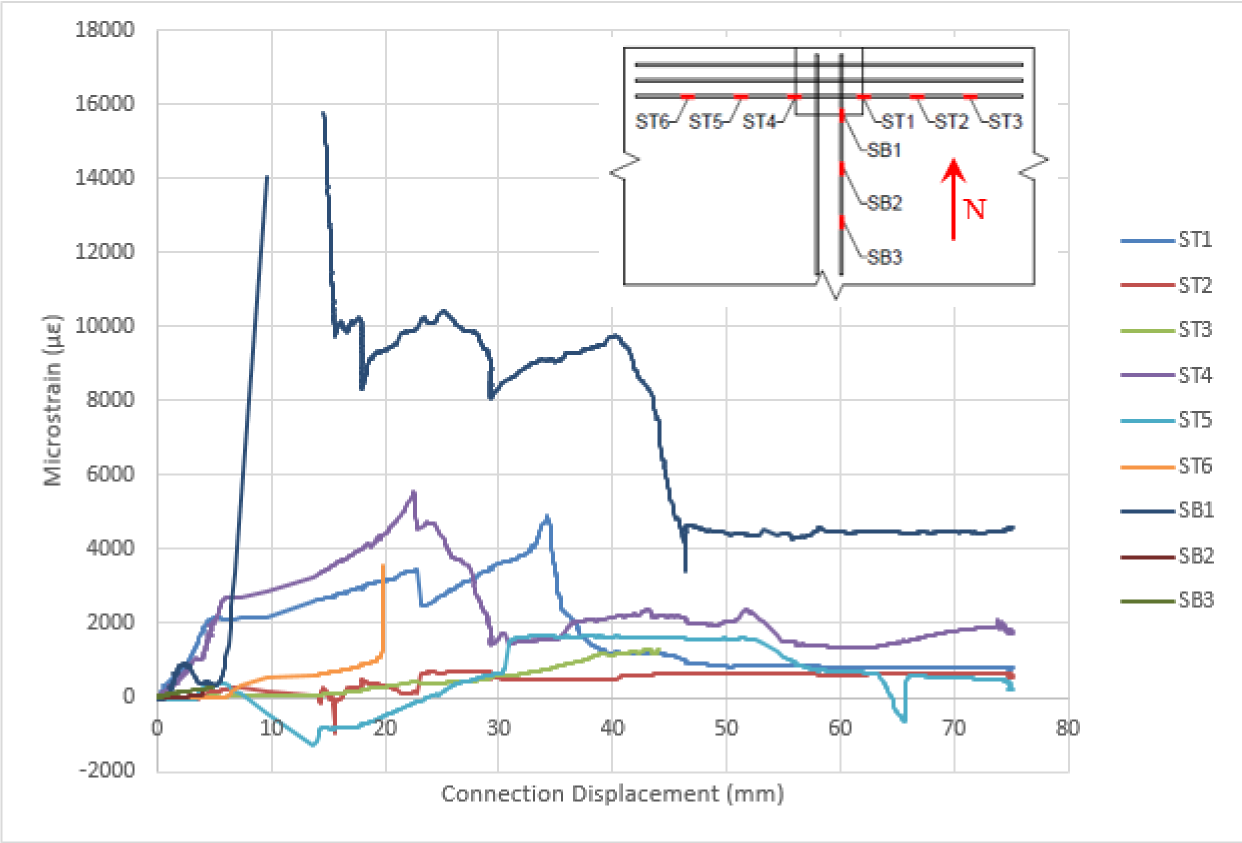

Figure 3-15: Measured strains in the structural integrity reinforcement vs. connection displacement for edge slab-column connection N

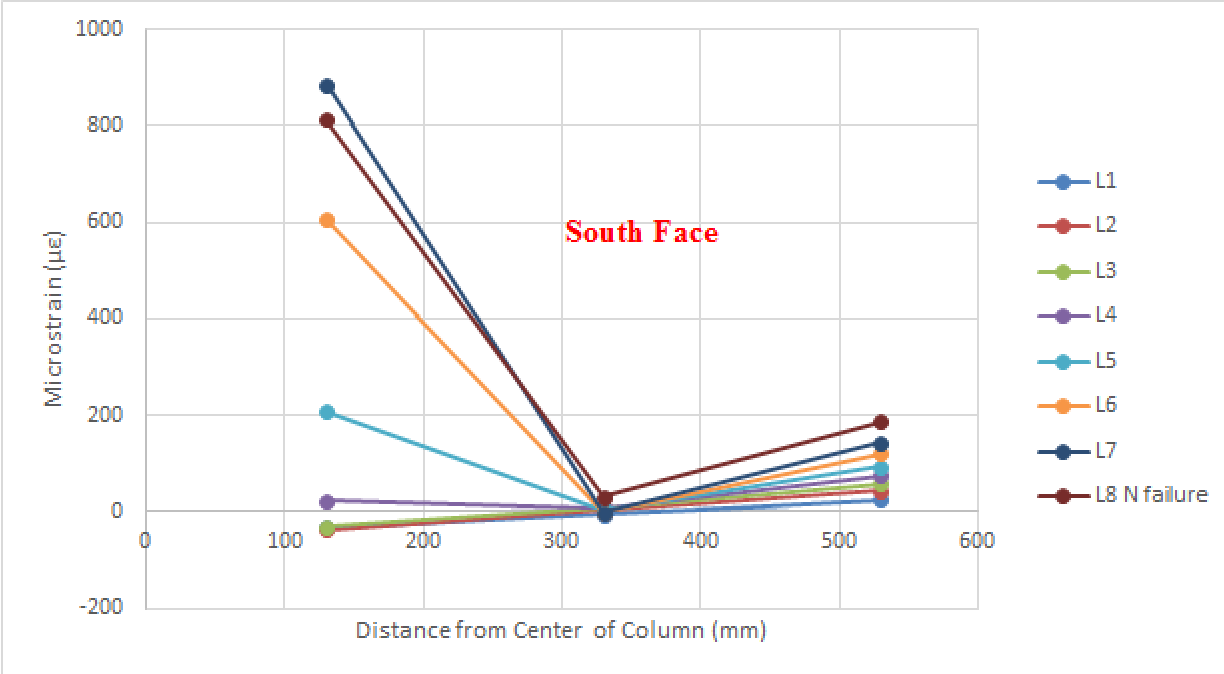

Figure 3-16: Strain distributions in the structural integrity reinforcement in the N-S direction at each load stage for edge slab-column connection N

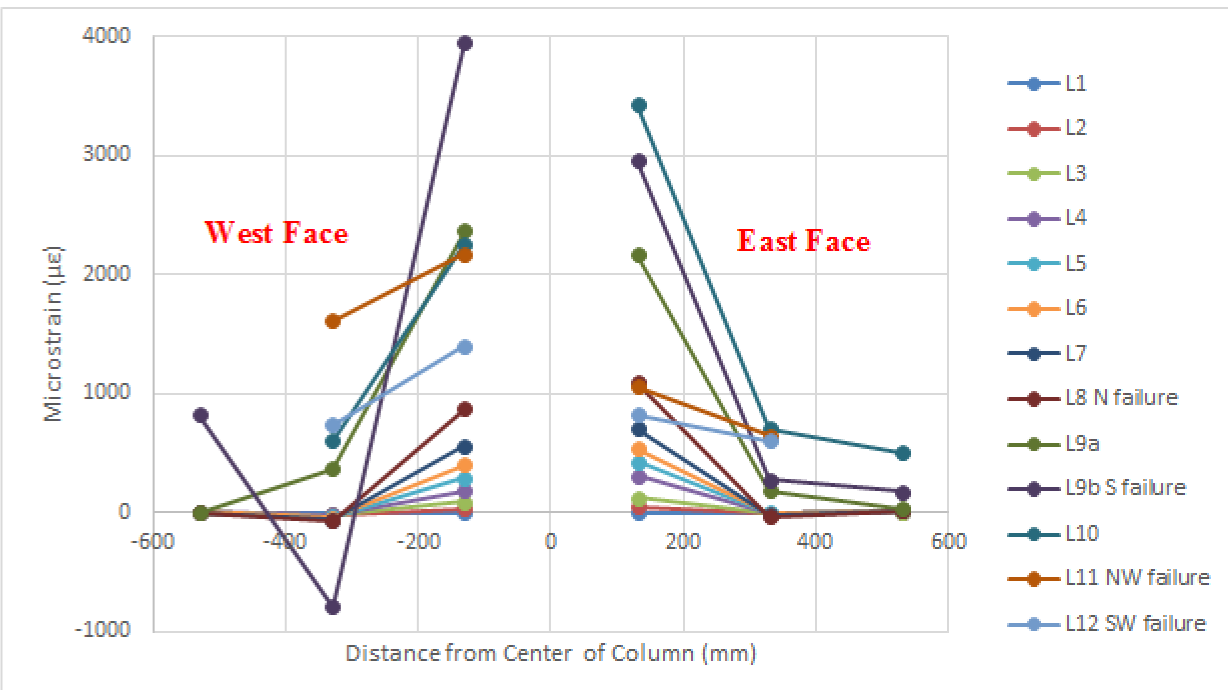

Figure 3-17: Strain distributions in the structural integrity reinforcement in the E-W direction at each load stage for edge slab-column connection N

3.4.2 Edge Slab-Column Connection S

3.4.2.1 Test Results

The punching shear failure of edge slab-column connection S occurred after punching shear failure occurred in slab-column connection N. Its shear versus connection displacement response curve is shown in Figure 3-18. The shear and displacement at key load stages are summarized in Table 3-4.

Hairline cracks appeared on the top slab surface surrounding the column at load stage 1 (see Figure 3-2) where the calculated shear was 55.3 kN at the slab-column connection. Flexural cracks continuously propagated and widened during the progression of loading. At load stage 8, the slab-column connection S reached its peak load of 209.7 kN and a punching shear cracking pattern was observed around the column (see Figure 3-5). Before the completion of punching shear failure, there were two rapid drops of shear at connection S: one of them was due to the large stiffness reduction caused by shear cracking, and the other was due to the punching failure of connection N. Column S punched through the slab entirely when the shear increased back to 201.1 kN at the end of load stage 9b (see Figure 3-7).

Edge slab-column connection S reached its maximum post-punching load of 105.6 kN in load stage 12 when a punching shear failure occurred at the west side corner connections. Further continuation of loading resulted in a decrease in the post-punching shear resistance at the connection.

At the end of the test, loose concrete was removed from the connection and inspection was done on the post-punching condition of the reinforcement, as shown in Figure 3-19. The final inclination angles of the top reinforcement which extended through the column and the structural integrity reinforcement were measured and summarized in Table 3-5 and Table 3-6, respectively. The average angles are 9.7 degrees for the top reinforcement, and 9.5 degrees for the structural integrity reinforcing bars.

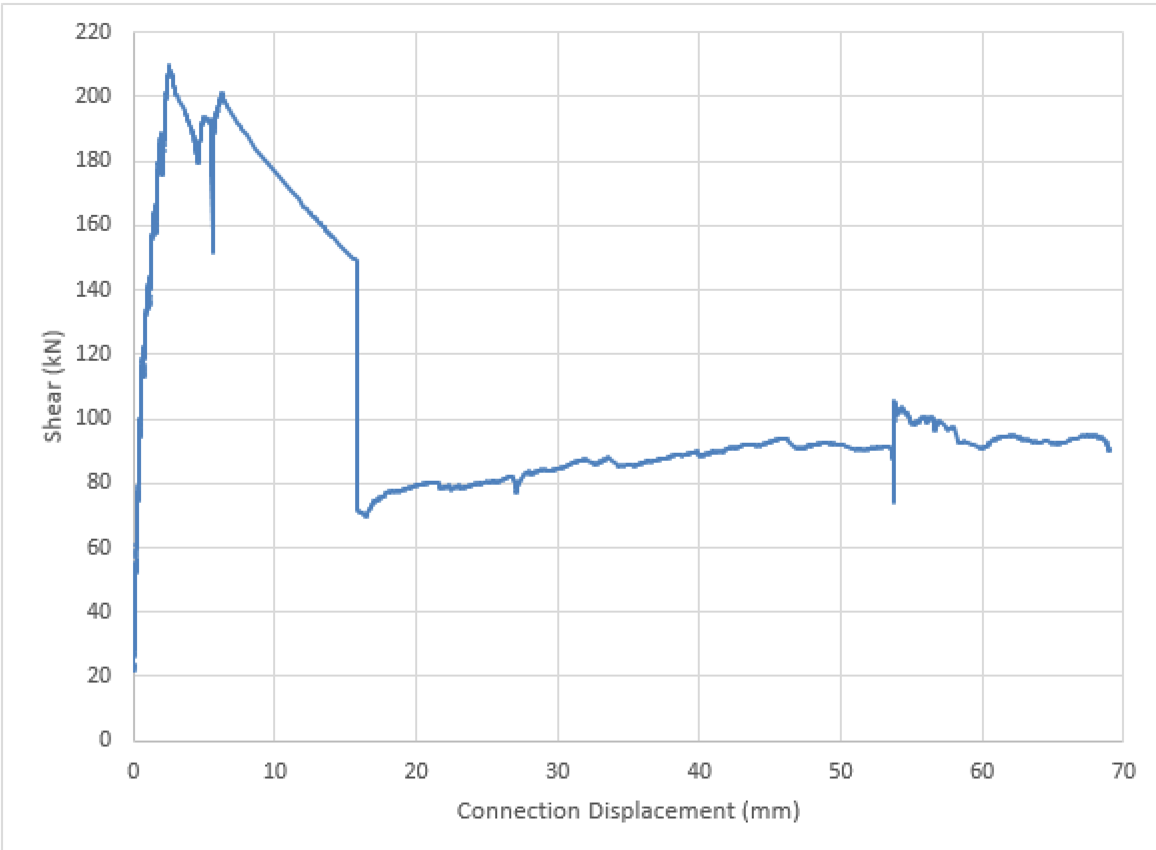

Figure 3-18: Shear vs. connection displacement curve for edge slab-column connection S

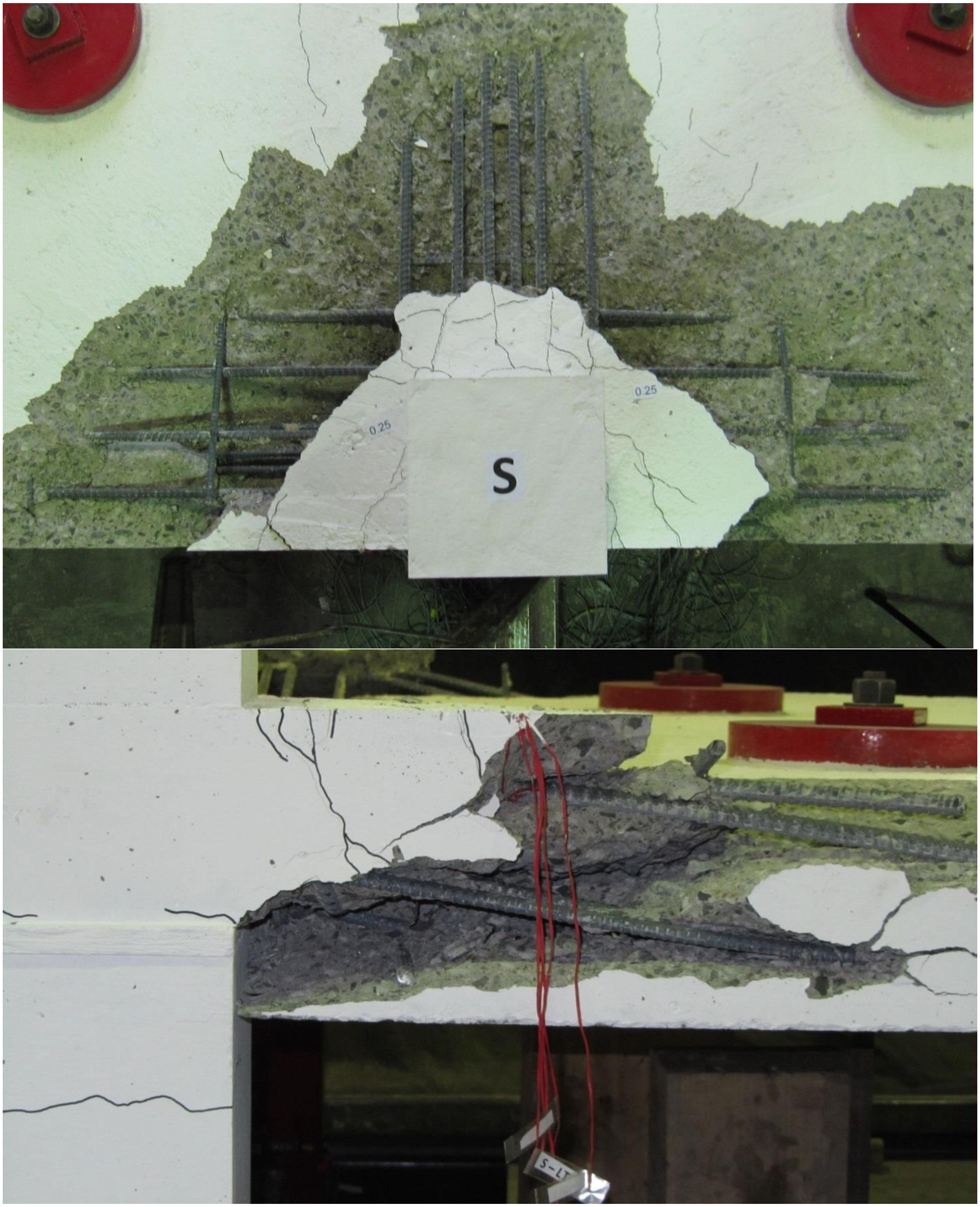

Figure 3-19: Post-punching shear condition of the edge slab-column connection S at the end of testing

Table 3-4: Summary of key load stages for edge slab-column connection S

Stage	Load (kN)	Displacement (mm)
First Cracking	55.3	0.18
First Yield (Top Bars)	NA	NA
First Yield (Structural Integrity Bars)	195.3	8.0
Punching Shear Failure	209.7	2.5
Max. Post-Punching Load	105.6	53.7

Table 3-5: Angle of top reinforcement for edge slab-column connection S

<table>
<tr><th>Steel Layout</th><th>Labels</th><th>Angle from Horizontal (Degree)</th></tr>
<tr><td rowspan="8">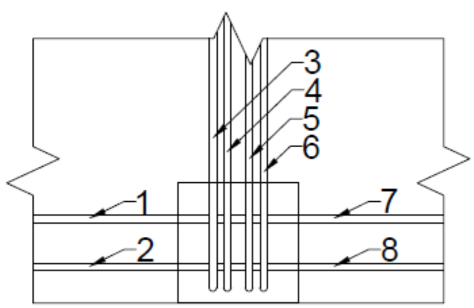</td><td>1</td><td>Free</td></tr>
<tr><td>2</td><td>9</td></tr>
<tr><td>3</td><td>10</td></tr>
<tr><td>4</td><td>10</td></tr>
<tr><td>5</td><td>10</td></tr>
<tr><td>6</td><td>10</td></tr>
<tr><td>7</td><td>Free</td></tr>
<tr><td>8</td><td>9</td></tr>
</table>

Table 3-6: Angle of structural integrity reinforcement for edge slab-column connection S

<table>
<tr><th>Steel Layout</th><th>Labels</th><th>Angle from Horizontal (Degree)</th></tr>
<tr><td rowspan="8">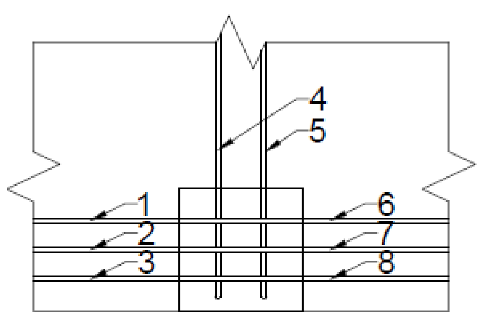</td><td>1</td><td>9</td></tr>
<tr><td>2</td><td>9</td></tr>
<tr><td>3</td><td>9</td></tr>
<tr><td>4</td><td>NA</td></tr>
<tr><td>5</td><td>NA</td></tr>
<tr><td>6</td><td>10</td></tr>
<tr><td>7</td><td>10</td></tr>
<tr><td>8</td><td>10</td></tr>
</table>

3.4.2.2 Concrete Cracking

Figure 3-21 shows the shear versus maximum crack width response for edge slab-column connection S. Flexural cracks first appeared on the top surface of the slab around the corners of the column, and spread to the edge of the slab (see Figure 3-2). As the loading progressed, more cracks appeared around the column stub, cracks also formed straight across the slab to connection N, and cracks formed on the edge surface of the slab and on the edge surface of the column (see Figure 3-3, 3-4 and 3-20). The crack width reached a maximum of 0.25 mm at edge slab-column connection S.

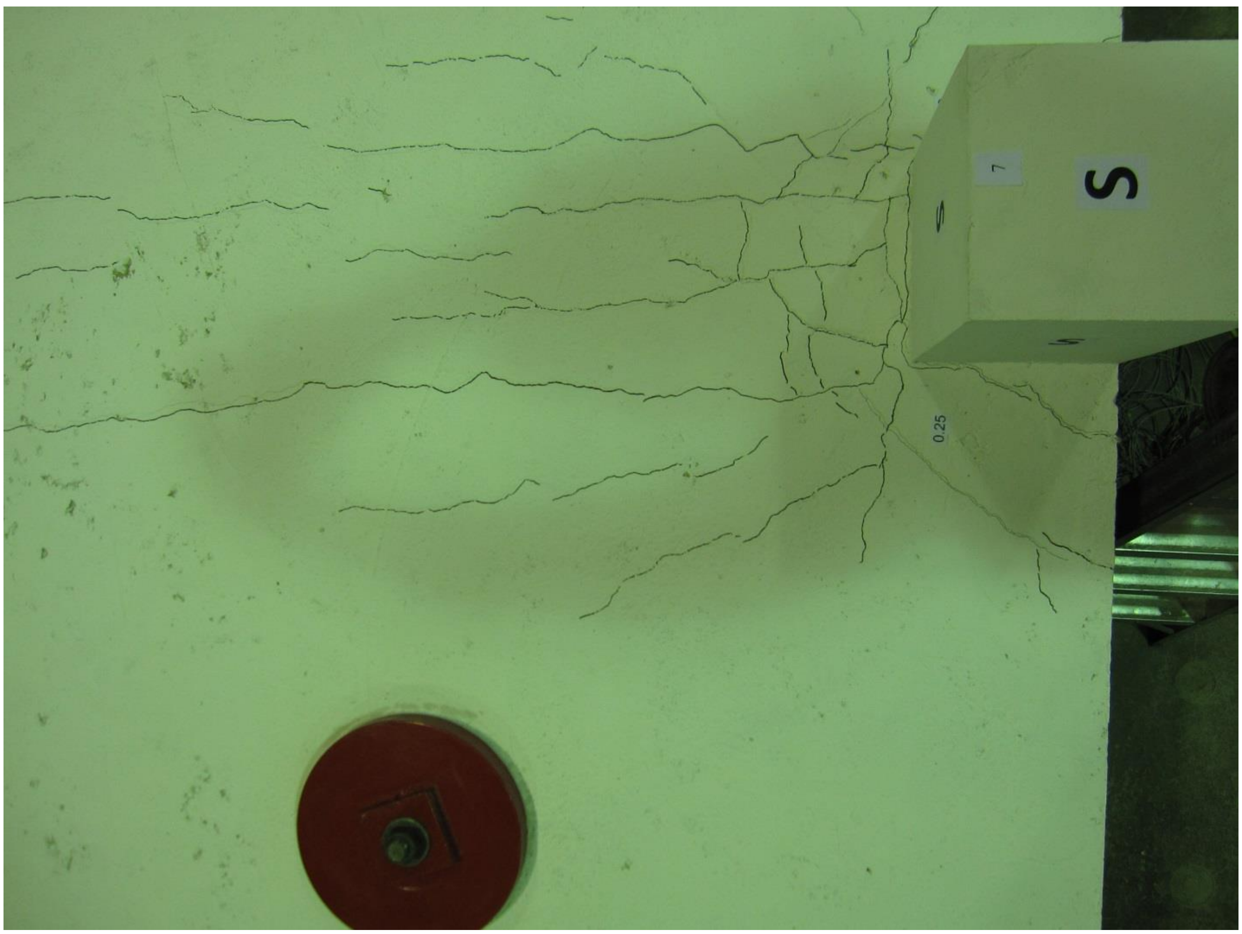

Figure 3-20: Crack pattern around edge slab-column connection S at load stage 7

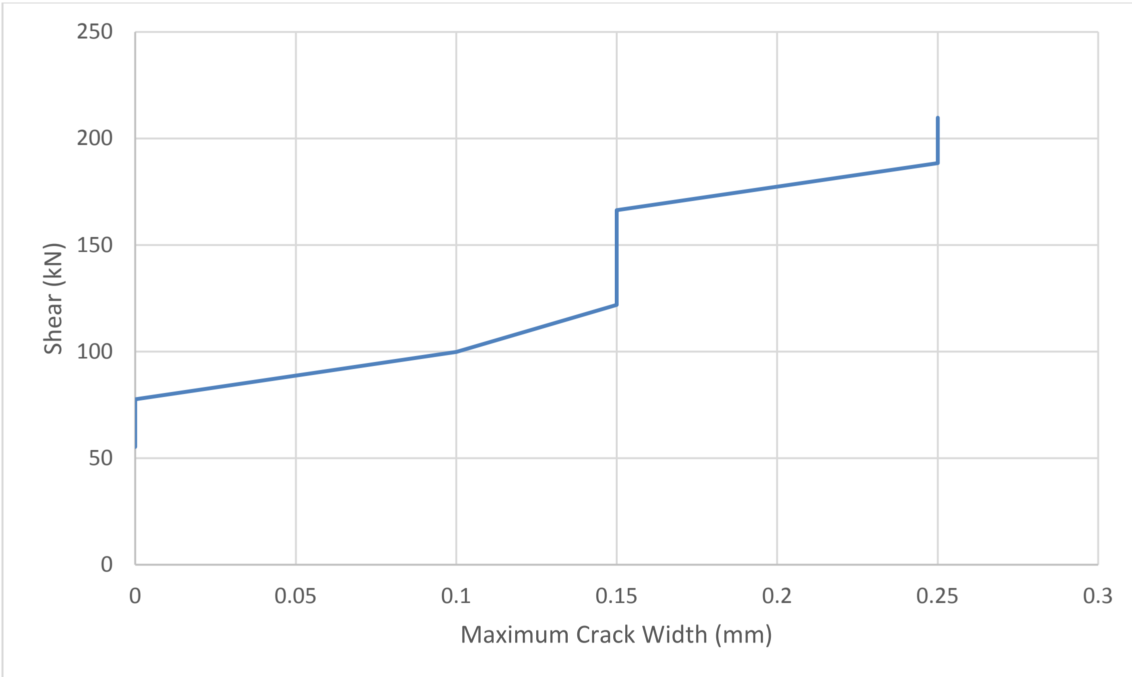

Figure 3-21: Shear vs. maximum crack width response for edge slab-column connection S

3.4.2.3 Top Reinforcement Strains

The strains development in the top reinforcement in slab-column connection S are presented in Figure 3-22. Similar to slab-column connection N, the highest strain was developed in gauge LT in the N-S outermost direction before punching shear failure. After the punching shear failure, the strain in gauge LT reduced while the strain in gauges LB1 and LB2 fluctuated in the range of 600 to 1100 με. The curves indicated that despite the breakout out from the concrete cover, the top reinforcement was able to provide limited post-punching strength to the edge slab-column connection.

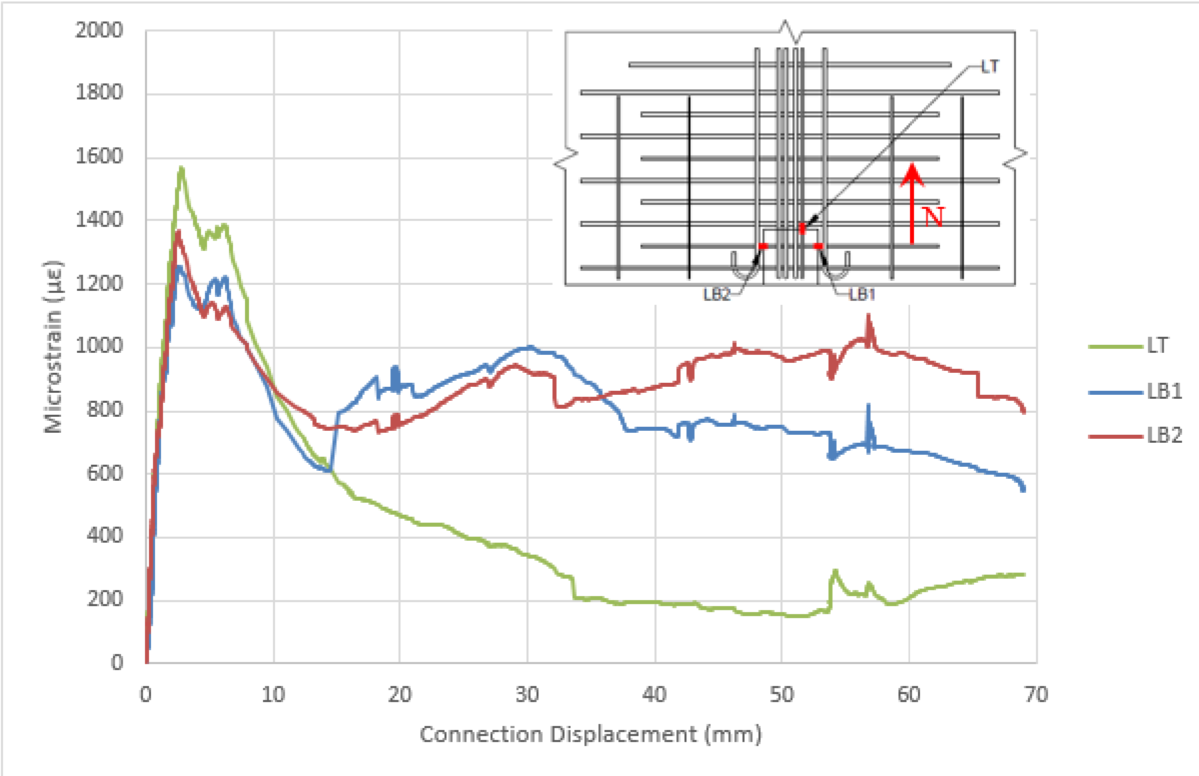

Figure 3-22: Measured strains in the top reinforcement vs. connection displacement for edge slab-column connection S

3.4.2.4 Structural Integrity Reinforcement Strains

The layout of strain gauges and the strain versus deflection responses of the selected structural integrity reinforcement on three sides of the edge slab-column connection S are shown in Figure 3-23.

Gauges located closest to the connection, including ST1, ST4 and SB1, were the first to produce noticeable strain readings before punching shear failure occurred, and were able to achieve 2260 με yield strain in the test. During the process of punching shear failure from displacement 2.5 to 6.7 mm, gauge SB1 was subjected to compression and its strain decreased to -7962 με. After punching, tension force was restored in SB1, and its strain increased rapidly and exceeded the recording range of 16000 με.

The continuation of post-punching loading resulted in damage in the strain gauges, including ST2, ST3, ST6, SB2 and SB3. It is observed that at the connection displacement of 32.5mm, the strain in ST4 peaked at 10238 με before dropping, and the strain in ST5 climbed from 0 to above 2000 με. This phenomenon indicated while the structural integrity reinforcement were providing effective support to the connection, concrete breakout had spread further away from the column stub and reached the location of gauge ST5.

The strain distribution at each load stage is shown in Figure 3-24 and 3-25. After punching shear failure of connection S, strain gauges in the N-S direction malfunctioned, and those on the E-W direction yielded at the location nearest the column. The event of punching shear failure at the west side corner slab-column connections resulted in significant increases of strain at the mid-length of the structural integrity reinforcing bars.

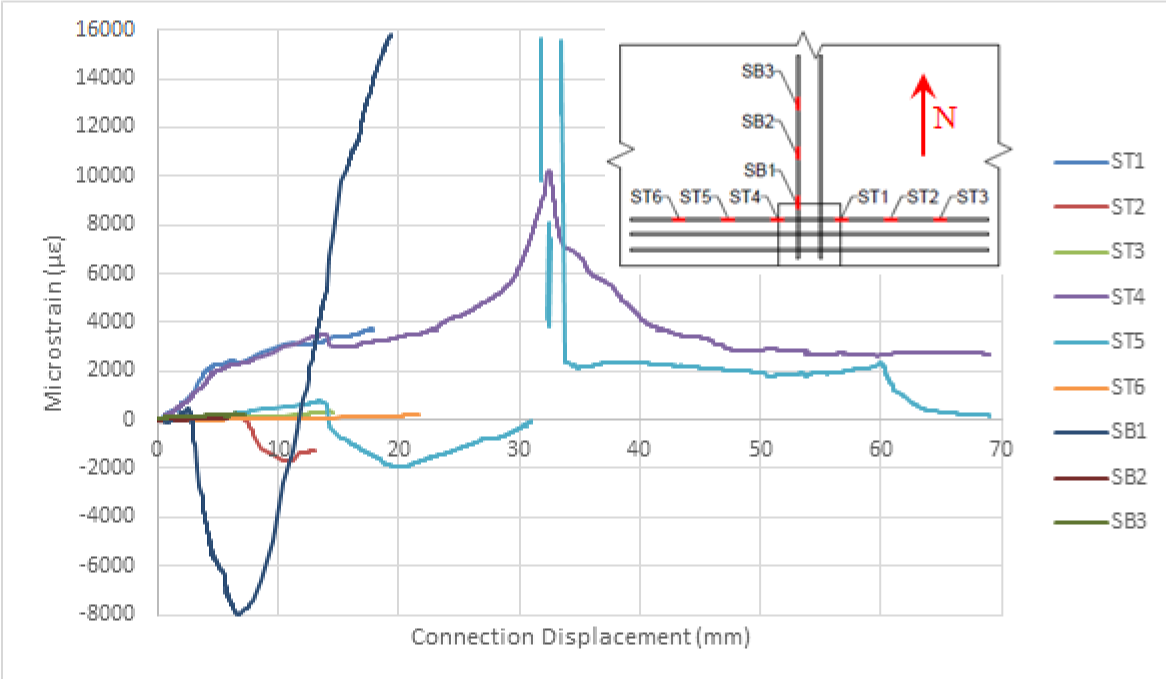

Figure 3-23: Measured strains in the structural integrity reinforcement vs. connection displacement for edge slab-column connection S

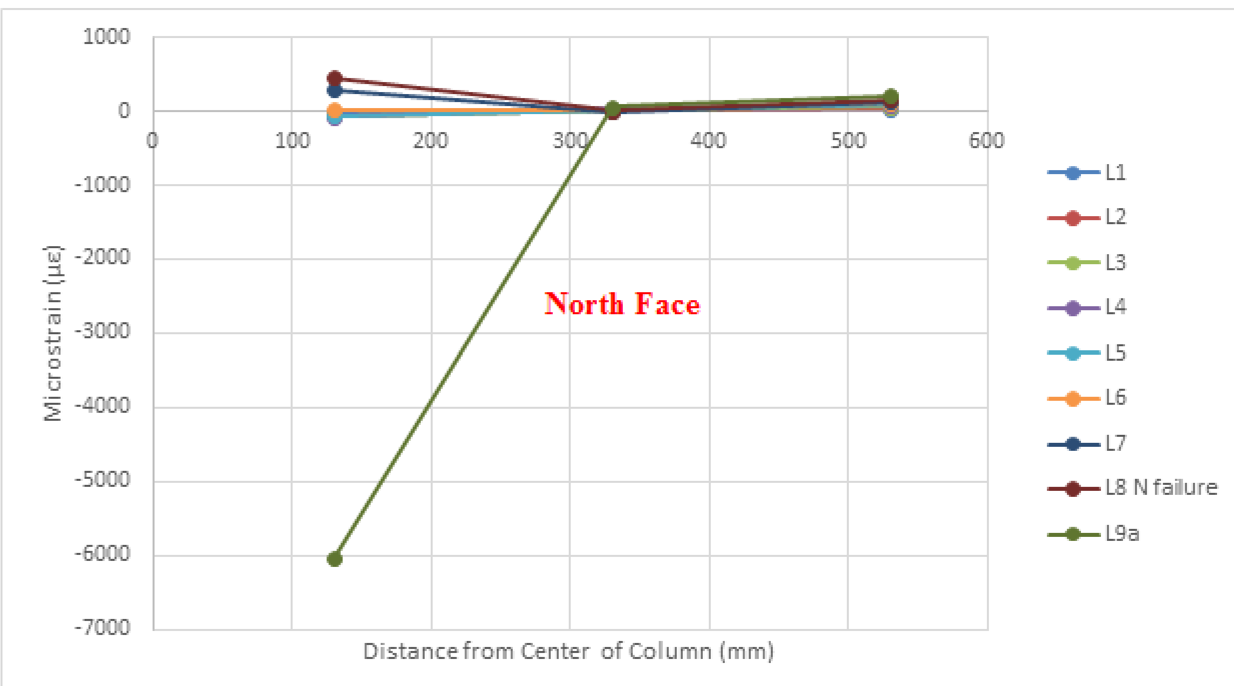

Figure 3-24: Strain distributions in the structural integrity reinforcement in the N-S direction at each load stage for edge slab-column connection S

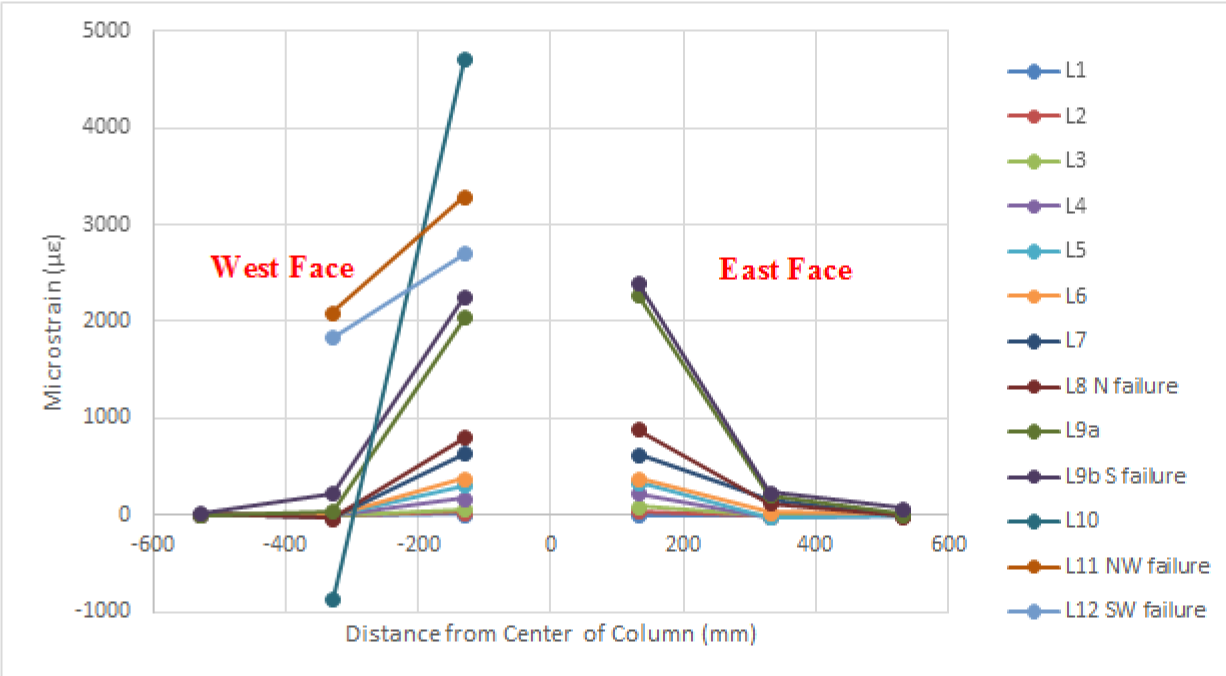

Figure 3-25: Strain distributions in the structural integrity reinforcement in the E-W direction at each load stage, for edge slab-column connection S

3.5 Corner Slab-Column Connections

3.5.1 Corner Slab-Column Connection NW

3.5.1.1 Test Results

Figure 3-26 illustrates the shear versus connection displacement response of corner slab-column connection NW. In this test, the west side corner slab-column connections failed in punching shear following punching shear failures at the two edge slab-column connections. Table 3-7 summarizes the corresponding shear and displacement data in each key load stage at slab-column connection NW.

Hairline cracking appeared on the top slab surface around the corner of the column stub, on the edge surface of the slab, and on the exterior corner at mid-height of the column at load stage 2 with a shear of 29.5 kN. At load stage 9a where edge slab-column connection N failed completely in punching, a substantial amount of load was redistributed on the north side columns, causing a spike of shear to 96.3 kN at slab-column connection NW at the connection displacement of 3.3 mm. Punching shear failure at edge slab-column connection S diminished the load spike, and response curve of NW resumed stable until a shear cracking pattern occurred at load stage 11 at a peak shear of 90.9 kN and a displacement of 5.2 mm (see Figure 3-8).

The gradual reduction of shear after the peak load represented the slow process of shear cracking within corner slab-column connection NW. Punching shear failure occurred at a displacement of 11.8 mm and the shear at the connection fell sharply from 71.6 kN to 50.9 kN.

The post-punching loading activity produced a relatively flat response, with shears in the range of 45 to 55 kN.

Inspection was done after loose concrete was removed from the connection (see Figure 3-27). The final inclinations of the top reinforcement and the structural integrity reinforcing bars are presented in Table 3-8 and Table 3-9, respectively. The average values of angle from horizontal are 11.6 degrees for the top reinforcement, and 14.8 degrees for the structural integrity reinforcing bars.

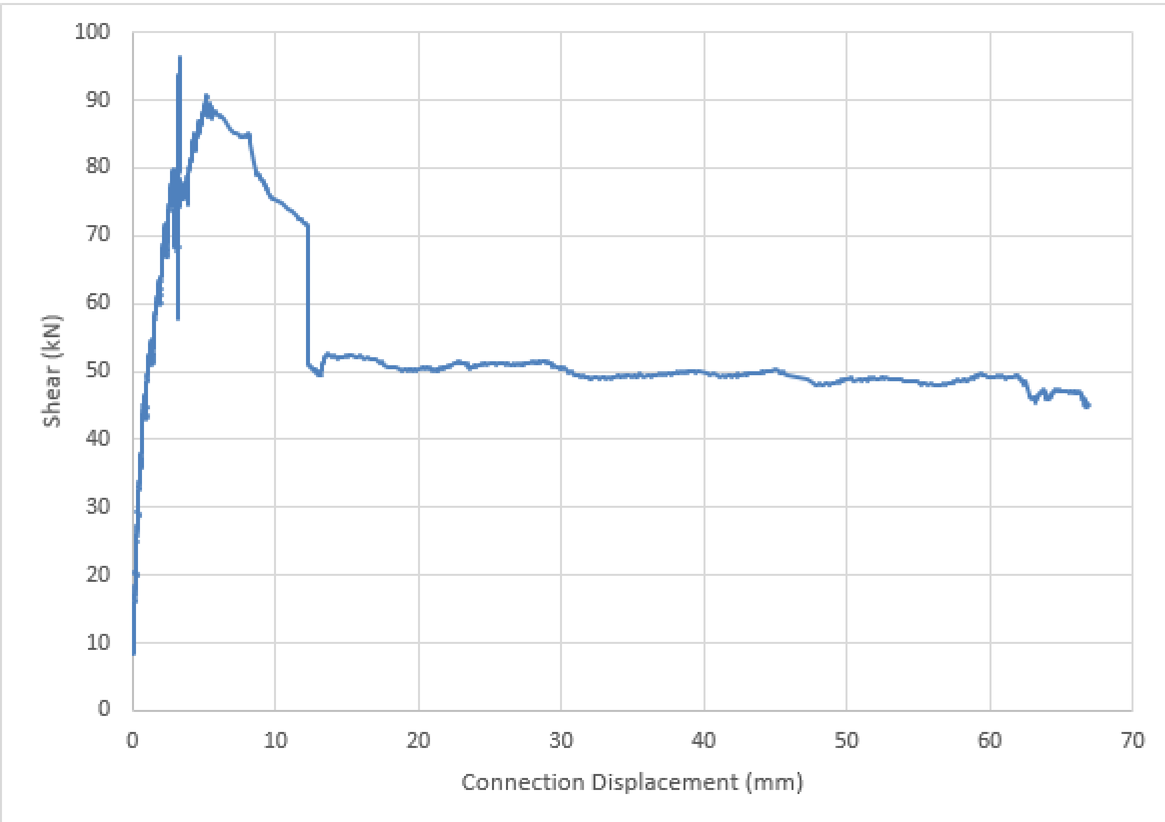

Figure 3-26: Shear vs. connection displacement curve for corner slab-column connection NW

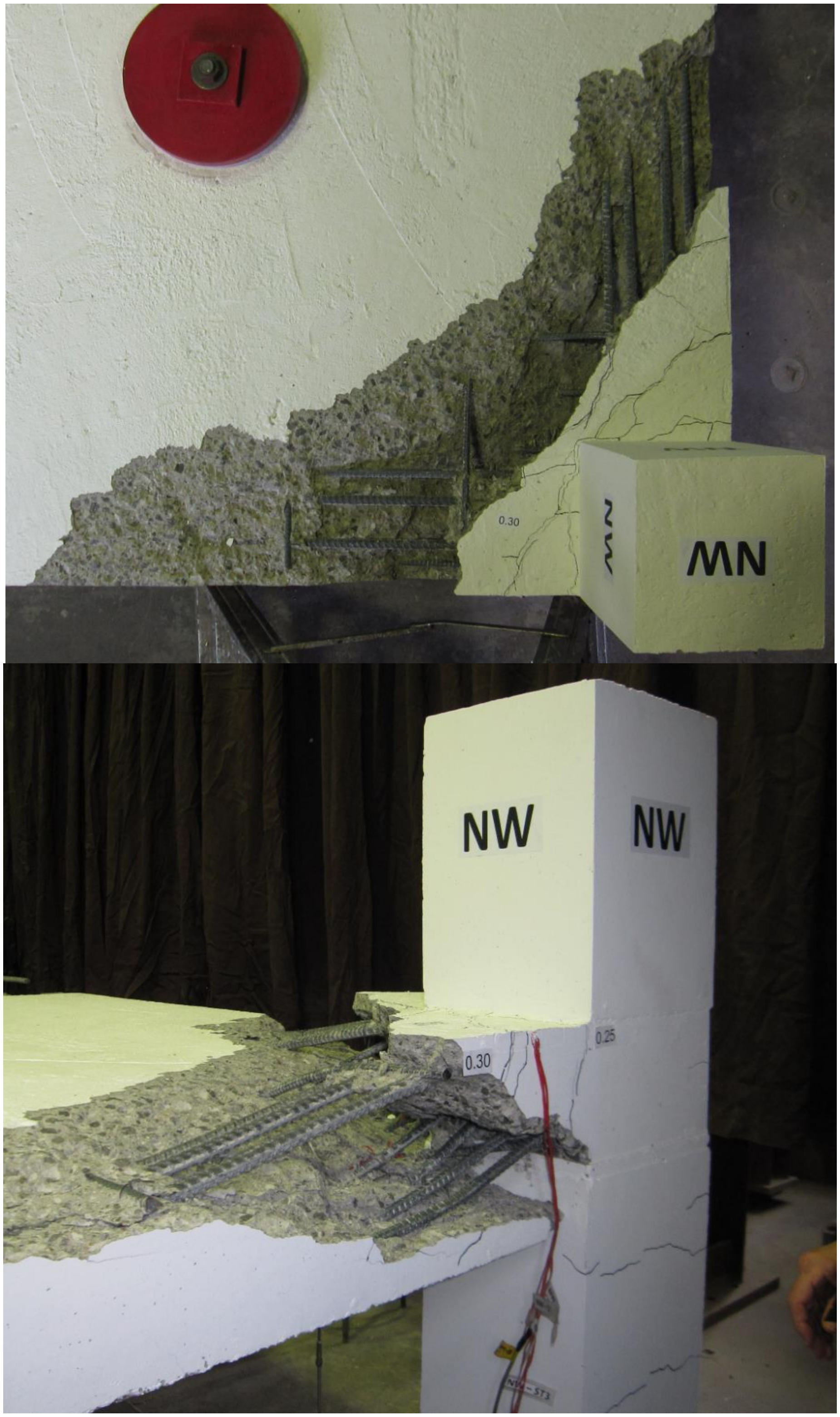

Figure 3-27: Post-punching shear condition of the corner slab-column connection NW at the end of testing

Table 3-7: Summary of key load stages for corner slab-column connection NW

Stage	Load (kN)	Displacement (mm)
First Cracking	29.5	0.37
First Yield (Top Bars)	75.8	3.6
First Yield (Structural Integrity Bars)	NA	NA
Punching Shear Failure	90.9	5.2
Max. Post-Punching Load	52.5	13.7

Table 3-8: Angle of top reinforcement for corner slab-column connection NW

<table>
<tr><th>Steel Layout</th><th>Labels</th><th>Angle from Horizontal (Degree)</th></tr>
<tr><td rowspan="7">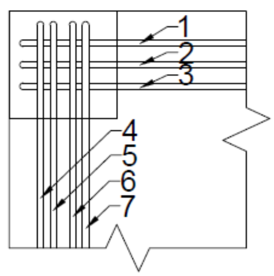
</td><td>1</td><td>13</td></tr>
<tr><td>2</td><td>13</td></tr>
<tr><td>3</td><td>12</td></tr>
<tr><td>4</td><td>10</td></tr>
<tr><td>5</td><td>10</td></tr>
<tr><td>6</td><td>12</td></tr>
<tr><td>7</td><td>11</td></tr>
</table>

Table 3-9: Angle of structural integrity reinforcement for corner slab-column connection NW

<table>
<tr><th>Steel Layout</th><th>Labels</th><th>Angle from Horizontal (Degree)</th></tr>
<tr><td rowspan="4">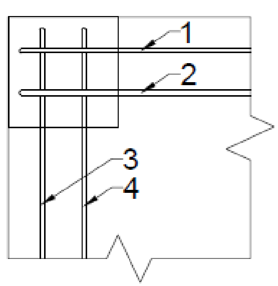
</td><td>1</td><td>12</td></tr>
<tr><td>2</td><td>20</td></tr>
<tr><td>3</td><td>12</td></tr>
<tr><td>4</td><td>15</td></tr>
</table>

3.5.1.2 Concrete Cracking

Figure 3-29 shows the shear versus maximum crack width curve for corner slab-column connection NW. Flexural cracks were observed on the top slab surface around the column stub, slab edge surface and column exterior faces (see Figure 3-3). As loading progressed, more cracks were produced diagonally across the slab at the location in front of the column stub (see Figure 3-28). The cracks reached a maximum width of 0.30 mm at load stage 8 where punching shear failure initiated at edge connections N and S. With further progression of loading the number of cracks increased. However, the maximum crack width still remained at 0.3 mm until shear failure occurred at corner slab-column connection NW.

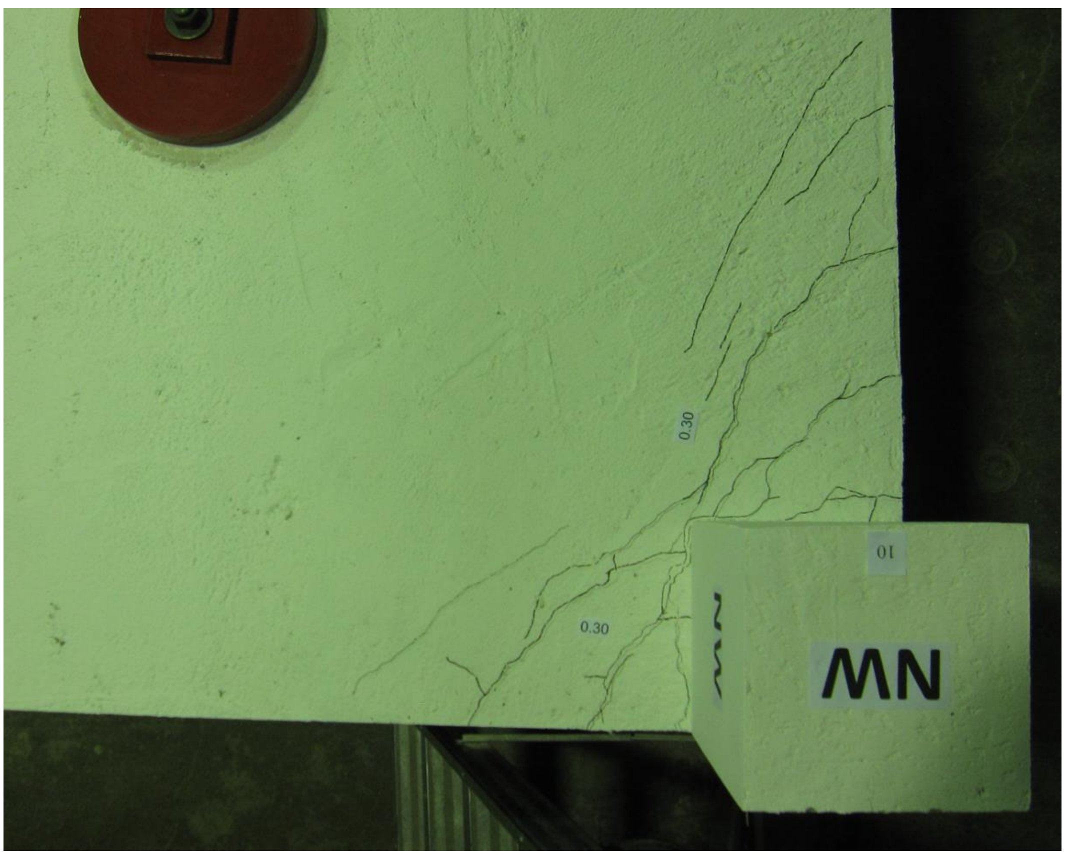

Figure 3-28: Crack pattern around corner slab-column connection NW at load stage 10

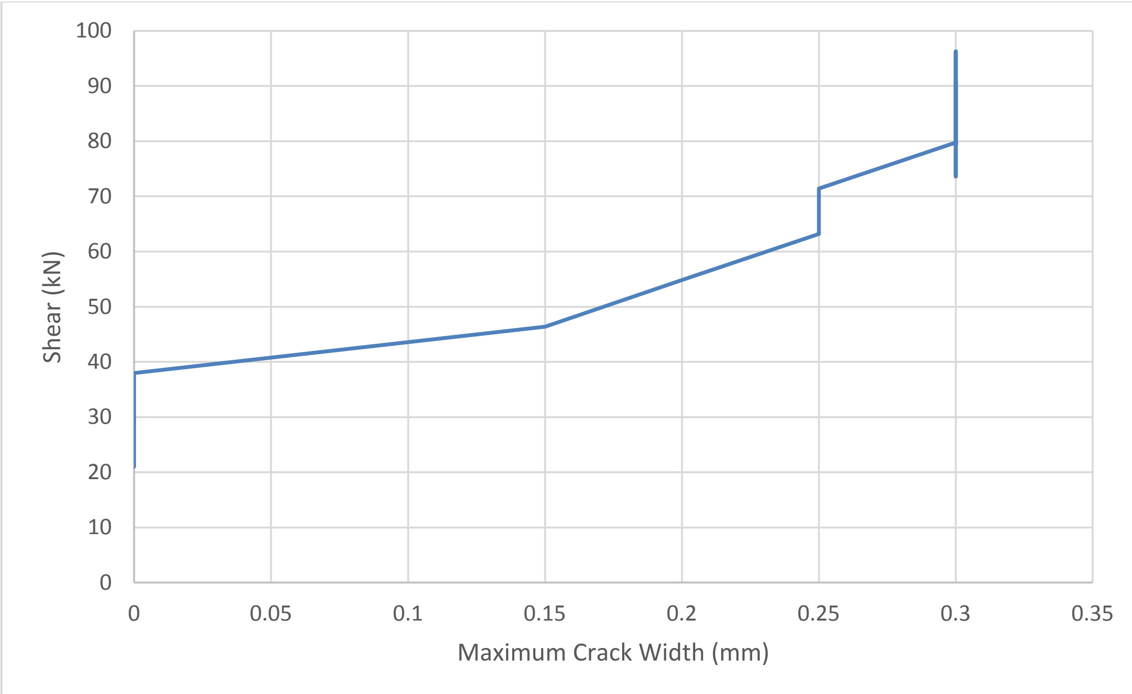

Figure 3-29: Shear vs. maximum crack width response for corner slab-column connection NW

3.5.1.3 Top Reinforcement Strains

Figure 3-30 presents the measured strains in the top reinforcement versus connection displacement responses of corner slab-column connection NW. The strain in both gauges LT and LB increased uniformly until the slab displacement close to the connection reached 2.9 mm where punching shear failure started at the edge slab-column connections. The resulting downward displacement of the center of slab imposed higher moment on the east face of corner connection NW. Hence, strain gauge LB positioned in the E-W direction experienced a sudden increase in strain, reaching the yield strain of 2260 με at the displacement of 3.6 mm and exceeding the upper recording limit of 16000 με at a displacement of 4.8 mm.

On the other hand, the slab region between connections NW and SW underwent smaller displacements. With less moment induced on the south face of the slab-column connection, gauge LT had a relatively flat response. Following shear failure at corner slab-column connection NW, the post-punching strain in gauge LT was stabilized in the range of 507 to 619 με.

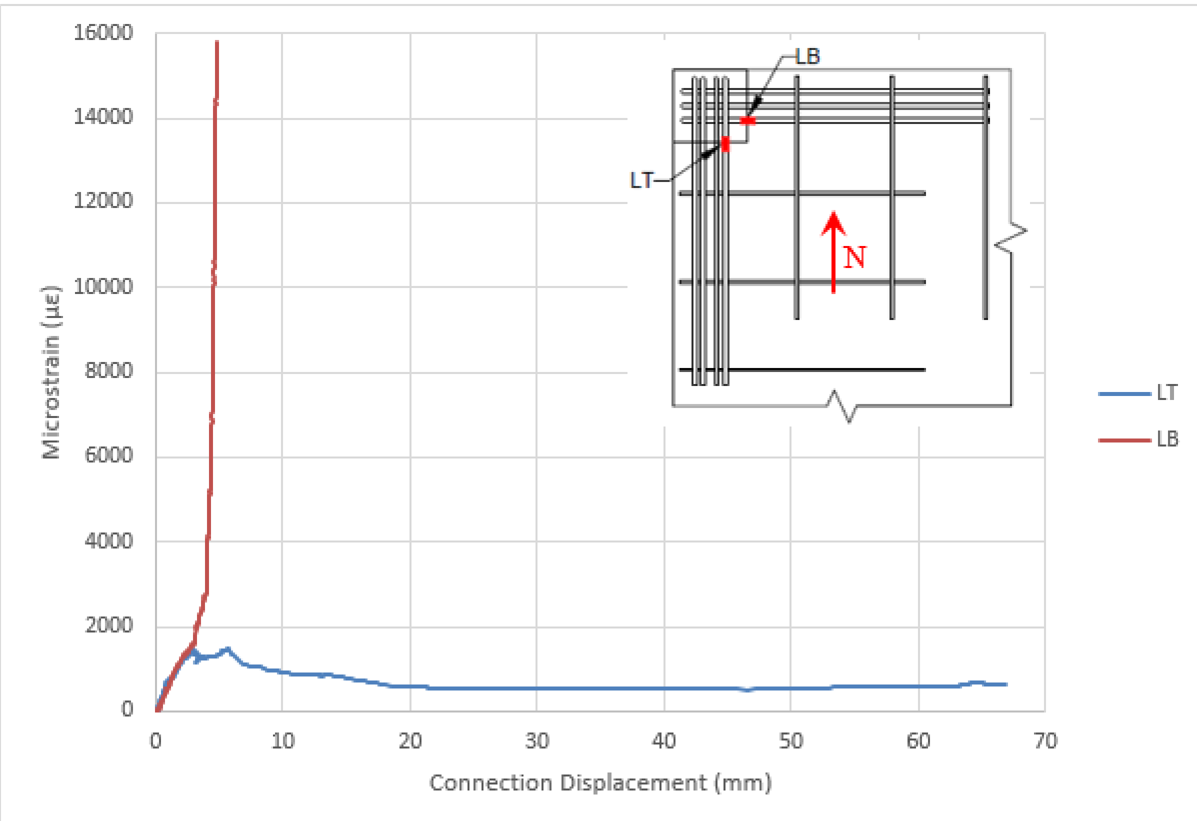

Figure 3-30: Measured strains in the top reinforcement vs. connection displacement for corner slab-column connection NW

3.5.1.4 Structural Integrity Reinforcement Strains

The strain gauge locations and the measured strains in the structural integrity reinforcing bars versus displacement responses for corner slab-column connection NW are shown in Figure 3-31.

Gauges ST1 and SB1, located closest to the column, were the first two strain gauges that showed a significant increase of strain. At the displacement of 2.4 mm, there was a sudden increase of strain in gauge ST2, suggesting that the integrity reinforcement at this location was subjected to tension in the early stage. When shear cracking started at corner connection NW at a displacement of 5.2 mm, a substantial decrease in strains were observed at the gauges close to the connection, including gauges ST1, SB1 and ST2.

After punching shear failure of the connection, the tendency of strain re-increase was observed in gauges ST3, SB1, SB2 and SB3. The regain of strain upon post-punching loading activity indicated that the structural integrity reinforcement were effective in providing secondary support to connection NW. Strain gauges ST3, SB1, SB2 and SB3 achieved maximum strains after punching at 357 $\mu\varepsilon$, 954 $\mu\varepsilon$, 872 $\mu\varepsilon$ and 222 $\mu\varepsilon$, respectively.

The strain distribution at each load stage is given in Figure 3-32 and 3-33. In the N-S direction, the gauges located nearest to the column responded with the highest strain in all of the load stages, and the overall strain in the structural integrity reinforcement increased progressively (see Figure 3-32). In the E-W direction, it can be seen that the effect of punching shear failure at the edge slab-column connections resulted in the malfunctioning of strain gauge ST2 at load stage 9 (see Figure 3-33).

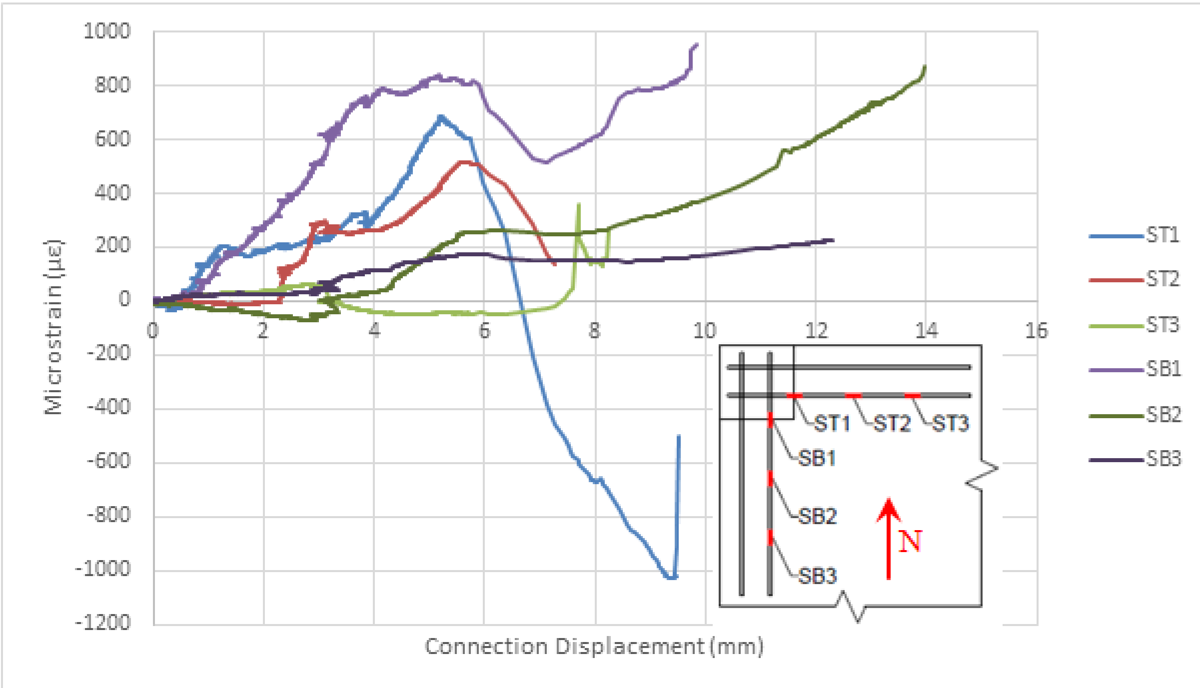

Figure 3-31: Measured strains in the structural integrity reinforcement vs. connection displacement for corner slab-column connection NW

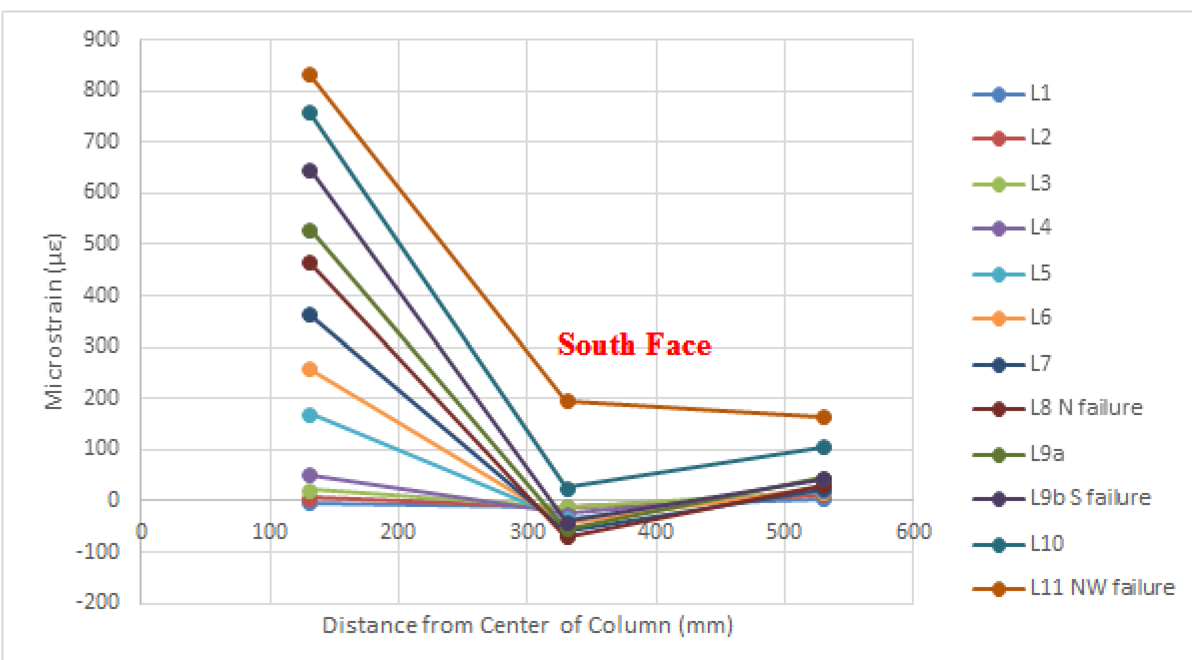

Figure 3-32: Strain distributions in the structural integrity reinforcement in the N-S direction at each load stage for corner slab-column connection NW

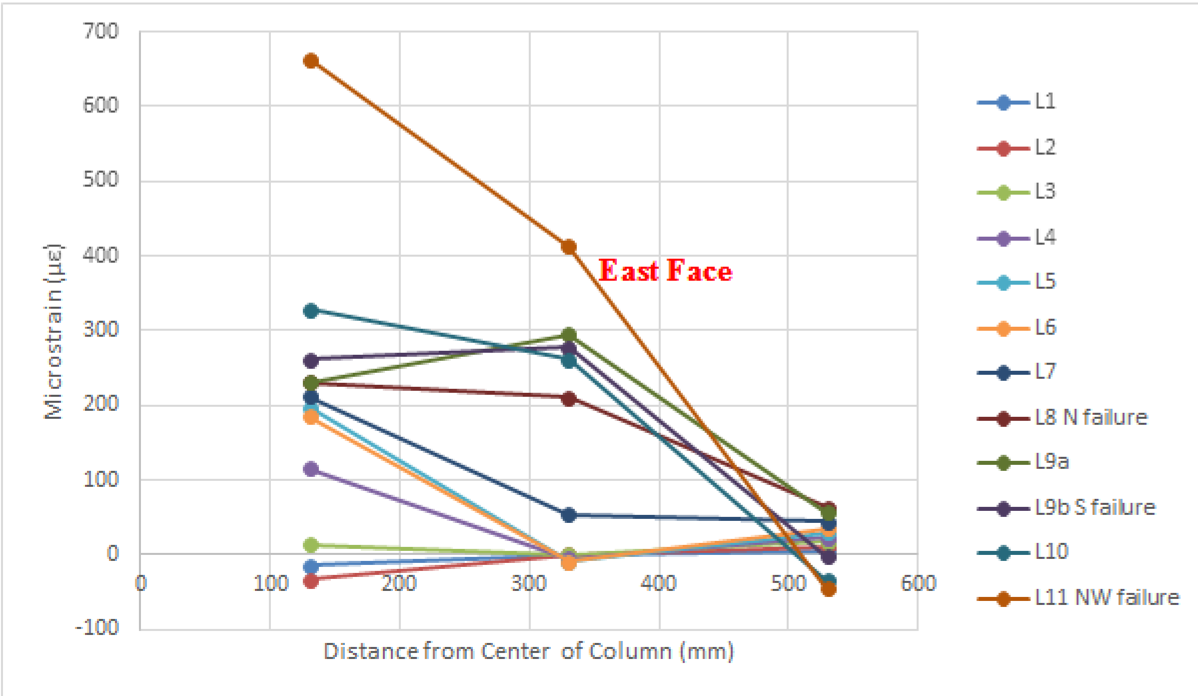

Figure 3-33: Strain distributions in the structural integrity reinforcement in the E-W direction at each load stage for corner slab-column connection NW

3.5.2 Corner Slab-Column Connection SW

3.5.2.1 Test Results

Figure 3-34 shows the shear versus connection displacement response of corner slab-column connection SW. Connection SW failed in punching shear after punching shear failure at slab-column connection NW. The data in key stages of this process, including shear and connection displacement, are presented in Table 3-10.

Hairline cracking was observed on the top of the slab around the corner of the column stub at load stage 2 at a shear of 29.3 kN. At load stage 9, due to the punching shear failure occurring at edge connection N which caused load redistribution to the north side corner columns, there was a sudden load reduction in slab-column connection SW to 44.6 kN at a displacement of 3.3 mm. The additional punching shear failure of edge slab-column connection S resulted in further redistribution of the loads to the corner slab-column connections. Due to this event, the shear in slab-column connection SW increased to 65.9 kN.

Torsional cracking occurred at corner slab-column connection SW at load stage 11 with a shear of 87.0 kN and a connection displacement of 5.5 mm. Torsional cracks can be observed diagonally across the slab surface, and only on the south edge of the slab (see Figure 3-9). Slab-column connection SW failed in punching at load stage 12 with a shear of 83.5 kN and a deflection of 9.2 mm.

The post-punching resistance of slab-column connection SW stabilized in the range of 46.5 to 51.8 kN until the end of test.

Inspection was done on the condition of the reinforcement after removal of loose concrete (see Figure 3-35). The post-punching inclinations of the top reinforcement and the structural integrity reinforcement are presented in Table 3-8 and Table 3-9, respectively. The average angles from horizontal are 10.0 degrees for the top reinforcement, and 18.0 degrees for the structural integrity reinforcing bars.

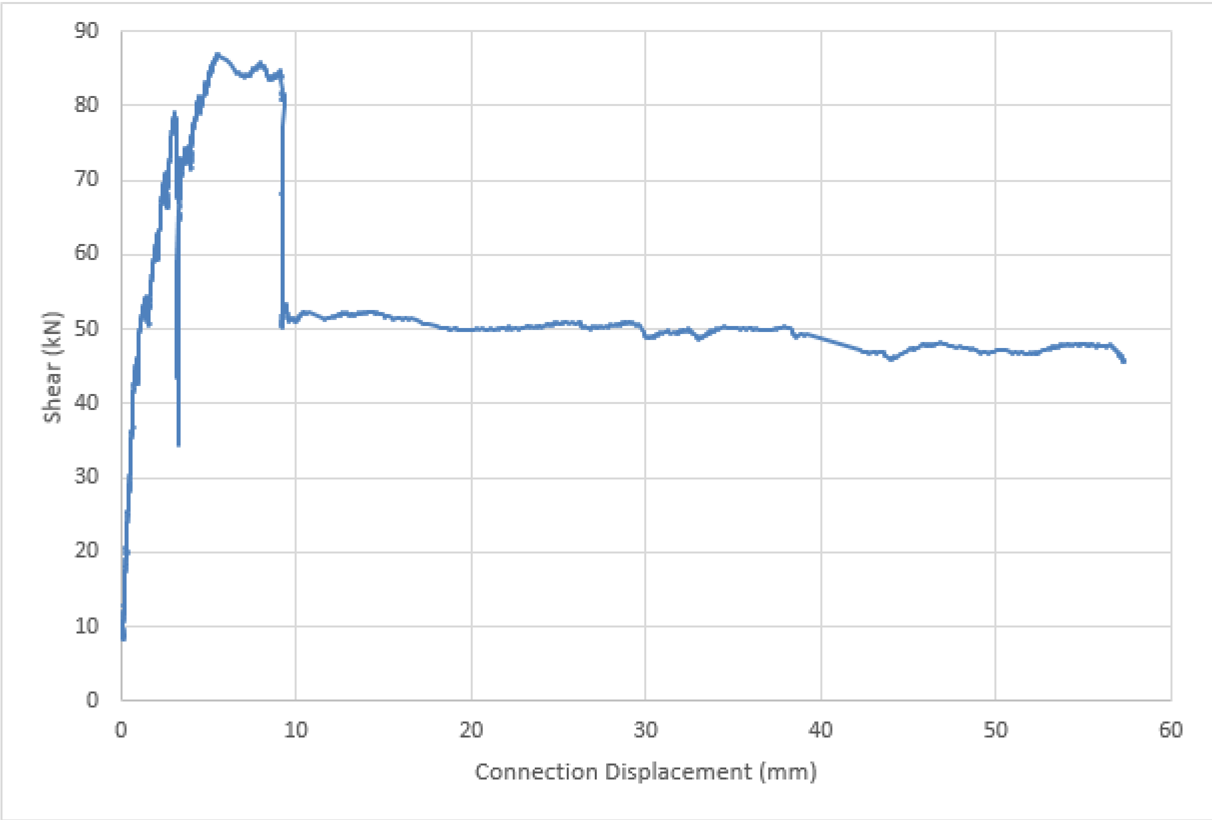

Figure 3-34: Shear vs. connection displacement curve for corner slab-column connection SW

Figure 3-35: Post-punching shear condition of the corner slab-column connection SW at the end of testing

Table 3-10: Summary of key load stages for corner slab-column connection SW

Stage	Load (kN)	Displacement (mm)
First Cracking	29.3	0.47
First Yield (Top Bars)	78.1	4.2
First Yield (Structural Integrity Bars)	NA	NA
Punching Shear Failure	87.0	5.5
Max. Post-Punching Load	53.5	9.3

Table 3-11: Angle of top reinforcement for corner slab-column connection SW

<table>
<tr><th>Steel Layout</th><th>Labels</th><th>Angle from Horizontal (Degree)</th></tr>
<tr><td rowspan="7">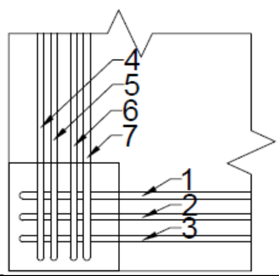
</td><td>1</td><td>12</td></tr>
<tr><td>2</td><td>12</td></tr>
<tr><td>3</td><td>13</td></tr>
<tr><td>4</td><td>Free</td></tr>
<tr><td>5</td><td>7</td></tr>
<tr><td>6</td><td>8</td></tr>
<tr><td>7</td><td>8</td></tr>
</table>

Table 3-12: Angle of structural integrity reinforcement for corner slab-column connection SW

<table>
<tr><th>Steel Layout</th><th>Labels</th><th>Angle from Horizontal (Degree)</th></tr>
<tr><td rowspan="4">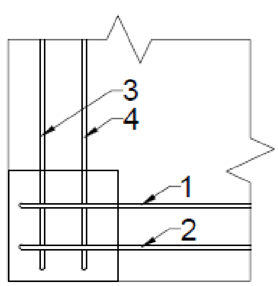
</td><td>1</td><td>21</td></tr>
<tr><td>2</td><td>18</td></tr>
<tr><td>3</td><td>15</td></tr>
<tr><td>4</td><td>NA</td></tr>
</table>

3.5.2.2 Concrete Cracking

Figure 3-37 presents the shear versus maximum crack width response for corner slab-column connection SW. Flexural cracks originated on the top slab surface around the corner of the column stub and extended diagonally towards the edge of slab. Increased loading resulted in cracks forming on the edge faces of the slab and on the exterior faces of the column (see Figure 3-3 and 3-36). The growth of crack widths stopped at a maximum of 0.30 mm at load stage 8 where edge slab-column connections N and S began to fail in punching shear. Load stages following the punching shear failures of the edge slab-column connections N and S resulted in an increase in the number of cracks with no increase in the maximum crack width.

Figure 3-36: Crack pattern around corner slab-column connection SW at load stage 10

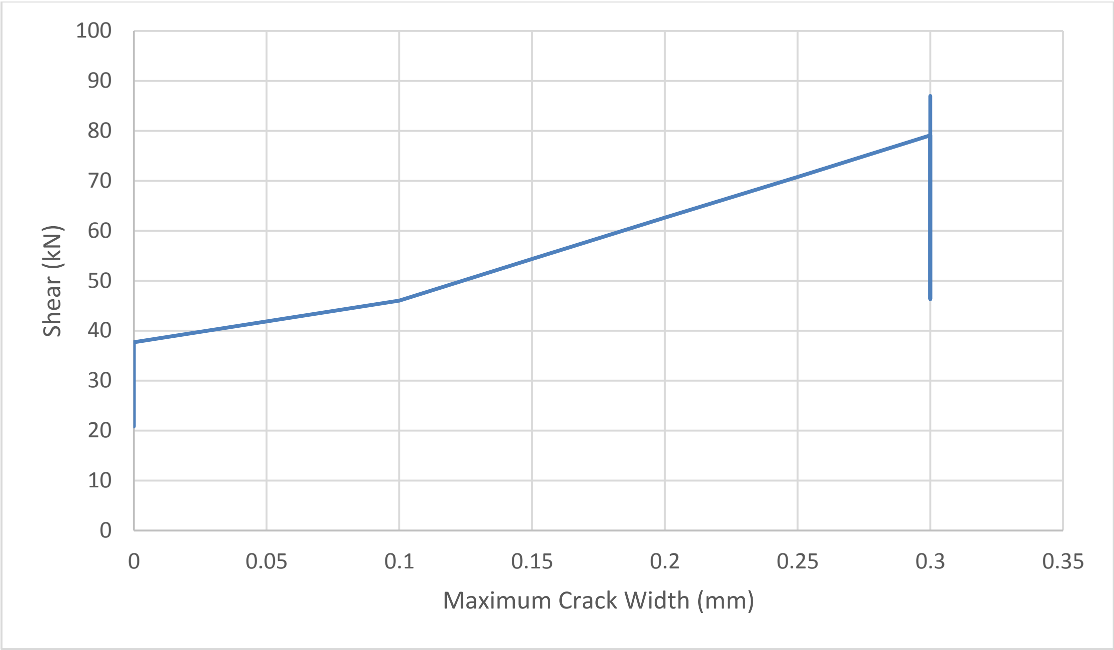

Figure 3-37: Shear vs. maximum crack width response for corner slab-column connection SW

3.5.2.3 Top Reinforcement Strains

Figure 3-38 shows the measured strains in the top reinforcement versus connection displacement responses in corner slab-column connection SW. The previous event of punching failure at the edge slab-column connections introduced a higher moment on the east face of west side corner connections. Therefore, the top reinforcement in the E-W direction responded with significant higher strains.

Gauge LB reached the yield strain of 2260 με at the beginning of shear cracking at connection NW. Both gauges, LT and LB, reached their maximum strain before punching shear failure occurred in slab-column connection SW at 1482 με and 3831 με, respectively.

Following the reduction of strain corresponding to the event of punching failure, the post-punching loading activity was unable to re-increase the overall strain in the top reinforcement.

This suggests that the breakout of the concrete cover limited the top reinforcement from providing effective post-punching strength to the connection.

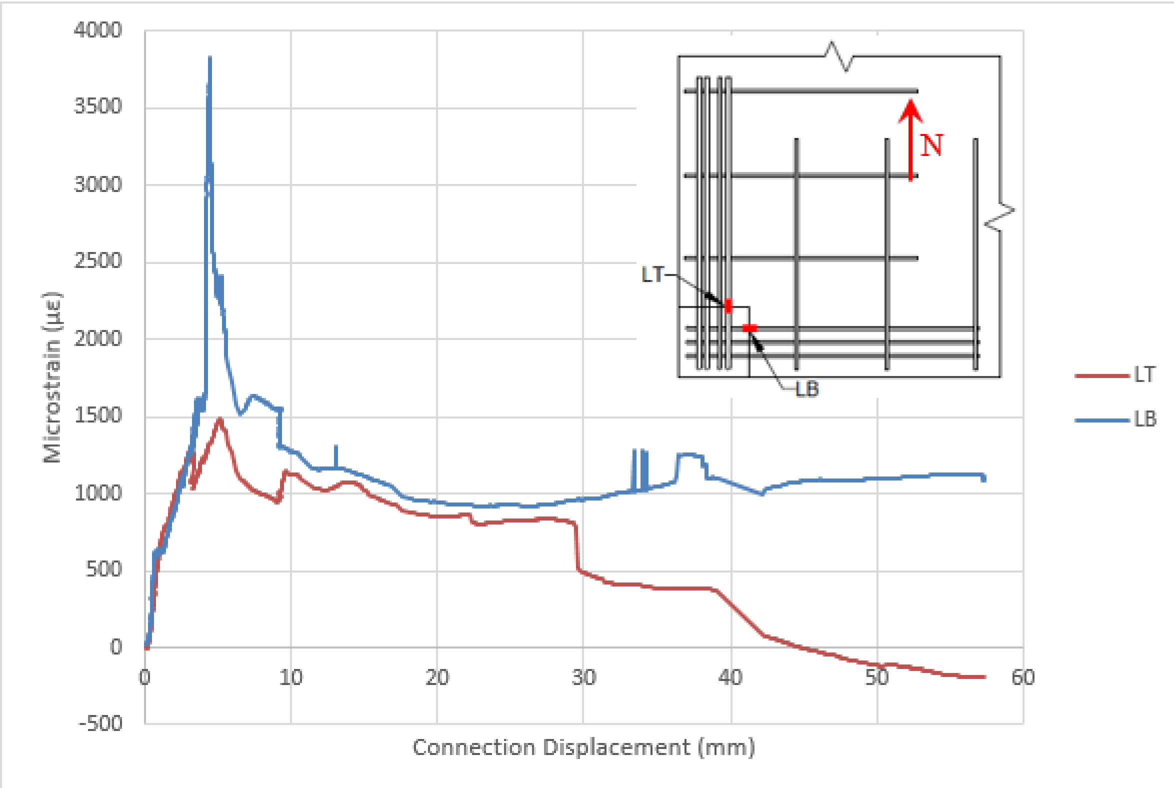

Figure 3-38: Measured strains in the top reinforcement vs. connection displacement for corner slab-column connection SW

3.5.2.4 Structural Integrity Reinforcement Strains

There were six strain gauges placed on two selected structural integrity reinforcing bars at corner slab-column connection SW. The measured strains in the structural integrity reinforcement versus connection displacement responses are shown in Figure 3-39. None of the strain gauges indicated yielding during testing.

Gauge ST1 was the only strain gauge that showed active response during the test due to the higher moment that occurred at the east face of the connection. In Figure 3-9, it could be observed that only inclined torsional cracking appeared on the south edge of the slab prior to complete punching shear failure. This cracking pattern caused gauge ST1, in the E-W direction, to reach an early peak strain of 1312 $\mu\varepsilon$ at a displacement of 5.3 mm. In the N-S direction, a peak strain of 1343 $\mu\varepsilon$ in gauge SB1 was reached at a displacement of 9.0 mm due to the delay of shear cracking on the west face of the slab.

The strain gauges were damaged as the shear cracks widened. The recording device was unable to detect whether the structural integrity reinforcement could reach yield strain after punching. However, strain gauges ST1, ST2, ST3, SB2 and SB3 showed traces of strain regain after the punching failure.

The strain distribution at each load stage was plotted in Figure 3-40 and 3-41. Most of the strain was developed in the region of the integrity reinforcement located closest to the face of the connection.

Due to the smaller moment occurring on the north face of the corner slab-column connection, the strain in gauge SB1 was low, below 200 $\mu\varepsilon$, until punching shear cracking started at corner slab-column connection NW (see Figure 3-41). On the other hand, the strain in gauge ST1 increased progressively as loading progressed.

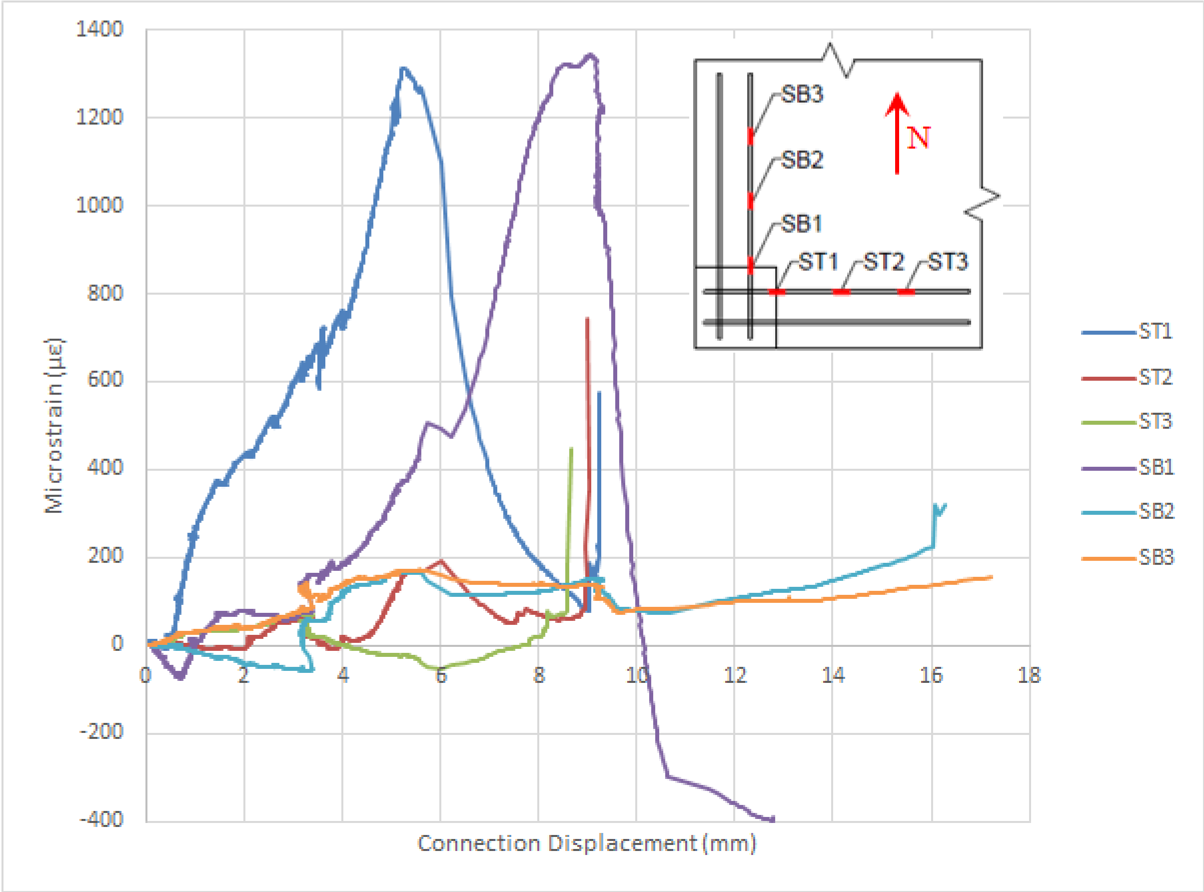

Figure 3-39: Measured strains in the structural integrity reinforcement vs. connection displacement for corner slab-column connection SW

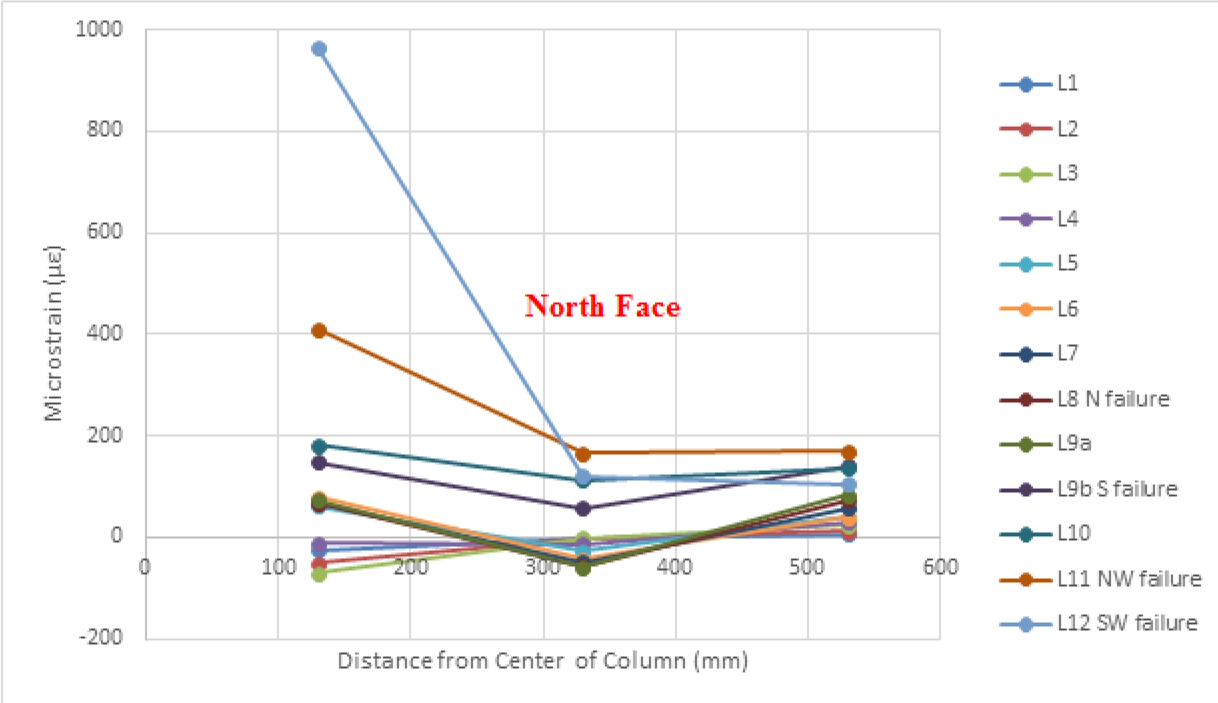

Figure 3-40: Strain distributions in the structural integrity reinforcement in the N-S direction at each load stage for corner slab-column connection SW

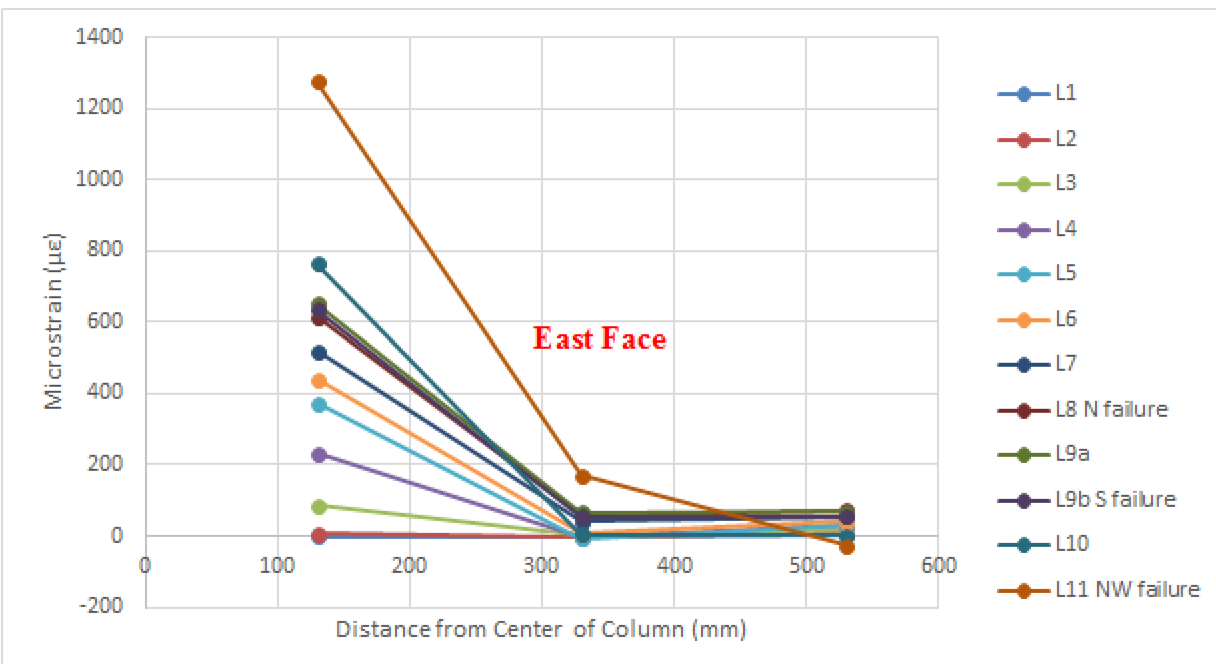

Figure 3-41: Strain distributions in the structural integrity reinforcement in the E-W direction at each load stage for corner slab-column connection SW

3.5.3 Corner Slab-Column Connection NE

3.5.3.1 Test Results

Punching shear failure procedure of east side corner connections was conducted in Part 2 of the test. Instead of uniform load covering the whole slab system, the incremental load was only applied by two hydraulic jacks adjacent to east-side corner connections. Figure 3-42 presents the shear versus connection displacement response of corner slab-column connection NE. The data in key stages of the test, including shear and connection displacement, are shown in Table 3-13.

Hairline cracking was observed on the slab surface around the corner of the column stub and extended to the edge of slab at load stage 2 at a shear of 32.0 kN. The response of corner connection NE in Part 1 of the test is similar to the response of corner slab-column connection NW. The failure of edge connection N during stage 9 resulted in a sudden increase in the shear to 100.7 kN at a deflection of 3.9 mm.

The pause between Part 1 and Part 2 loading of the test resulted in an increase in deflections. The shear on slab-column connection NE was reduced to 41.3 kN.

In Part 2 of the loading, corner slab-column connection NE was loaded until failure. Unlike other connections that experienced a delay between initiation of shear cracking and the punching shear failure, connection NE failed in punching immediately after reaching a peak shear of 107.4 kN at a displacement of 7.7 mm. This could be attributed to the concentration of applied load near the east side corner connections, resulting in a sudden punching shear failure at corner slab-column connection NE.

In the post-punching response of connection NE, the failure of slab-column connection SE is apparent at a deflection of 54.6 mm as a sharp drop in shear from 50.6 kN to 39.2 kN. After this event, the shear in connection NE regained slightly and reached a maximum post-punching shear of 53.2 kN at a connection displacement of 76.0 mm.

Inspection was done on the condition of the reinforcement after removal of the loose concrete. Complete ripping out of the top reinforcing bars was observed on the south face of the connection (see Figure 3-43). The post-punching inclinations of the top reinforcement and the structural integrity reinforcement are presented in Table 3-14 and 3-15, respectively. The average angles from horizontal are 14.0 degrees for the top reinforcement, and 20.0 degrees for the structural integrity reinforcing bars.

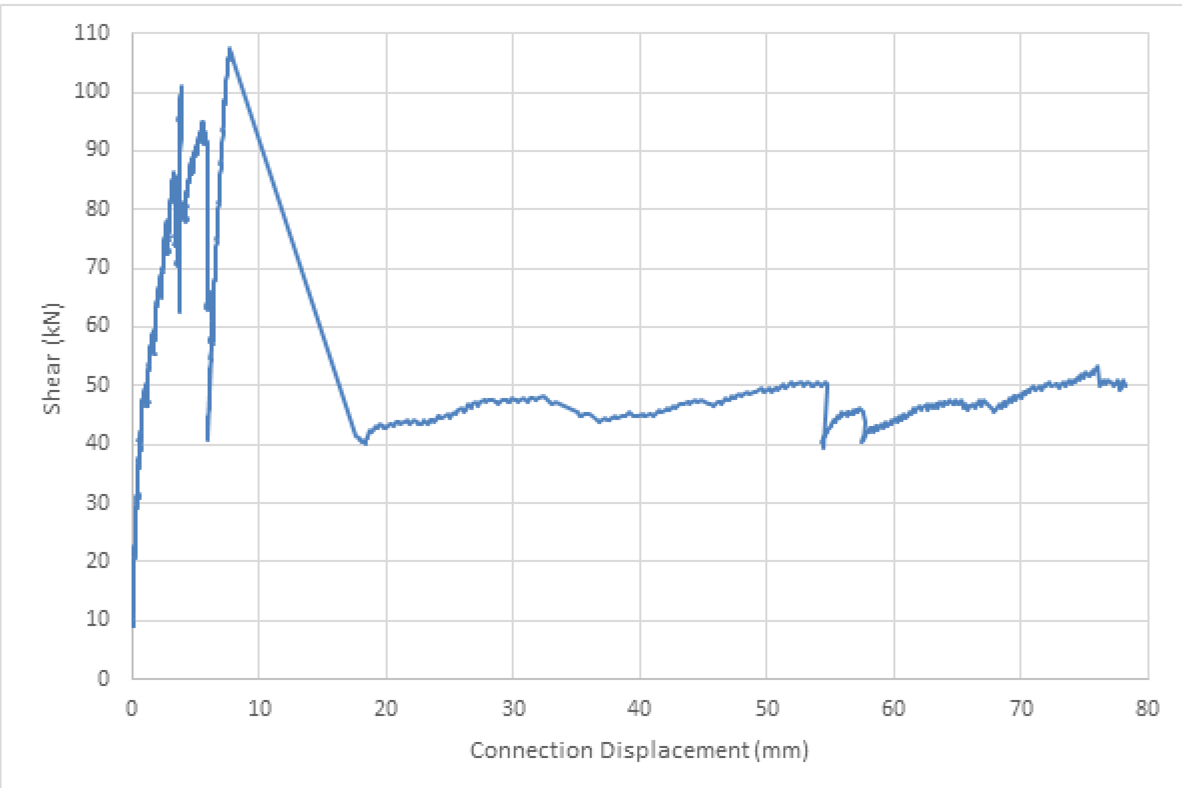

Figure 3-42: Shear vs connection displacement curve for corner slab-column connection NE

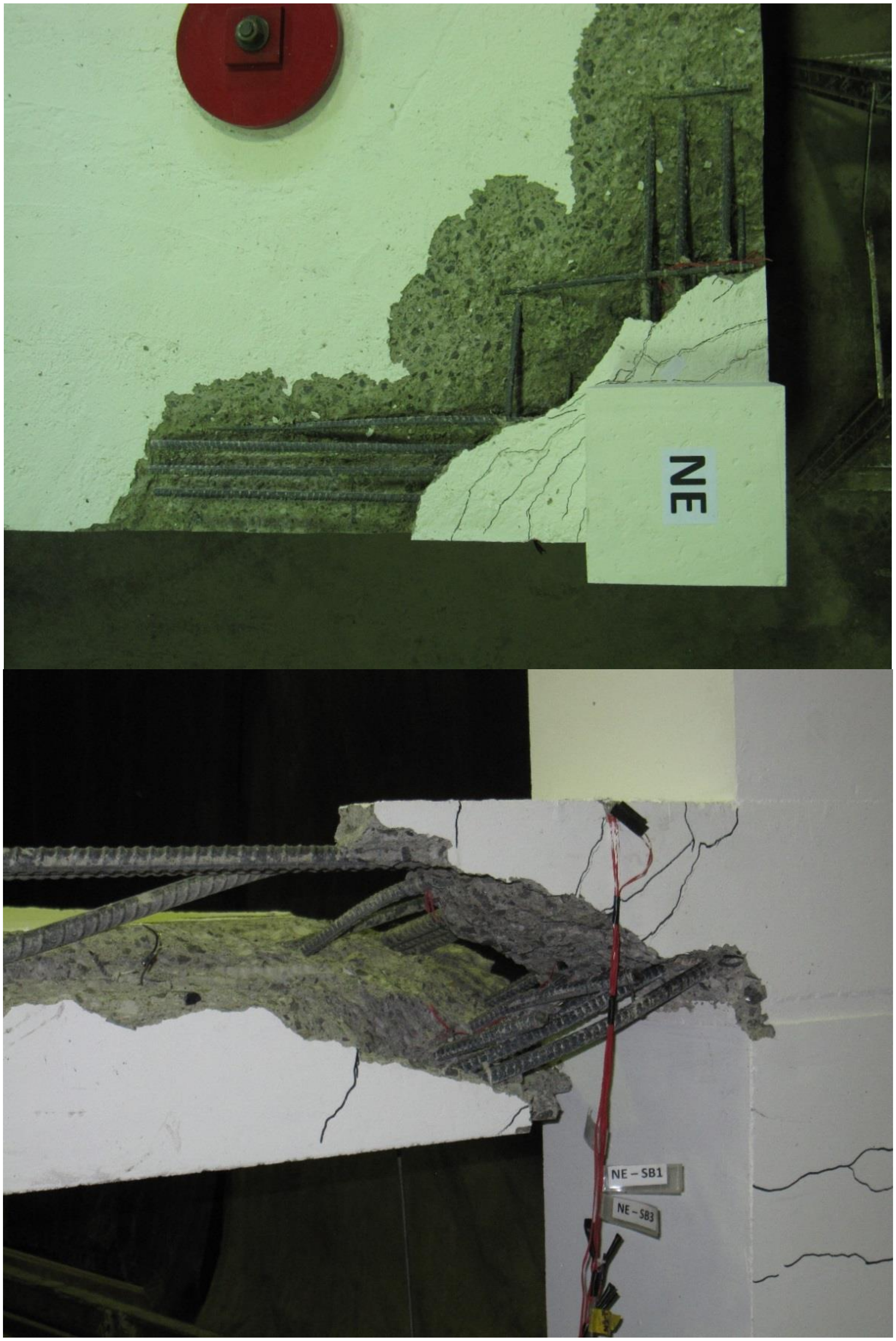

Figure 3-43: Post-punching shear condition of the corner slab-column connection NE at the end of testing

Table 3-13: Summary of key load stages for corner slab-column connection NE

Stage	Load (kN)	Displacement (mm)
First Cracking	32.0	0.43
First Yield (Top Bars)	64.8	3.7
First Yield (Structural Integrity Bars)	NA	NA
Punching Shear Failure	107.4	7.7
Max. Post-Punching Load	53.2	76.0

Table 3-14: Angle of top reinforcement for corner slab-column connection NE

<table>
<tr><th>Steel Layout</th><th>Labels</th><th>Angle from Horizontal (Degree)</th></tr>
<tr><td rowspan="7">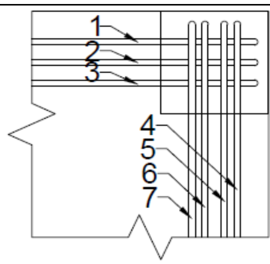</td><td>1</td><td>14</td></tr>
<tr><td>2</td><td>14</td></tr>
<tr><td>3</td><td>14</td></tr>
<tr><td>4</td><td>14</td></tr>
<tr><td>5</td><td>Free</td></tr>
<tr><td>6</td><td>Free</td></tr>
<tr><td>7</td><td>Free</td></tr>
</table>

Table 3-15: Angle of structural integrity reinforcement for corner slab-column connection NE

<table>
<tr><th>Steel Layout</th><th>Labels</th><th>Angle from Horizontal (Degree)</th></tr>
<tr><td rowspan="4">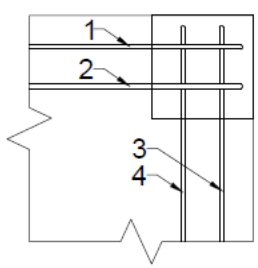</td><td>1</td><td>16</td></tr>
<tr><td>2</td><td>21</td></tr>
<tr><td>3</td><td>24</td></tr>
<tr><td>4</td><td>19</td></tr>
</table>

3.5.3.2 Concrete Cracking

Figure 3-45 shows the shear versus maximum crack width response for corner slab-column connection NE. Flexural cracks were observed on the top surface of slab, edge faces of the slab, and the exterior faces of the column (see Figure 3-3 and 3-44). The crack width reached a maximum of 0.30 mm at load stage 8 when shear cracking started at edge slab-column connections N and S.

In Part 1 of the test, after connections N, S, NW and SW failed in punching, significant load redistribution occurred as concrete breakout took place at the edge slab-column connections. Therefore, with the Part 1 loading, the necessary shear at connections NE and SE to cause punching failure could not be achieved. The continuation of slab displacement in the Part 2 loading increased the shear and moments at connection NE and produced more flexural cracks (see Figure 3-44).

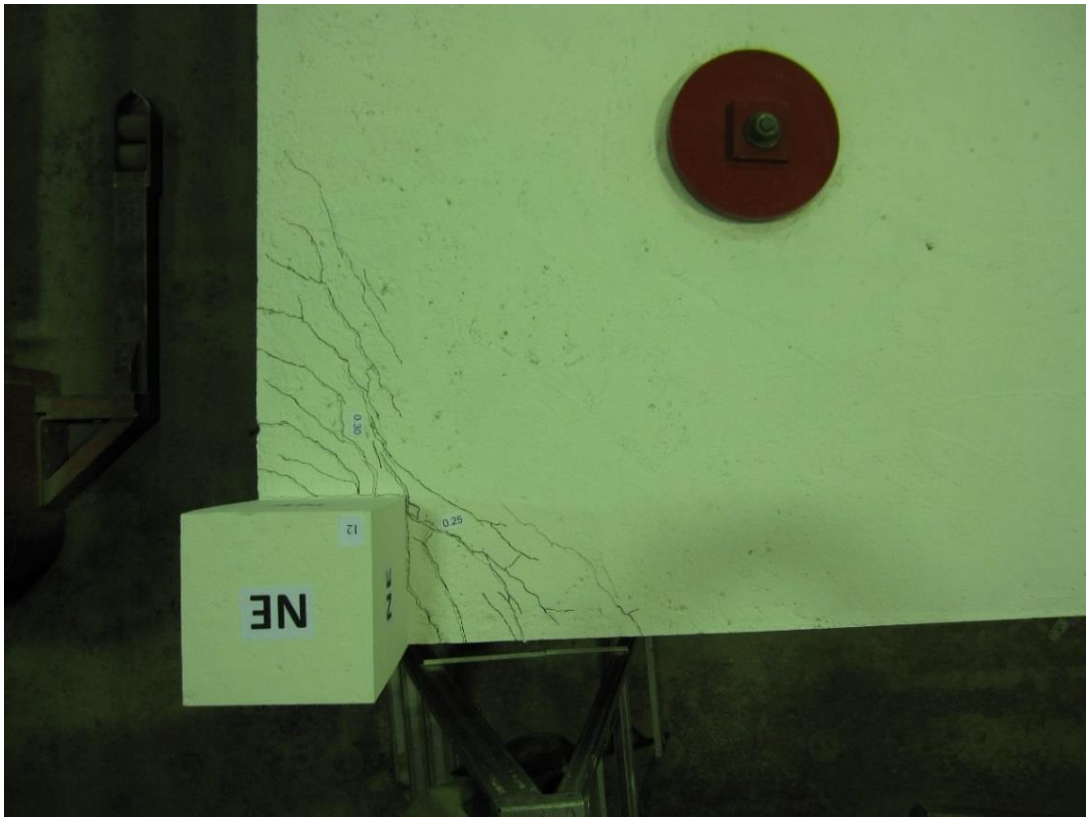

Figure 3-44: Crack pattern around corner slab-column connection NE at load stage 12

Figure 3-45: Shear vs. maximum crack width response for corner slab-column connection NE

3.5.3.3 Top Reinforcement Strains

Figure 3-46 shows the measured strains in selected top reinforcing bars versus connection displacement responses for corner slab-column connection NE.

The flexural deformations of the slab caused higher strain occurred in the top reinforcement in the E-W direction. Strain gauge LB reached the yield strain of 2260 με at a displacement of 3.7 mm shortly after punching shear failure of edge slab-column connections N and S. The maximum strain in gauge LB was achieved when corner slab-column connections NW and SW failed in punching shear, and far exceeded the 16000 με upper recording limit of the strain gauge.

The pause between Part 1 and Part 2 of the test resulted in reduced strains in the reinforcement. The strain in gauge LB dropped from 13125 με to 9796 με during this delay. In Part 2 loading, the reloading of the east side of the slab led to a small strain increase. Gauge LB reached a strain of 9963 με at a deflection of 7.6 mm before slab-column connection NE failed in punching shear. During the post-punching loading, the strain in gauge LB was relatively constant, varying between 8700 and 9000 με until the end of the test.

The strain in gauge LT remained below 2000 με throughout the test.

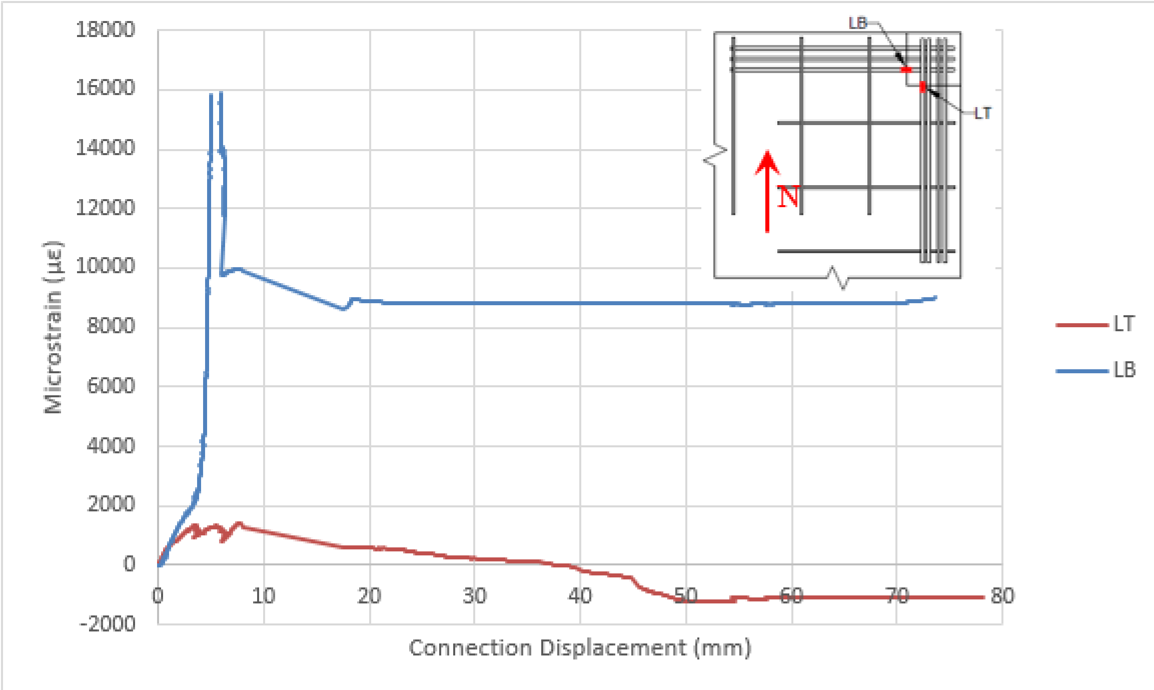

Figure 3-46: Measured strains in the top reinforcement vs. connection displacement for corner slab-column connection NE

3.5.3.4 Structural Integrity Reinforcement Strains

The strains in the structural integrity reinforcement versus connection displacement responses at corner slab-column connection NE are given in Figure 3-47.

Being in the E-W direction and at the location closest to the column, strain gauge ST1 had the highest strains during the test. The punching shear failures of other connections can be identified as peaks on the response curve of gauge ST1 at their respective deflections. Before conducting Part 2 of the test, there was a decline of strain to 1006 με at the deflection of 6.0 mm. The strain in gauge ST1 re-increased as the loading was continued until punching shear failure occurred at slab-column connection NE.

The majority of the strain gauges at connection NE, including ST1, ST2, SB1, SB2 and SB3, were damaged by the punching shear failure at a deflection of 8.0 mm.

Strain gauge ST3, located furthest from the column in the EW direction, was able to function after punching failure at connection NE. It could be seen that the strain started to develop significantly after the punching shear failure, indicating that the integrity reinforcement was providing post-punching resistance to the corner slab-column connection. Gauge ST3 malfunctioned with a peak strain of 738 $\mu\varepsilon$ at a deflection of 18.0 mm. It was not clear whether the structural integrity reinforcement yielded during the post-punching response.

Figure 3-48 shows the measured strain distributions in the structural integrity reinforcing bars at each load stage on the south face of corner connection NE. This plot indicates that at the location closest to the column, the structural integrity reinforcement underwent increasing compressive strains until punching shear failure occurred at load stage 9. The compression strains at this location of the structural integrity reinforcing bars then became tensile.

On the other hand, Figure 3-49 shows that the section of structural integrity reinforcing bars closest to the face of corner connection was experiencing the highest strain throughout the test, and the overall strain in the integrity reinforcement in the E-W direction increased progressively as loading progressed.

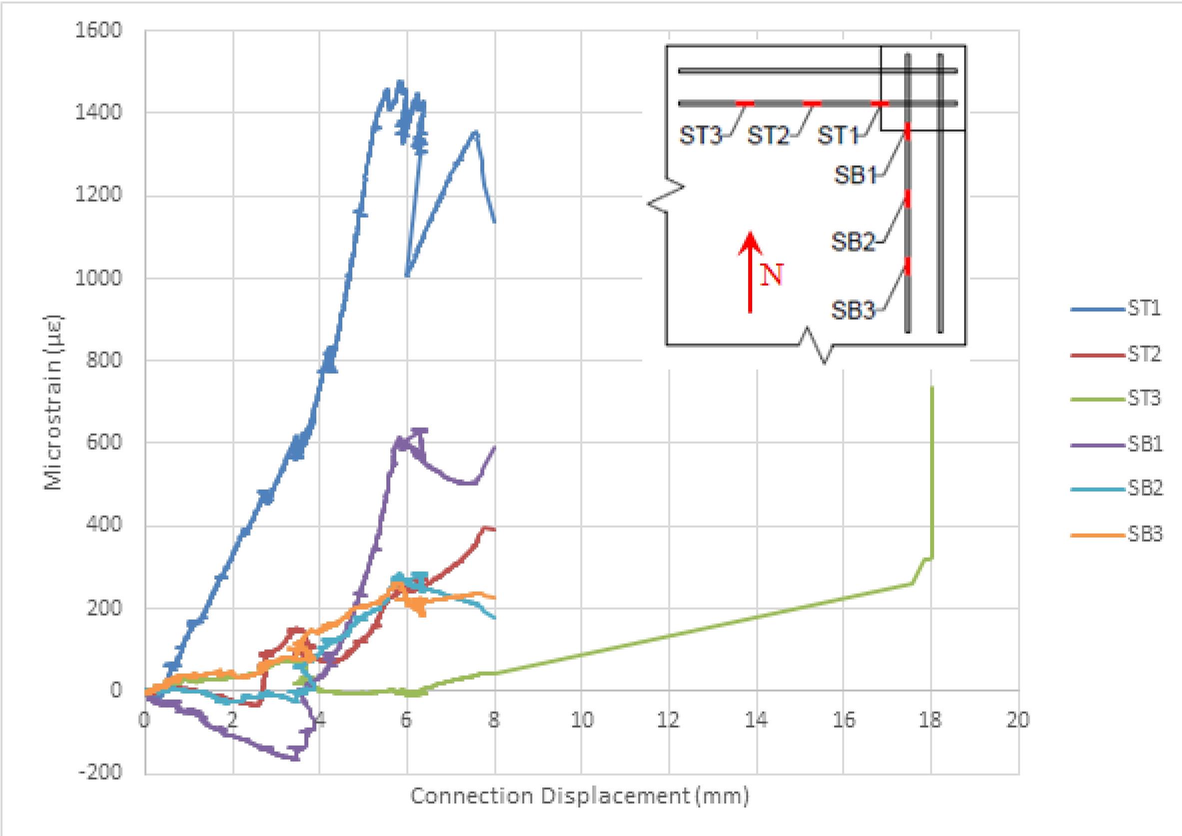

Figure 3-47: Measured strains in the structural integrity reinforcement vs. connection displacement for corner slab-column connection NE

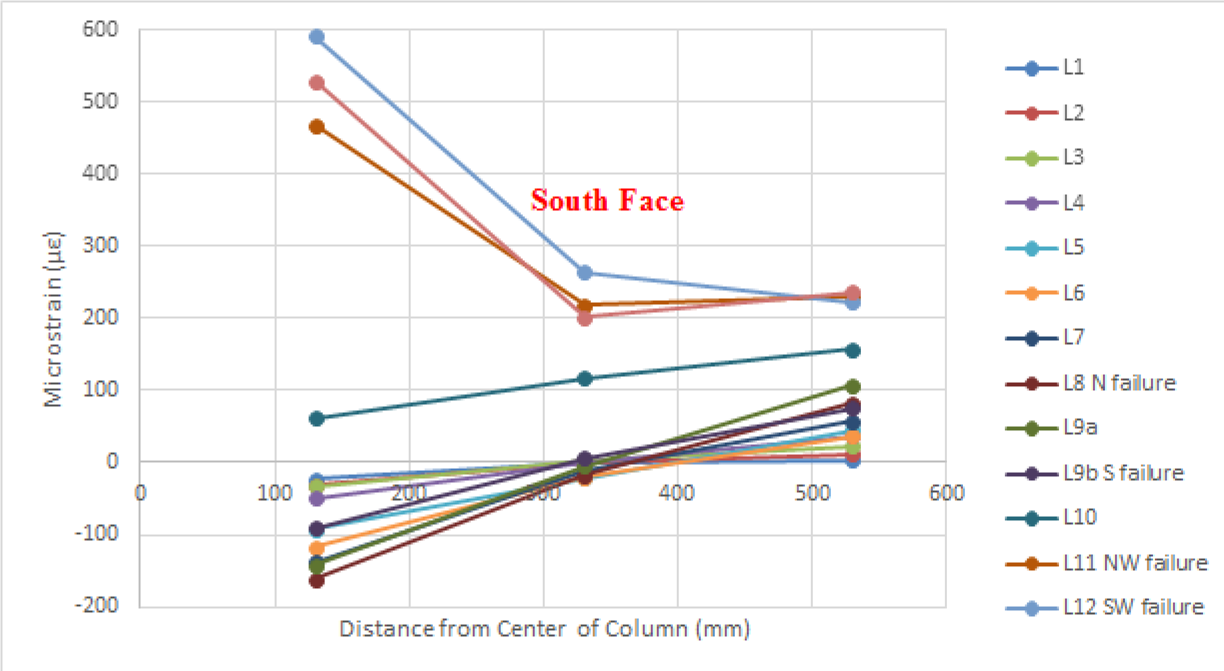

Figure 3-48: Strain distributions in the structural integrity reinforcement in the N-S direction at each load stage for corner slab-column connection NE

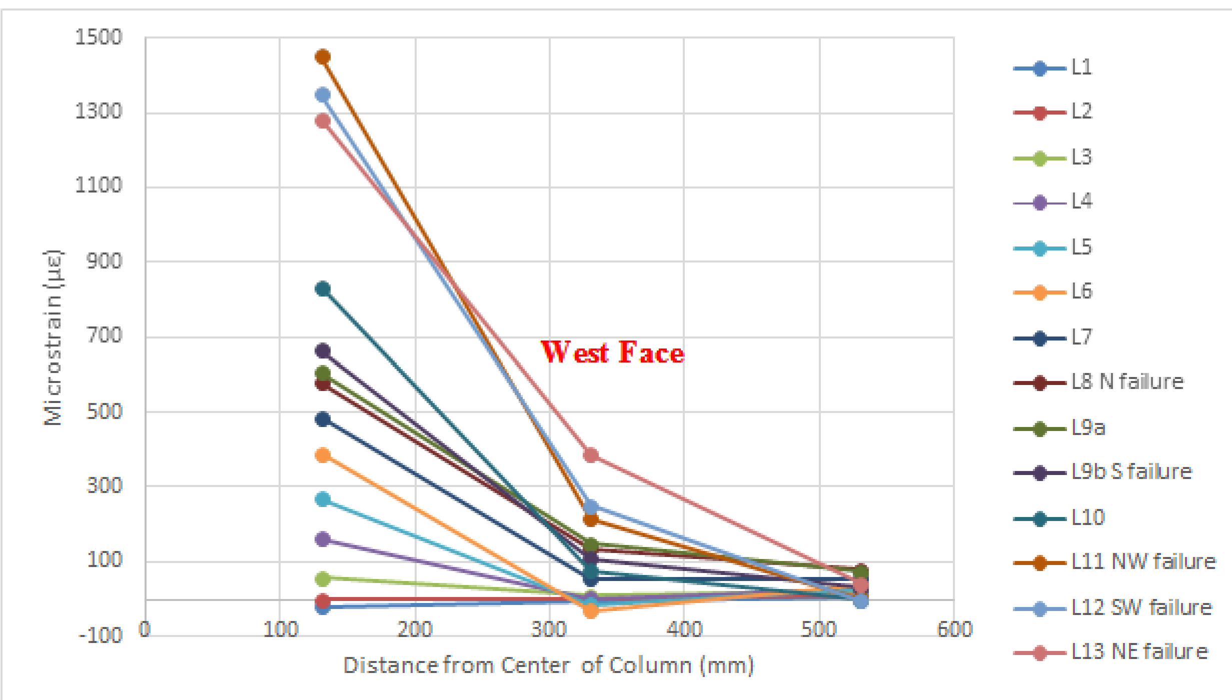

Figure 3-49: Strain distributions in the structural integrity reinforcement in the E-W direction at each load stage for corner slab-column connection NE

3.5.4 Corner Slab-Column Connection SE

3.5.4.1 Test Results

Corner slab-column connection SE failed in punching after connection NE. Figure 3-50 presents its shear versus connection displacement response. The shear and displacement at key load stages are shown in Table 3-16.

Connection SE was the only corner slab-column connection that developed hairline cracks at load stage 1 at a shear of 21.7 kN and a displacement of 0.19 mm (see Figure 3-2). During Part 1 of the test, the response curve of connection SE was similar to the response curve of slab-column connection SW. The punching shear failure of the edge slab-column connection N at stage 9 can be identified as a sudden drop of shear at a deflection of 3.3 mm.

The pause between Part 1 and Part 2 resulted in a drop of shear in slab-column connection SE to 39.0 kN. In Part 2, slab-column connection SE was loaded to failure after punching shear failure of slab-column connection NE. The punching failure of NE was apparent in the response curve as a small drop of shear to 93.7 kN at a displacement of 7.0 mm.

The punching failure happened abruptly after shear cracking appeared at corner slab-column connection SE. The sudden releasing of high concrete stresses resulted in a sudden breakout of the concrete cover at the connection. The recorded punching shear failure load was 107.6 kN at a displacement of 8.7 mm. The shear then dropped rapidly in the post-punching response.

The ongoing loading activity showed that structural integrity reinforcement in slab-column connection SE was able to develop post-punching shear strength. The shear in SE increased to a maximum post-punching shear of 49.9 kN at a displacement of 56.3 mm.

The inspection on the final condition of the reinforcement revealed that two top reinforcement bars at the north face of the connection were entirely ripped out (see Figure 3-51). The post-punching inclinations of the top reinforcement and the structural integrity bars are presented in Table 3-17 and 3-18, respectively. The average angles from horizontal are 11.2 degrees for the top reinforcement, and 18.0 degrees for the structural integrity reinforcement.

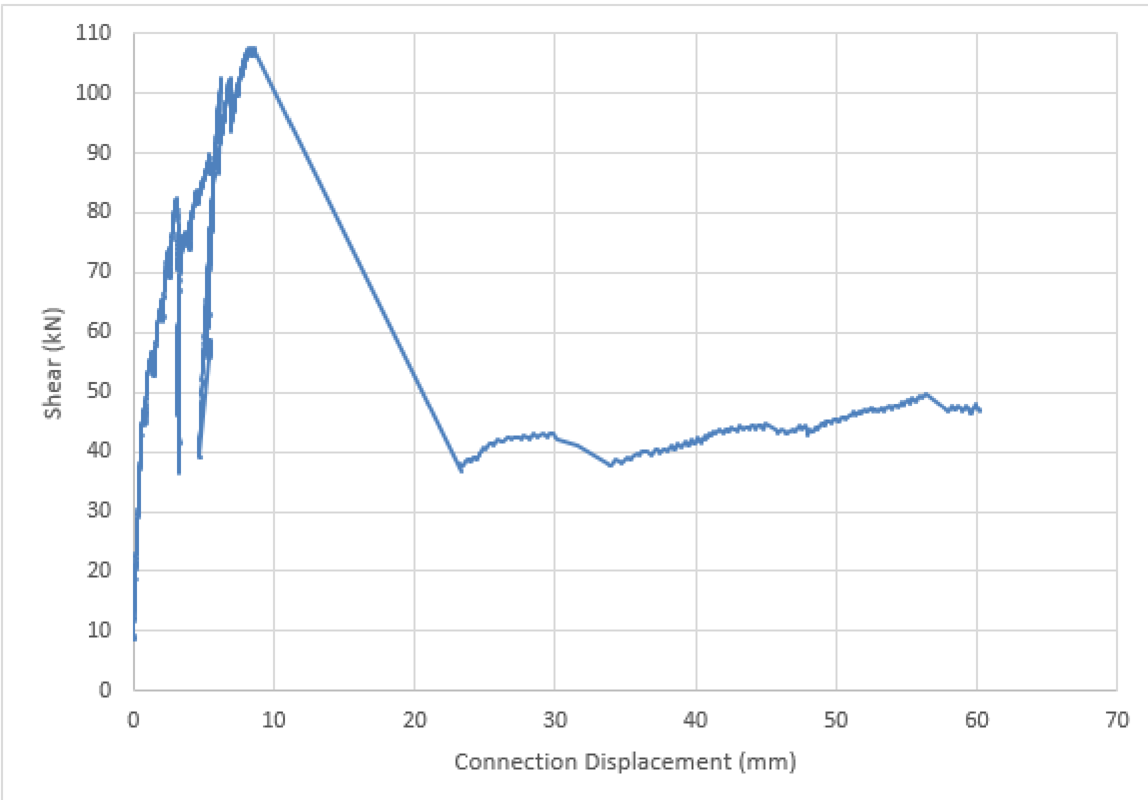

Figure 3-50: Shear vs. connection displacement curve for corner slab-column connection SE

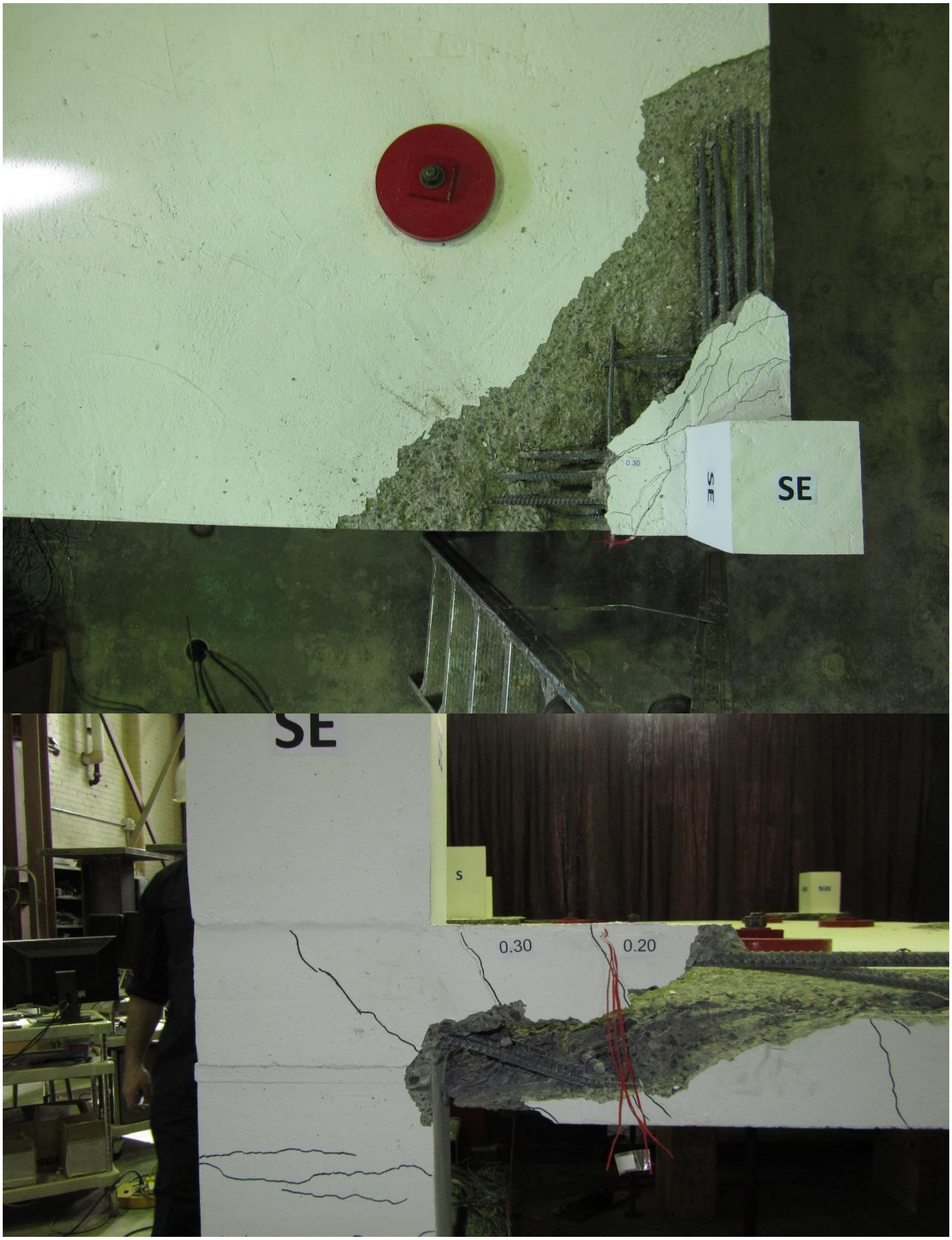

Figure 3-51: Post-punching shear condition of the corner slab-column connection SE at the end of testing

Table 3-16: Summary of key load stages for corner slab-column connection SE

Stage	Load (kN)	Displacement (mm)
First Cracking	21.8	0.19
First Yield (Top Bars)	82.7	4.4
First Yield (Structural Integrity Bars)	NA	NA
Punching Shear Failure	107.6	8.7
Max. Post-Punching Load	49.9	56.3

Table 3-17: Angle of top reinforcement for corner slab-column connection SE

<table>
<tr><th>Steel Layout</th><th>Labels</th><th>Angle from Horizontal (Degree)</th></tr>
<tr><td rowspan="7">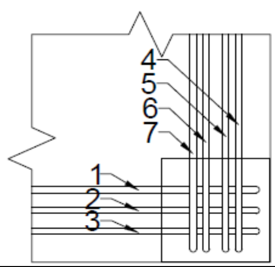
</td><td>1</td><td>13</td></tr>
<tr><td>2</td><td>11</td></tr>
<tr><td>3</td><td>12</td></tr>
<tr><td>4</td><td>10</td></tr>
<tr><td>5</td><td>10</td></tr>
<tr><td>6</td><td>Free</td></tr>
<tr><td>7</td><td>Free</td></tr>
</table>

Table 3-18: Angle of structural integrity reinforcement for corner slab-column connection SE

<table>
<tr><th>Steel Layout</th><th>Labels</th><th>Angle from Horizontal (Degree)</th></tr>
<tr><td rowspan="4">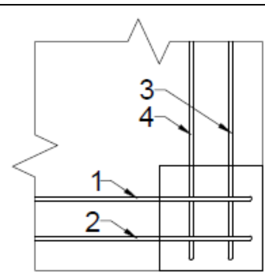
</td><td>1</td><td>17</td></tr>
<tr><td>2</td><td>15</td></tr>
<tr><td>3</td><td>20</td></tr>
<tr><td>4</td><td>20</td></tr>
</table>

3.5.4.2 Concrete Cracking

Figure 3-53 presents the shear versus maximum crack width response for corner slab-column connection SE. Flexural cracks were observed on the top surface of the slab, edge face of the slab, and exterior faces of the column (see Figure 3-3 and 3-52). The maximum crack width was reached at load stage 8 where shear cracking started at edge connections N and S. The continuation of load application led to an increase in the number of cracks, while the maximum crack width remained at 0.30 mm.

In Part 1 of the test, due to the fact that applied load was reduced through deformation and concrete breakout action at slab-column connections N, S, NW and SW that failed in punching shear, it was unable to cause shear cracking at corner connections NE and SE. On the other hand, compared to corner connections NW and SW which failed previously in Part 1, more flexural cracks were originated at slab-column connection SE due to the larger moment produced by large slab displacements (see Figure 3-52).

Figure 3-52: Crack pattern around corner slab-column connection SE at load stage 12

Figure 3-53: Shear vs. maximum crack width response for corner slab-column connection SE

3.5.4.3 Top Reinforcement Strains

Figure 3-54 shows the measured strains in the top reinforcement versus connection displacement responses for corner slab-column connection SE.

Strain gauge LB reached the yield strain of 2260 με at a deflection of 4.4 mm during the loading process to cause shear failure at west side corner slab-column connections. The strain in gauge LB increased abruptly, and reached a maximum strain of 11847 με at a displacement of 6.2 mm.

Unlike corner slab-column connection NE, the pause between Part 1 and Part 2 loading did not lead to release of large amount of strain in the top reinforcement in the E-W direction at connection SE. The strain in gauge LB was able to stay above 11401 με until punching shear failure occurred at a displacement of 8.4 mm. In the post-punching response, the strain in gauge LB reduced gradually from 10084 με to 9287 με.

Connection SE was the only corner slab-column connection that achieved the yield strain in the top reinforcement in the N-S direction. Gauge LT experienced significant strain increase during the loading process in Part 2 of the test. The yield strain was reached at a displacement of 6.1 mm and a maximum strain of 3166 με was achieved at the displacement of 8.4 mm shortly before the slab-column connection SE failed in punching shear.

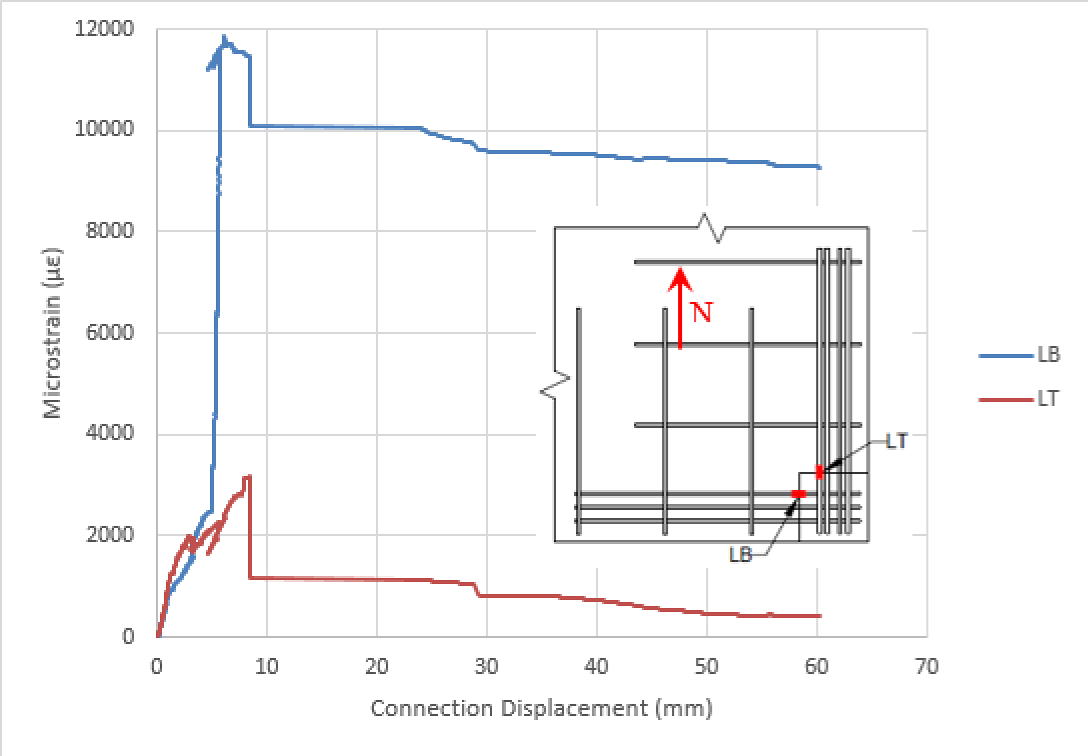

Figure 3-54: Measured strains in the top reinforcement vs. connection displacement for corner slab-column connection SE

3.5.4.4 Structural Integrity Reinforcement Strains

The strains in the structural integrity reinforcing bars versus displacement responses for corner slab-column connection SE are shown in Figure 3-55. The majority of strain gauges displayed active response during the test. The corner slab-column connection SE was the last connection of the slab structure to fail in punching shear.

The maximum strain was reached in gauge ST1 during punching shear failure on the west side, with a strain of 864 με and a displacement of 5.7 mm. Before the start of Part 2 loading, the strains reduced in all of the gauges and there was a small recovery of slab deflections.

Following the failure of connection NE at a displacement 6.2 mm, the strain in gauges ST1, SB1, SB2 and SB3 started decreasing, while signs of strain increases were apparent in gauges ST2 and

ST3. The strain in gauges SB1 and SB2 indicated that prior to punching failure at slab-column connection SE, compressive strains occurred in the structural integrity reinforcement on the north face of the connection. All of the gauges malfunctioned immediately upon punching shear failure and it was unable to determine whether the structural integrity reinforcing bars yielded during the post-punching response.

The strain distributions at each load stage are shown in Figure 3-56 and 3-57. The strains in gauges located 130 mm and 330 mm from the center of the column increased gradually as loading progressed. The punching shear failure at connections NE and SE reduced the strain drastically in gauges located nearest to the column.

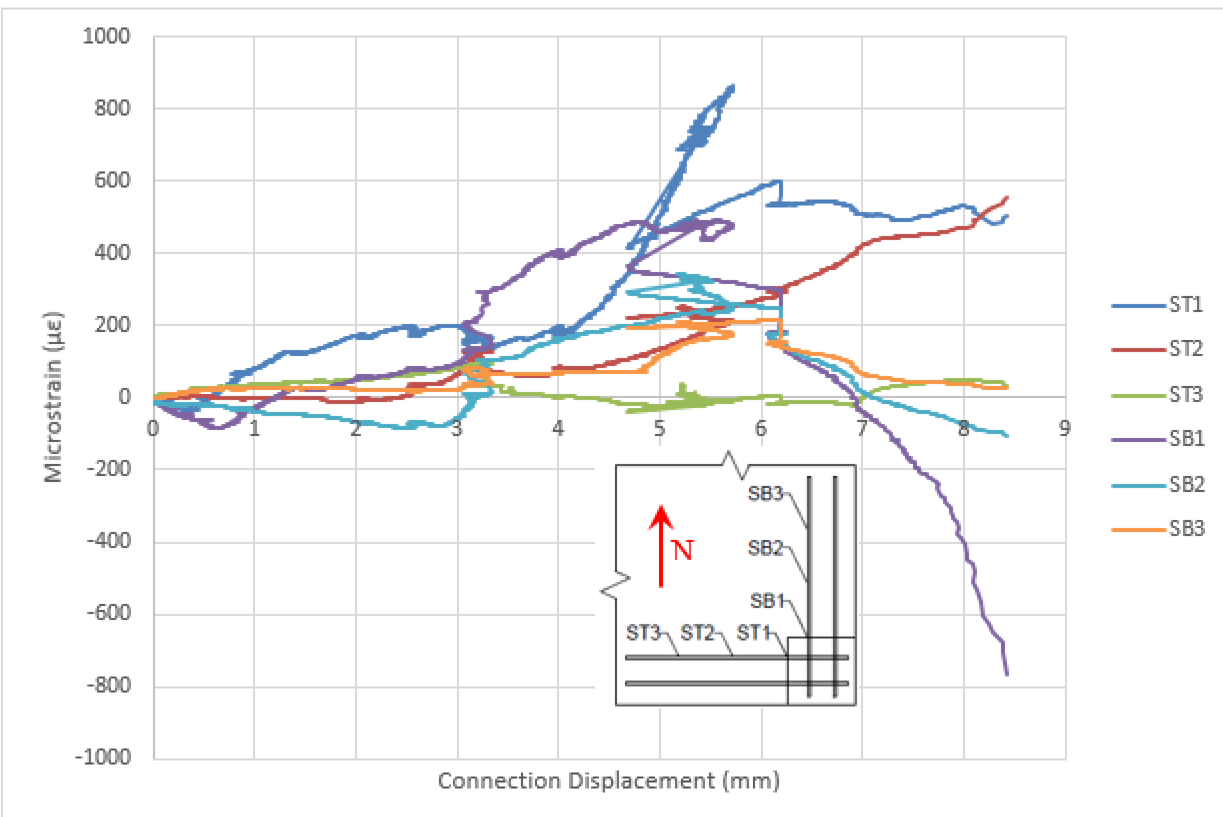

Figure 3-55: Measured strains in the structural integrity reinforcement vs. connection displacement for corner slab-column connection SE

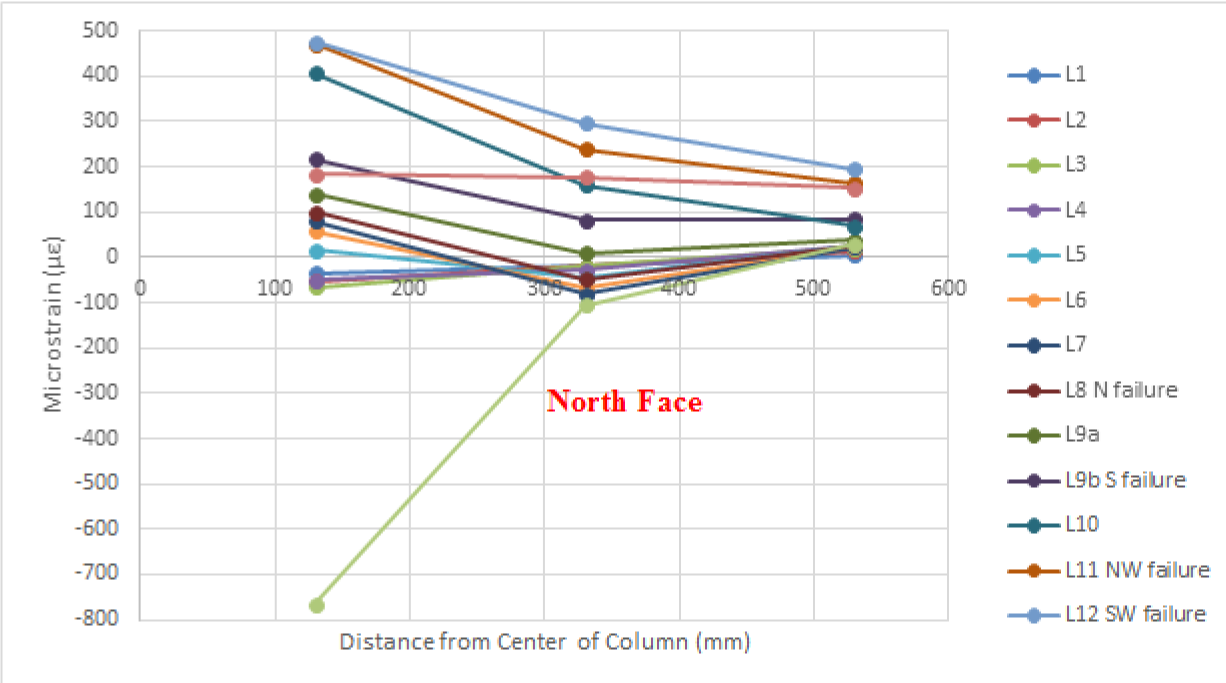

Figure 3-56: Strain distributions in the structural integrity reinforcement in the N-S direction at each load stage for corner slab-column connection SE

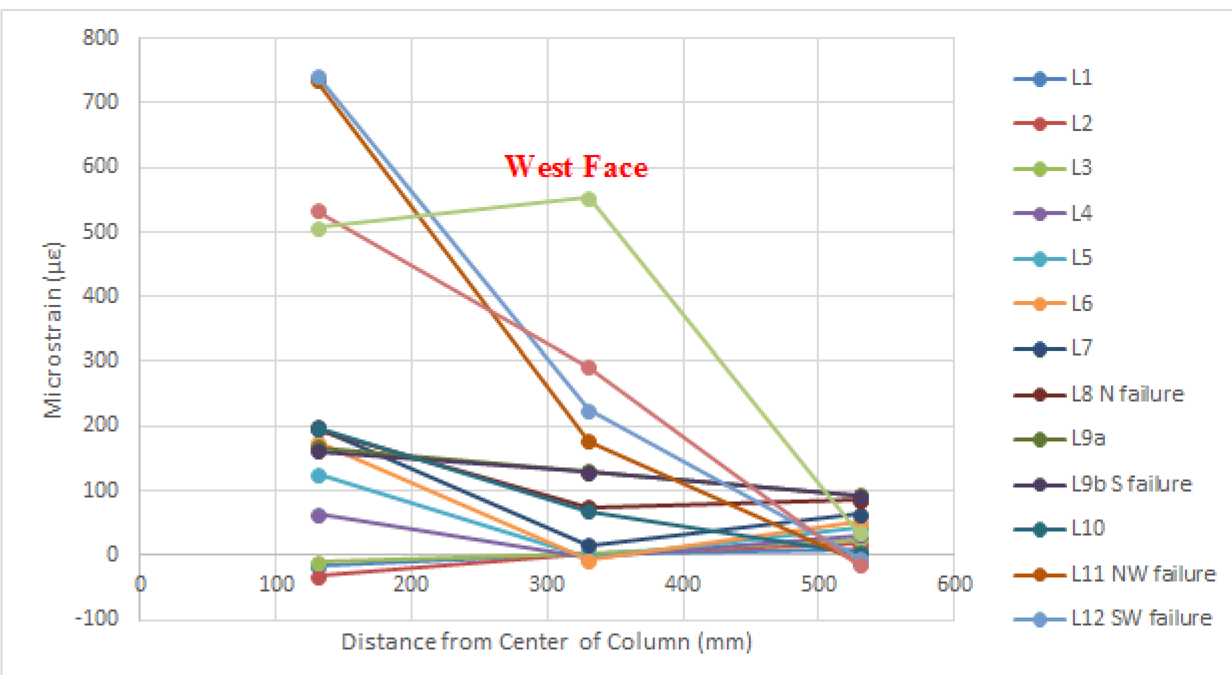

Figure 3-57: Strain distributions in the structural integrity reinforcement in the E-W direction at each load stage for corner slab-column connection SE

4. ANALYSIS AND COMPARISON OF RESULTS

4.1 Introduction

The methodology used to determine the shear at each slab-column connection from the total load at different intervals of failure is discussed in detail in this chapter.

The experimental results for individual slab-column connections, including the shear, the shear stress and the moment at punching shear failure, as well as the ultimate shear after punching shear failure, are compared with the code predictions using the 2014 CSA A23.3 Standard. The overall performance of the slab structure is also assessed in comparison to its design loads calculated in Chapter 2.

4.2 Calculation of Shear Distribution

4.2.1 Prediction of Post-Punching Shear Failure Stiffness

The ACI Code for Nuclear Safety Related Concrete Structures (ACI Committees 349, 1978) provides a guideline to calculate the concrete breakout strength of multiple embedded reinforcing bars when the bars are loaded vertically to the free edge.

Using this concept, Habibi et al. (2014) developed an analytical model for predicting the post-punching shear response of slab-column connections. This model predicts the non-linear post-punching response of slabs by taking into consideration the individual layers of both the top reinforcement and the structural integrity reinforcement. It is also capable of predicting the failure modes of each layer of reinforcement, including rupture of reinforcement, concrete breakout, and pullout of the reinforcing bars.

The analytical model proposed by Habibi et al. (2014) was adopted to predict the post-punching shear responses for edge and corner slab-column connections. These predictions are presented in Figure 4-1 and Figure 4-2, respectively. The calculation results indicated that the edge and the corner slab-column connections would experience concrete breakout, yielding of the reinforcement and pullout of the structural integrity bars from the slab. It can be observed from the response predictions that the complete pullout of each layer of reinforcement (the upper top reinforcement, lower top reinforcement, upper integrity reinforcement and lower integrity reinforcement) results in a sharp drop in the predicted post-punching response.

The stiffness of the slab-column connections following punching failure can be estimated by calculating the slope of the curve in the linear response region. The predicted post-punching stiffness for the edge and corner slab-column connections are 6631 kN/m and 3189 kN/m, respectively.

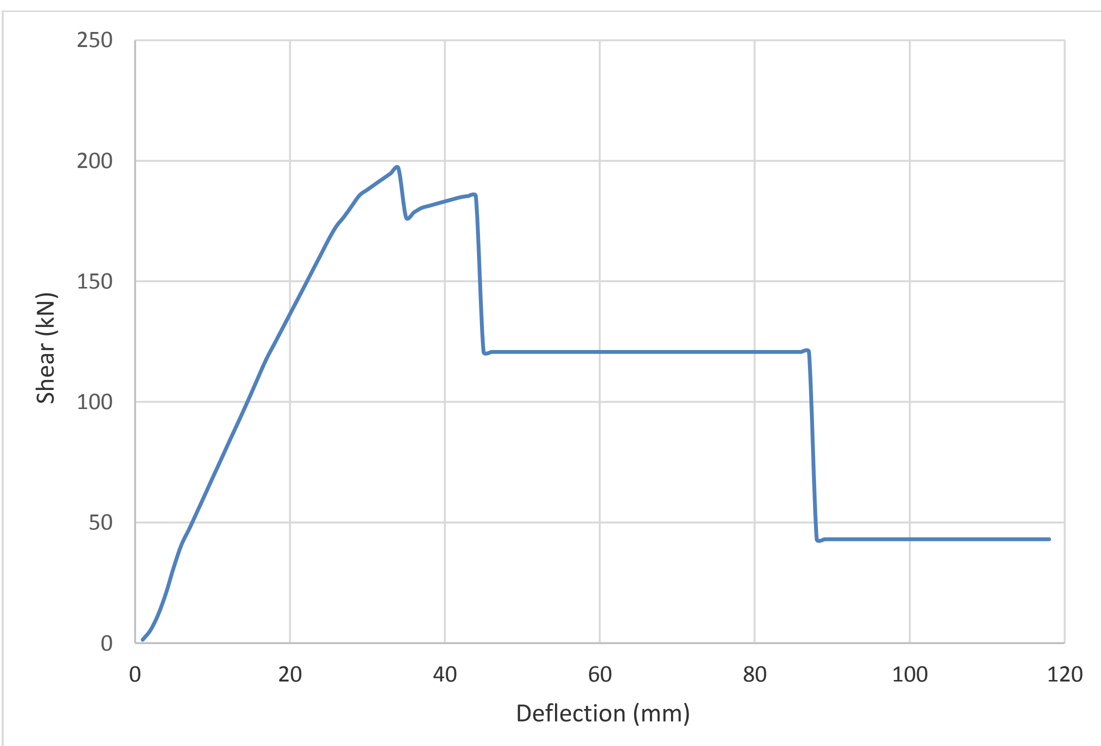

Figure 4-1: Predicted post-punching shear response of edge slab-column connection

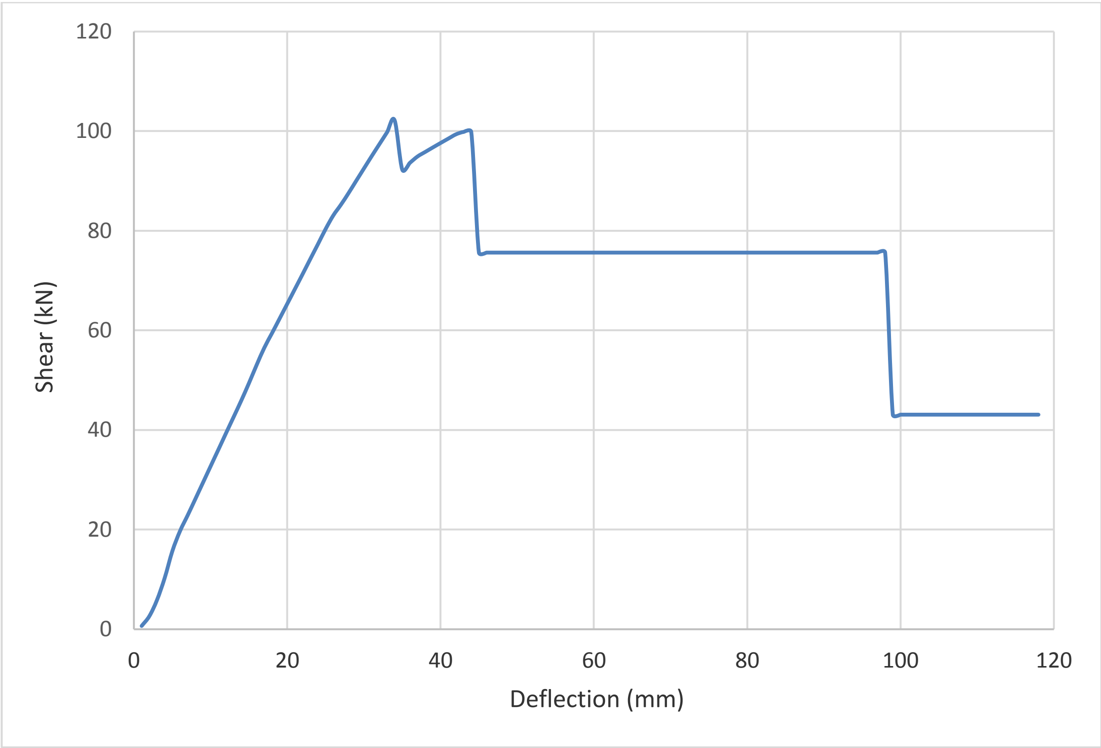

Figure 4-2: Predicted post-punching shear response of corner slab-column connection

4.2.2 SAP2000 Model

It is found that the calculated shear at each slab-column connection, based on tributary areas does not accurately reflect the distribution of loads in the slab structure. Therefore, a computer model was constructed in SAP2000 to better estimate the shear and moment at each slab-column connection.

This structural model, shown in Figure 4-3, is configured in accordance with the design specification of the slab structure: 6000 × 3000 × 150 mm slab supported by six 250 × 250 × 1000 mm exterior columns. The slab was modeled with linear elastic plate bending elements and the columns were modeled as beam frame elements. The reinforcement and concrete properties used in the model are adjusted to match the measured values, as specified in Chapter 2.

To represent the post-punching condition of a slab-column connection in this computer model, the corresponding column was replaced by a vertical spring support with the stiffness obtained from the analytical model developed by Habibi et al. (2014). As an example, Figure 4-4 demonstrates the model configuration following the punching failure of edge connection N, in which the original column N was replaced by a spring support with a stiffness of 6631 kN/m.

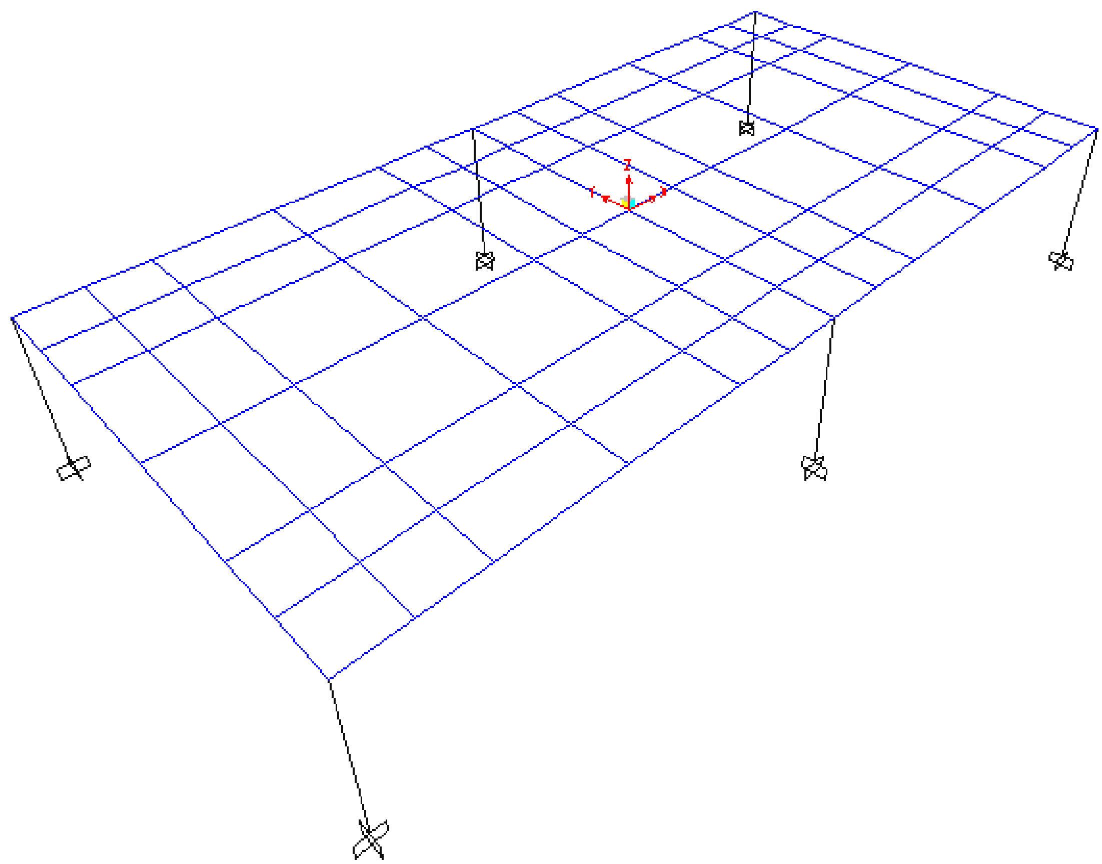

Figure 4-3: SAP2000 model of slab structure, before punching shear failure

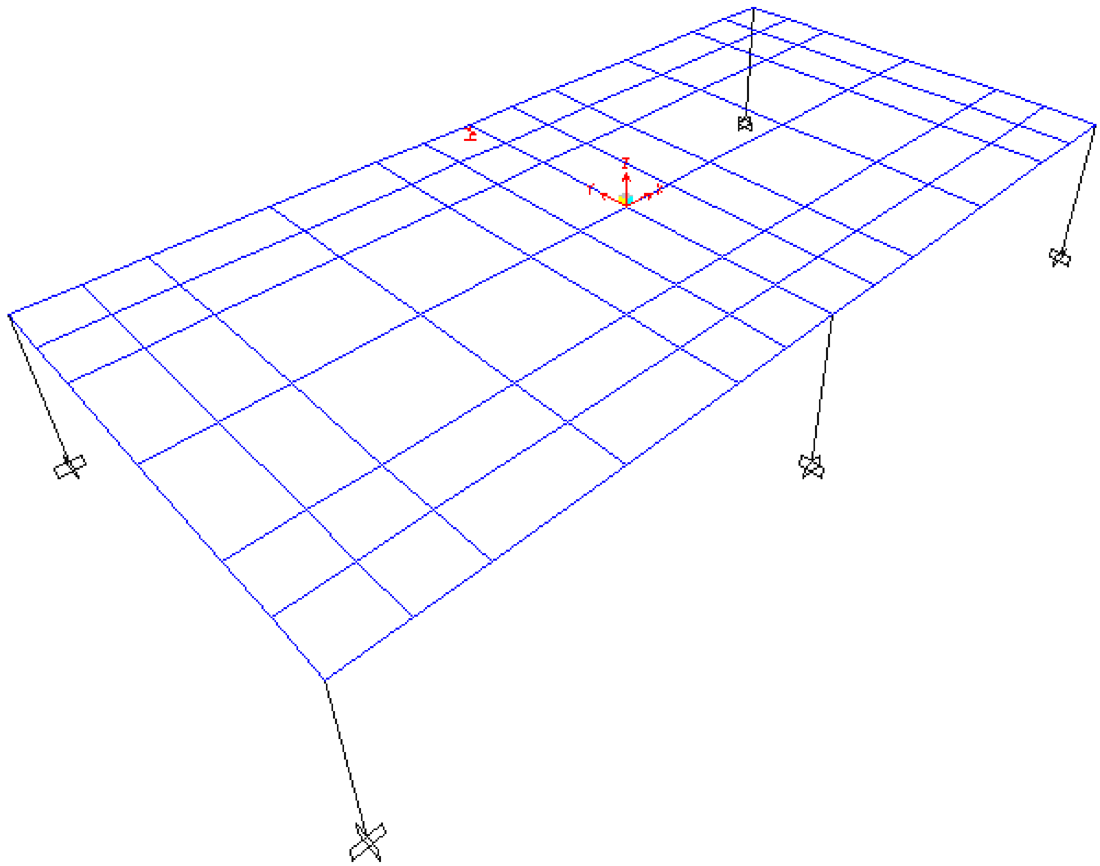

Figure 4-4: SAP2000 model of slab structure, after punching failure of edge connection N

4.2.3 Calculation of Shear Distribution Ratio at the Slab-Column Connections

4.2.3.1 Calculations for Part 1 of the Test

In Part 1 of the test, the slab structure was loaded with simulated uniform distributed load. For a slab system loaded with uniform distributed load, the ratio of load distribution at each support is constant until the structural support system changes, for example, when one or multiple slab-column connections fail in punching shear. Based on this principle, the calculation of load distribution ratio at the connections for Part 1 of the test is divided into five intervals. Each of the intervals is distinguished by a specific event that changed the condition of the slab supports. There intervals include:

1. Load distribution ratio before punching shear failure;
2. Load distribution ratio following punching shear failure of connection N;
3. Load distribution ratio following punching shear failure of connection S;
4. Load distribution ratio following punching shear failure of connection NW;
5. Load distribution ratio following punching shear failure of connection SW.

The support conditions are adjusted in the computer model for each interval. Along with the dead load from slab and loading apparatus, one set of typical loads obtained from the load cells within the interval would be applied to their respective loading points in the SAP2000 model. The resulting load distribution ratios were determined for each interval and are listed in Table 4-1, 4-2, 4-3, 4-4, and 4-5. For example in the first interval the shear at column N is 0.288 times the total load carried by the slab (see Table 4-1). The equation to calculate shear at each connection is:

$$V = P \times R \tag{4.1}$$

where:

V = shear at a particular slab-column connection.

P = total load, including slab self-weight, loading apparatus self-weight and applied load.

R = calculated load distribution ratio for a particular column.

It is apparent from these tables that as different events occur the distribution of shear at the columns changes. These distribution factors were used to determine the shears at the different slab-column connections in Chapter 3.

Table 4-1: Load distribution ratio for interval 1 – before punching shear failure

Connections	Load Distribution Ratio, *R*
N	0.288
S	0.278
SW	0.105
NE	0.114
NW	0.106
SE	0.109

Table 4-2: Load distribution ratio for interval 2 – post-punching failure of connection N

Connections	Load Distribution Ratio, *R*
N	0.131
S	0.354
SW	0.082
NE	0.178
NW	0.169
SE	0.086

Table 4-3: Load distribution ratio for interval 3 – post-punching failure of connection S

Connections	Load Distribution Ratio, *R*
N	0.177
S	0.170
SW	0.157
NE	0.171
NW	0.164
SE	0.162

Table 4-4: Load distribution ratio for interval 4 – post-punching failure of connection SW

Connections	Load Distribution Ratio, *R*
N	0.228
S	0.167
SW	0.198
NE	0.176
NW	0.085
SE	0.145

Table 4-5: Load distribution ratio for interval 5 – post-punching failure of connection NW

Connections	Load Distribution Ratio, *R*
N	0.234
S	0.235
SW	0.119
NE	0.149
NW	0.117
SE	0.145

4.2.3.2 Calculations for Part 2 of the Test

Similar to Part 1 of the test, the load distribution ratio calculation for Part 2 is divided into 3 intervals, including:

6. Load distribution ratio before punching shear failure of connections NE and SE;
7. Load distribution ratio following punching shear failure of connection NE;
8. Load distribution ratio following punching shear failure of connection SE.

It is noted that in Part 2 of the test, the slab structure was loaded with pattern loading. Therefore, the methodology for deriving load distribution ratio on each connection was adjusted accordingly. Based on the fact that increased loading were generated only from the two hydraulic jacks adjacent to the east side connections, while the condition of the rest of the jacks remained unchanged, the loads were separated into three loading components and load distribution ratio were calculated individually for each component. The load distribution ratios are assumed to remain constant during each interval. These loading components include:

A. Load distribution ratio from the self-weight of slab and loading apparatus;
B. Load distribution ratio from the six hydraulic jacks that remained unchanged;
C. Load distribution ratio from the two hydraulic jacks generating increasing load.

The equation to calculate the shear at each connection is given by:

$$V = P_A \times R_A + P_B \times R_B + P_C \times R_C \tag{4.2}$$

where:

V = shear at a particular slab-column connection.

P_A = summation of slab and loading apparatus self-weight.

R_A = calculated load distribution ratio for a particular column from component A.

P_B = summation of load from the six hydraulic jacks that remained unchanged.

R_B = calculated load distribution ratio for a particular column from component B.

P_C = summation of load from the two hydraulic jacks generating increasing load.

R_C = calculated load distribution ratio for a particular column from component C.

Table 4-6: Load distribution ratio for interval 6 – before punching shear failure of NE and SE

	Part A	**Part B**	**Part C**
Connections	Load Dist. Ratio, R_A	Load Dist. Ratio, R_B	Load Dist. Ratio, R_C
N	0.235	0.289	0.107
S	0.235	0.278	0.104
SW	0.124	0.169	-0.003
NE	0.141	0.048	0.407
NW	0.124	0.174	-0.002
SE	0.141	0.042	0.388

Table 4-7: Load distribution ratio for interval 7 – post-punching failure of connection NE

	Part A	**Part B**	**Part C**
Connections	Load Dist. Ratio, R_A	Load Dist. Ratio, R_B	Load Dist. Ratio, R_C
N	0.282	0.307	0.223
S	0.225	0.281	0.070
SW	0.114	0.162	-0.029
NE	0.079	0.022	0.240
NW	0.123	0.167	-0.005
SE	0.176	0.061	0.500

Table 4-8: Load distribution ratio for interval 8 – post-punching failure of connection SE

	Part A	**Part B**	**Part C**
Connections	Load Dist. Ratio, R_A	Load Dist. Ratio, R_B	Load Dist. Ratio, R_C
N	0.280	0.328	0.218
S	0.280	0.287	0.201
SW	0.110	0.155	-0.044
NE	0.110	0.036	0.342
NW	0.110	0.170	-0.041
SE	0.110	0.024	0.323

4.3 Comparison of Code Predictions with Experimentally Determined Punching Shear Strength

The structural parameters for the edge and corner slab-column connections are presented in Table 4-9. The slab and apparatus self-weights, the applied loads, and the support condition at the punching shear failure event for each connection were modeled in the structural analysis software SAP2000. The direct shear and moment transfer at punching shear failure of the slab-column connections were then obtained from the structural analysis.

Based on the two-way shear stress given by Eq. 4.1, the amount of maximum shear stress v_{test} at a slab-column connection is influenced by direct shear V_{test} and moment transfer in two directions, $M_{test\text{-}x}$ and $M_{test\text{-}y}$. In order to determine the shear stress at failure, this equation is solved, knowing the shear at failure as well as the moment-to-shear ratio in each direction, calculated from the analytical results of the test (see Eq. 4.2a and 4.2b). Solving these equations results in the nominal shear stress, v_{test}, (Eq. 4.3a) and the nominal shear V_{test} corresponding to the punching shear failure at each column. The moment-to-shear ratios in the two directions for each column are given in Table 4-10.

$$v_{test} = \frac{V_{test}}{b_0 d} + \frac{\gamma_{vx} M_{test-x} e_x}{J_x} + \frac{\gamma_{vy} M_{test-y} e_y}{J_y} \qquad 4.1$$

$$R_x = \frac{M_{test-x}}{V_{test}} \qquad 4.2a$$

$$R_y = \frac{M_{test-y}}{V_{test}} \qquad 4.2b$$

$$v_{test} = \frac{V_{test}}{b_0 d} + \frac{\gamma_{vx} (R_x \times V_{test}) e_x}{J_x} + \frac{\gamma_{vy} \left(R_y \times V_{test}\right) e_y}{J_y} \qquad 4.3a$$

$$V_{test} = \frac{v_{test}}{\left(\frac{1}{b_0 d} + \frac{\gamma_{vx} R_x e_x}{J_x} + \frac{\gamma_{vy} R_y e_y}{J_y}\right)} \qquad 4.3b$$

Table 4-10 summarizes the analytical results at punching shear failure at each column, including the direct shear, transferred moment, and comparison of calculated nominal shear stress to the code nominal shear stress. The 2014 CSA A23.3 Standard uses a nominal punching shear stress of $0.33\sqrt{f_c'} = 0.33\sqrt{43} = 2.16\ MPa$.

The analytical results indicate that the calculated punching shear stress is much higher than the nominal shear stress predicted by the CSA Standard. At the edge slab-column connections, the ultimate shear stress exceeded the nominal value by 66%; at the corner slab-column connections, the maximum shear stress exceeded the nominal value by 73% to 78%.

Table 4-9: Parameters of tested exterior slab-column connections

Type	f'_c (MPa)	h (mm)	c (mm)	d (mm)	b_o (mm)	e_x (mm)	γ_{vx}	J_x (mm^4)	e_y (mm)	γ_{vy}	J_y (mm^4)
Edge	43	150	250	110	970	95.9	0.38	1.17E+9	180.0	0.42	2.64E+9
Corner	43	150	250	110	610	76.3	0.40	6.84E+8	76.3	0.40	6.84E+8

Table 4-10: Analytical shear, moments and shear stress in comparison to the nominal stress predicted by code (ACI, 2011 and CSA, 2014)

Slab-Column Connections	V_{test} (kN)	In the E-W direction		In the N-S direction		v_{test} (MPa)	v_n (MPa)	v_{test} / v_n
		Moment to shear ratio, R_x (m)	M_{test-x} (kN·m)	Moment to shear ratio, R_y (m)	M_{test-y} (kN·m)			
N (edge)	215.1	0.23	50.5	0	0	3.59	2.16	1.66
S (edge)	196.8	0.28	56.0	0	0	3.59	2.16	1.66
NW (corner)	87.2	0.21	18.2	0.42	36.3	3.73	2.16	1.73
SW (corner)	87.5	0.29	25.6	0.36	31.6	3.85	2.16	1.78
NE (corner)	106.2	0.22	23.4	0.25	26.6	3.81	2.16	1.76
SE (corner)	103.9	0.28	29.6	0.19	20.1	3.76	2.16	1.74

4.4 Comparison of Code Predictions with Experimentally Determined Post-Punching Strength of Individual Connections

The experimental and predicted maximum post-punching shear strength of edge and corner slab-column connections are presented in Table 4-11 and 4-12, respectively. The post-punching strength of slab-column connections are predicted using equation $V_{se} = \Sigma A_{sb} \times f_y / 2$ which is derived from Eq. 1.14. It is found that in this test, the experimental post-punching strength of both edge and corner connections are lower than the predicted values at a consistent percentage of 62.4% to 66.9%.

There are two factors that lead to the lower than expected post-punching performance:

1. The minimum permitted slab thickness of 150 mm used in this test.
2. Torsional cracking in the slab reduced the breakout resistance of the top and structural integrity reinforcement (Figure 4-5).
3. The slab was subjected to an overload over its entire area.

Table 4-11: Experimental and Predicted Maximum Post-Punching Shear Strength of Edge Slab-Column Connections

Edge Slab-Column Connection	Experimental Post-Punching Strength V_{exp} (kN)	ΣA_{sb} (mm^2)	f_y (MPa)	Predicted Post-Punching Strength V_{pred} (kN)	$\frac{V_{exp}}{V_{pred}}$
N	105.3	800	400	160	0.658
S	105.6				0.660

Table 4-12: Experimental and Predicted Maximum Post-Punching Shear Strength of Corner Slab-Column Connections

Corner Slab-Column Connection	Experimental Post-Punching Strength V_{exp} (kN)	ΣA_{sb} (mm^2)	f_y (MPa)	Predicted Post-Punching Strength V_{pred} (kN)	$\frac{V_{exp}}{V_{pred}}$
NW	52.5	400	400	80	0.656
SW	53.5				0.669
NE	53.2				0.665
SE	49.9				0.624

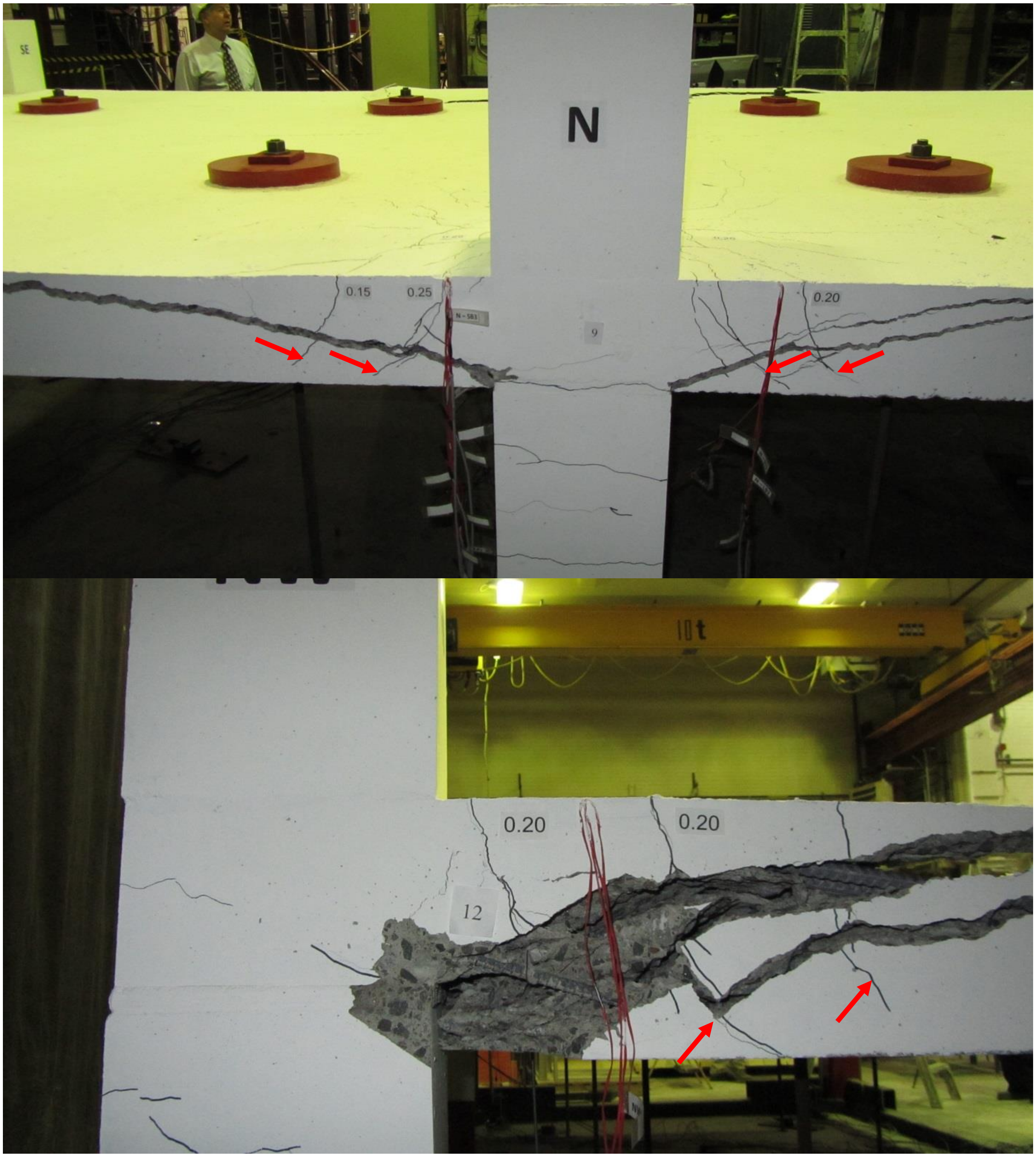

Figure 4-5: Typical torsional cracking in slab for edge and corner slab-column connections

4.5 Comparison of Overall Post-Punching Performance during Uniform Loading to Design Loads

Figure 4-6 shows the overall response of the slab structure. This figure also shows the design loads, including service load, factored load and nominal load which were calculated in Chapter 2.

The ultimate total load was 754.7 kN which greatly exceeded the design factored load of 434.3 kN. During the continuous loading following the failure of the edge slab-column connections, the slab was able to undergo significant displacements from 15.3 mm to 37.5 mm, and withstand a load level higher than the total service load of 306.7 kN. The slab structure was able to provide a resistance well above the service load level, even after two punching shear failures occurred. Some important aspects in interpreting the test results are as follows:

1. The actual concrete compressive strength was 43 MPa, that is significantly higher than the design value of 35 MPa, that resulted in increased punching shear strength.
2. The slab structure was over-designed for flexure to ensure that punching shear failures would occur.
3. The edge slab-column connections hung by structural integrity reinforcement allowed the slab to resist considerable loading while enduring large displacements without additional shear failure during post-punching loading.
4. The design post-punching shear resistances are 160 kN and 80 kN for the edge and corner slab-column connections, respectively. Hence, for the slab structure, with two edge and four corner slab-column connections, the total post-punching resistance is 640 kN. It is noted that for this slab, which was subjected to an extreme overload, the post-punching resistance of 555.1 kN was attained. This represents 87% of the design post-punching resistance.

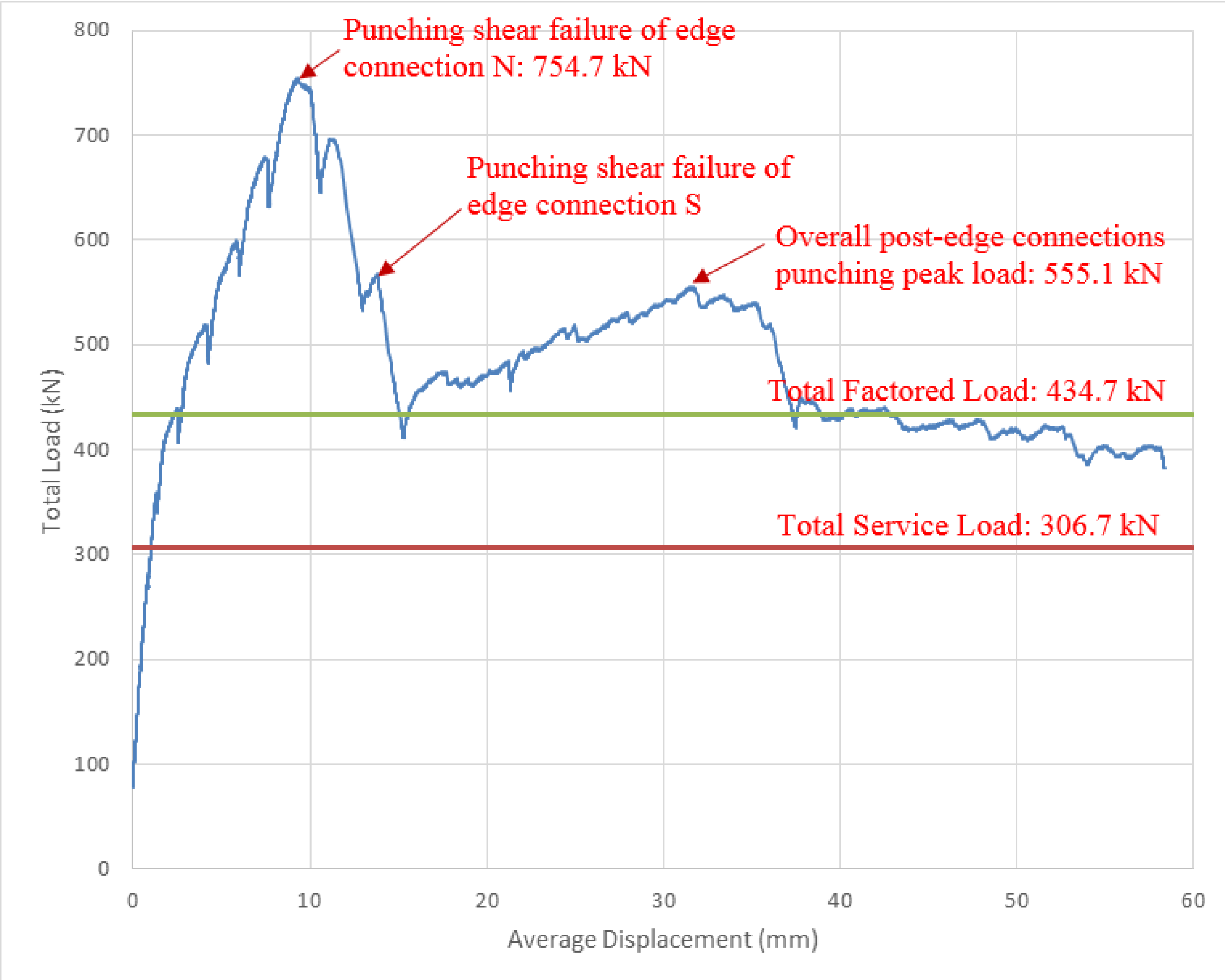

Figure 4-6: Comparison of overall response during uniform loading to design loads

5. CONCLUSIONS AND RECOMMENDATIONS

The objective of this thesis was to investigate the sequence of punching shear failures and examine the post-punching shear behaviour of structural integrity reinforcing bars in a slab system comprised of corner and edge slab-column connections that were designed in accordance with the CSA A23.3-14 Standard. The analytical model developed by Habibi et al. (2014) for predicting the post-punching shear response of slab-column connections was used to assist the computation of load distribution on each connection from the slab loading. The punching shear strength and post-punching shear strength of individual slab-column connections were compared with predictions using the CSA A23.3-14 Standard design expressions. The slab structure's overall performance under uniform loading was compared to its design loads, including service load and factored load. The conclusions made based on this study are as follows:

1. The slab structure reinforcement was designed assuming that the uniform load is distributed based on the tributary areas of each slab-column connection. From structural analysis it is apparent that the edge slab-column connections resist more load than that calculated with an assumed tributary area, while the corner slab-column connections receive less load than that calculated based on their tributary area.
2. The thin, 150 mm, slab thickness limits the breakout resistance of the concrete above the structural integrity reinforcement hence limiting the stresses that can be achieved in the reinforcing bars.
3. Torsional cracks caused by unbalanced moment at the edge and corner slab-column connections effectively reduced concrete breakout resistance, and further decreased the post-punching resistance of the edge and corner slab-column connections.

4. An additional effect that was observed in the test was the significant tension that was developed in the slab causing flexural cracking in the edge and corner columns.
5. The analytical model, developed by Habibi et al. (2014), was adjusted accordingly to the configuration of exterior slab-column connections to predict their post-punching response. The post-punching stiffness of slab-column connection calculated from this model allowed a reasonable estimation of post-punching load redistribution in the slab system following punching shear failures.
6. The top reinforcement anchored into or passing through the columns can provide limited post-punching shear resistance. In the corner slab-column connections, more tensile stress was developed in the top reinforcement extending towards the previously failed edge slab-column connections due to moment redistribution after the punching shear failures.
7. Predictions using the CSA A23.3-14 Standard approach results in conservative estimates of the punching shear strength for both edge and corner slab-column connections. The punching shear stress corresponding to the maximum shear during testing surpassed the nominal stress by 66% for the edge slab-column connections, and by 73% to 78% for the corner slab-column connections.
8. The combined effect of post-punching shear resistance of two edge slab-column connections and punching shear resistance of four corner slab-column connections offered an overall post-punching shear resistance for the slab structure that was 80.9% more than the design service load.
9. Even though the slab structure was subjected to an extreme overload the slab was able to resist post-punching loading greater than the design service load. The structural integrity reinforcement was not designed for the case of general overloading of a slab. The overall

maximum post-punching resistance was 555.1 kN. This represents a total resistance equal to 87% of the design structural integrity reinforcement resistance.

10. The overall performance of the slab structure indicated the ability to provide significant resistance while undergoing large displacements following punching shear failures.

Based on the findings from this experiment, recommendations on performing future research on full-scale slab structure are:

1. For a slab structure, load readings can be taken at each support instead of the loading points to better measure the load distribution in the test and load variation due to the change of support conditions.
2. Additional experiments to be conducted on full-scale slab structures with slabs of greater thicknesses. The effect of increased slab thickness on the improvement of developing post-punching strength should be studied and the required length of the structural integrity reinforcement should also be studied.

REFERENCES

ACI Committee 318, 1977. ACI 318-77, Building Code Requirements for Reinforced Concrete. American Concrete Institute, Detroit, MI.

ACI Committee 318, 2008. ACI 318-08, Building Code Requirements for Structural Concrete. American Concrete Institute, Farmington Hills, MI.

ACI Committee 318, 2011. ACI 318-11, Building Code Requirements for Structural Concrete. American Concrete Institute, Farmington Hills, MI.

ACI Committee 349, 1978. "Proposed Addition to: Code Requirements for Nuclear Safety Related Concrete Structures (ACI 349-76)," *Journal of the American Concrete Institute,* Vol. 75, No. 8, pp. 329-335.

ASTM, 2014. ASTM A370-14, Standard Test Methods and Definitions for Mechanical Testing of Steel Products. ASTM International, West Conshohocken, PA.

Aoude, H., Cook, W. D., and Mitchell, D. 2013. "Two-Way Slab Parking Structures in Canada," *Concrete International*, Vol. 35, No. 12, pp. 47-55.

Correa, C. 2003. *Shear Strength of Slab-Corner Column Connections*. M. Eng. Thesis, McGill University, Montreal, QC.

CSA, 1984. CSA A23.3-84, Design of Concrete Structures. Canadian Standards Association, Rexdale, ON.

CSA, 1992. CSA G30.18-M92, Billet-Steel Bars for Concrete Reinforcement. Standards Council of Canada, Ottawa, ON.

CSA, 1994. CSA A23.3-94. Design of Concrete Structures. Canadian Standards Association, Mississauga, ON.

CSA, 2004. CSA A23.3-04, Design of Concrete Structures. Canadian Standards Association, Mississauga, ON.

CSA, 2014. CSA A23.3-14, Design of Concrete Structures. Canadian Standards Association, Mississauga, ON.

CSI, 2010. SAP2000 (Version 14.2.4) [Computer Software]. Walnut Creek, CA.

Dilger, W. 2000. “Flat Slab-Column Connections,” *Progress in Structural Engineering and Materials.* Vol. 2, No. 3, pp. 386-399.

Egberts, M. J. L. 2009. *Preventing Progressive Collapse of Flat Plate Structures with an Irregular Layout of Structural Reinforcement*. M. Eng. Thesis, McGill University, Montreal, QC.

Elgabry, A. A., and Ghali, A. 1996. “Moment Transfer by Shear in Slab-Column Connections,” *ACI Structural Journal*, Vol. 93, No. 2, pp. 187-196.

El-Salakawy, E. F., Polak, M. A., and Soliman, M. H. 1998. “Slab-column edge connections subjected to high moments,” *Canadian Journal of Civil Engineering*, Vol. 25, No. 3, pp. 526-538.

Habibi, F. 2012. *Post-Punching Shear Response of Two-Way Slabs*. Ph.D. Thesis, McGill University, Montreal, QC.

Habibi, F., Redl, E., Egberts, M., Cook, W. D., and Mitchell, D., 2012. “Assessment of CSA A23.3 Structural Integrity Requirements for Two-Way Slabs,” *Canadian Journal of Civil Engineering*, Vol. 39, No. 4, pp. 351-361.

Habibi, F., Cook, W. D., and Mitchell, D., 2014. “Predicting Post-Punching Shear Response of Slab-Column Connections.” *ACI Structural Journal,* Vol. 111, No. 1, pp. 123-134.

Hammil, N., and Ghali, A. 1994. “Punching Shear Resistance of Corner Slab-Column Connections,” *ACI Structural Journal*, Vol. 91, No. 6, pp. 697-705.

Hawkins, N.M., and Mitchell, D. 1979. “Progressive Collapse of Flat Plate Structures,” *Journal of the American Concrete Institute*, Vol. 76, No. 7, pp. 775-808.

Melo, G. S. S. A., and Regan, P. E. 1998. “Post-Punching Resistance of Connections between Flat Slabs and Interior Columns,” *Magazine of Concrete Research*, Vol. 50, No. 4, pp. 319-327.

Mirzaei, Y. 2008. “Post Punching Behavior of Reinforced Slab-Column Connections.” *In 7th fib PhD Symposium, in Stuttgart Germany, September*, pp. 11-13.

Mitchell, D., and Cook, W. D. 1984. “Preventing Progressive Collapse of Slab Structures,” *Journal of Structural Engineering,* American Society of Civil Engineers, Vol. 110, No.7, pp. 1513-1532.

Mitchell, D., Adams, J., DeVall, R.H., Lo, R.C., and Weichert, D. 1986. “Lessons from the 1985 Mexican Earthquake,” *Canadian Journal of Civil Engineering*, Vol. 13, No. 5, pp. 535-557.

Mitchell, D. 1993. “Controversial Issues in the Seismic Design of Reinforced Concrete Frames,” *Recent Developments in Lateral Force Transfer in Buildings, Thomas Paulay Symposium, American Concrete Institute, La Jolla, CA,* pp.73-93.

Moehle, J. P. 1988. “Strength of Slab-Column Edge Connections,” *ACI Structural Journal*, Vol. 85, No. 1, pp. 89-98.

Reilly, J. L. 2013. *Effects of Delamination on the Response of Slab-Column Connections in Parking Structures*. M. Eng. Thesis, McGill University, Montreal, QC.

Ruiz, M. F., Mirzaei, Y., and Muttoni, A. 2013. “Post-Punching Behavior of Flat Slabs,” *ACI Structural Journal*, Vol. 110, No. 5, pp. 801-811.